CENTRAL UNIVERSITY OF TECHNOLOGY, FREE STATE

Multi material structures for biomedical applications

William Allan Kinnear

Dissertation Submitted
in fulfilment of the
requirements for the degree
MAGISTER TECHNOLOGIAE ENGINEERING: MECHANICAL

Supervisor: Prof. Ihar Yadroitsau, D. Eng
Co-supervisors: Dr. Ina Yadroitsava, Ph. D
Mr. Marinus Potgieter, M. Tech

Bloemfontein
March 2016

DECLARATION OF INDEPENDENT WORK

DECLARATION WITH REGARD TO INDEPENDENT WORK

I, William Allan Kinnear, identity number [redacted] and student number [redacted], do hereby declare that this research project submitted to the Central University of Technology, Free State (CUT, FS) for the MAGISTER TECHNOLOGIAE DEGREE ENGINEERING: MECHANICAL, is my own independent work; and complies with the code of Academic integrity, as well as other relevant policies, procedures, rules and regulations of the Central University of Technology, Free State; and has not been submitted previously to any institution by myself or any other person in fulfilment of the requirements for the attainment of any qualification.

SIGNATURE OF STUDENT.....DATE.....

ACKNOWLEDGEMENTS

I would first like to express my deep gratitude to Prof Ihar Yadroitsau (I.Yadroitsev), Dr Ina Yadroitsava and Marinus Potgieter for their continual support and guidance. I am privileged to learn from their vast knowledge of Additive Manufacturing.

I would like to thank the staff at the CRPM, CUT for their help and expertise. I would personally like to thank Johan Els and Ian van Zyl for their continual support and readiness to assist. I would like to extend a special thanks to Dr Olga de Smidt at the CAFSaB, CUT for her guidance and assistance.

I would like to express my gratitude to the staff at PDTS for allowing me to take time off from work to finish my dissertation. I would personally like to thank Ludrick Barnard and Marinus Potgieter for their guidance and support.

A special word of thanks to the South African Research Chairs Initiative as part of the Department of Science and Technology, the National Research Foundation of South Africa (Grant №97994) for their financial support.

I would like to thank my family and friends for all the support they provided me with. I would personally like to thank my parents, William and Valmae' Kinnear for always leading me in the right direction and their unconditional love. I dedicate this dissertation to them. Furthermore I would like to thank my grandmother Dawn Hobbs for her continual support. I would also like to thank Dane Kinnear, Cindy Kinnear and Werner Smit for their support.

Lastly I would like to honor the Lord Jesus Christ for his unending grace in my life. For it is the hope in him that I will profess.

"But by the grace of God I am what I am, and his grace to me was not without effect"

- 1 Corinthians 15:10 -

ABSTRACT

In this study Direct Metal laser Sintering (DMLS) multi material structures are investigated. The study is developed in two main sections, firstly the conceptualization, validation and optimization of a DMLS multi material DMLS powder deposition system. An "ideal" multiple powder deposition system deposits a homogeneous powder layer with interlocking interface between the different powders. The system need to be time efficient yet deposit powder accurately. In the study a multiple hopper powder deposition system is conceptualized. An experimental was manufactured to establish optimal design specifications with parametric data for powder flow through hoppers. A prototype hopper is developed to validate the hopper system. Ti6Al4V and copper (Cu) powder is deposited side by side and following one another to determine the quality and accuracy of the deposited powder layer.

Secondly, DMLS Ti6Al4V and Cu multi material structures are validated as an antibacterial implant interface that reduces the risk of bacterial infection. Ti6Al4V is a commonly used biomaterial because of its suitable mechanical and biocompatible properties. Cu is a proven antibacterial agent and at low percentages is not toxic to the human body. In the study optimal single track process parameters for pure Cu on a Ti6Al4V substrate are determined. Ti6Al4V-1%Cu structures are manufactured in two proposed processes. Firstly by in-situ alloying Ti6Al4V-1%Cu. Secondly, producing pure Cu areas on a Ti6Al4V substrate so that the surface contains 1% Cu by means of surface area. The produced DMLS samples are exposed to *Escherichia coli* and *Staphylococcus aureus*. Recommendations are made on the development of more effective antibacterial Ti6Al4V-Cu structures.

The work in this study aims to lay a foundation for advanced implant development at the Centre of Rapid Prototyping and Manufacturing (CRPM), Central University of Technology (CUT). By producing medical implants with property specific regions in a single manufacturing cycle will greatly improve the efficiency and functionality of medical implants.

Contents

LIST OF FIGURES

LIST OF TABLES

GLOSSARY

.STL	Stereolithography data file
3D-CAD	Three Dimensional-Computer Aided Drawing
ASTM	American society for testing and material
BSE	Back scatter detector
CFU	Colony forming unit
CNC	Computer numerical control
CRPM	Centre for Rapid Prototyping and Manufacturing
CSIR	Council for Scientific and Industrial Research
CT	Computed tomography
CUT, FS	Central University of Technology, Free State
DMLS	Direct Metal Laser Sintering
E. coli	*Escherichia coli*
EDS	Energy dispersive X-ray
ELI	Extra low interstitials
EOS	Electro optical system
ES	Bacterial cell mixture of *E. coli* and *S. aureus*
FGM	Functionally graded material
HAP	Hydroxyapatite
hMSC	Human mesenchymal stem cells
ILT	Institute for Laser Technology
LED	Light-emitting diode
ND	No disc control
NSF	National Science Foundation
PGLSS	Part Generation by Layer wise Selective Sintering
S. aureus	*Staphylococcus aureus*
SCC	Stress corrosion cracking
SE	Secondary electron
SEM	Scanning electron microscopy
SLM	Selective laser melting
SLS	Selective laser sintering
SS	Stainless steel

NOMENCLATURE

ρ	Density
ρ_{tap}	Tap density
$\rho_{apparent}$	Apparent density
h	Layer thickness
P	Laser power
V	laser scanning speed
p	Probability

PUBLICATIONS AND PRESENTATIONS TO DATE

- Kinnear A., Dzogbewu T.C., Yadroitsava I., Yadroitsev I. Multi material powder delivering system for direct metal laser sintering. 16th International conference RAPDASA, 4-6 November 2015, Pretoria, South Africa
- Kinnear, A., Yadroitsava, I., Yadroitsev, I. Multi material powder delivering systems for selective laser melting, *INTERIM*, Central University of Technology, Free State, 2015, 14 (1), pp. 11-23.
- Kinnear A., I. Yadroitsava, I. Yadroitsev. Multi material structures for biomedical applications, *Light Metals Technology Conference* 27-29 July 2015, Port Elizabeth, South Africa (*poster*).

Chapter 1. INTRODUCTION

1.1. Background

Direct Metal Laser Sintering (DMLS) also referred to as Selective laser melting (SLM) has revolutionized the manufacturing arena; objects that were previously impossible to produce are now simply formed with the DMLS process. The layer by layer manufacturing process of DMLS allows for functional parts and tools with complex shape to be produced (Figure 1.1.1). Geometrical features such as hollows, internal structures, thin walls and undercuts can be manufactured with DMLS (Fraunhofer Institut, 2003). DMLS is effective in producing light weight structures and parts with functional surface properties.

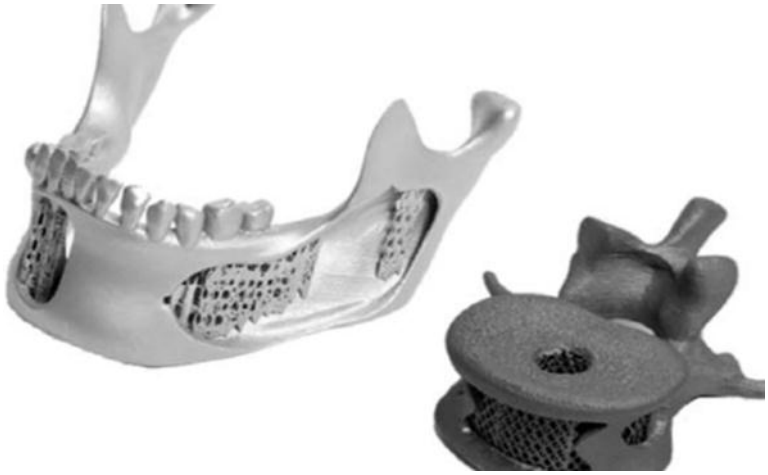

Figure 1.1.1. Manufactured medical implants (Wehmöller *et al.*, 2005)

The DMLS process is revealing new opportunities in the prototyping and manufacturing for aerospace, medical and tooling industries. The extent of DMLS's applications is still growing with the process even being used in the art and fashion industries. The biomedical sector utilizes the benefits of DMLS to manufacture complex geometries and structures in high grade biocompatible materials. Patient specific medical implants, assistive devices and prosthetics are manufactured from the DMLS process. Facial reconstruction has also benefited from the DLMS. Facial features such as noses and jaw lines can be reconstructed due to the ability of DMLS to produce complex and accurate shapes from Computer Aided Design (CAD) designs (Vaezi *et al.*, 2013). Wehmöller *et al.* (2005) conducted a study on the feasibility of metal implants

constructed using the DMLS process. Computer Tomography (CT) scans of a plastic skeleton were used to create CAD data of a jaw bone, lumbar vertebra as well as a middle segment of the tubular femoral bone. For the first time complex bio-structures were manufactured from stainless steel utilizing DMLS.

In August 2014 the Centre of Rapid Prototyping and Manufacturing (CRPM) at the Central University of Technology (CUT) in conjunction with Kimberley Hospital Complex implanted South Africa's first prosthetic jaw bone. The jaw bone was manufactured using the DMLS process. The customized jaw was manufactured on site at the CRPM from Ti6Al4V powder on an EOS M280 machine to replace the cancer infected facial bone (Figure 1.1.2).

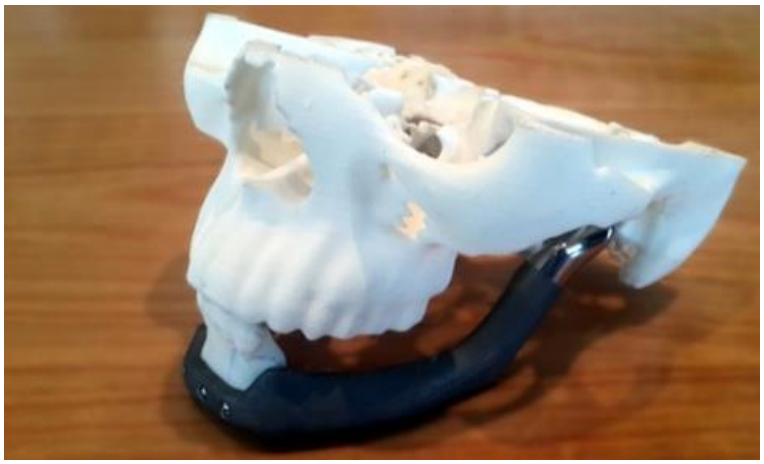

Figure 1.1.2. CRPM's prosthetic jaw bone

Using multiple biocompatible materials on a medical implant has many advantages. Implants can be constructed to have different mechanical, chemical and physical properties in desired areas of the implant. For example a bone where the middle section is made from a material with a higher Young's modules and the outer shell from a material with less hardness to improve the functionality of the implant and reduce stress shielding on the bone. Utilizing DMLS, screw connections or weld joints can be avoided when considering the joint connections of different material in current implants. Copper (Cu) is a proven antibacterial agent. Implants can be constructed to have a biocompatible Ti6Al4V structure with Cu additions at the implant interface in a single manufacturing cycle. These Cu additions will reduce the risk of bacterial infection and implant failure.

With the current DMLS process multi material objects are possible but only with material differences between layers (Z-axis). The current DMLS powder delivery system limits the process to a single material per layer. New approaches are needed to develop a process that produce multi material objects not only in the Z axis, but also allows for material differences on a single layer (X-Y axis). The multi material process will need to dispense multiple material powders on a single layer and between layers. Multi material objects with complex shapes and properties produced in single manufacturing cycle has great potential in growing the AM market.

1.2. The aim of the project

The aim of the project is to investigate multiple material structures for biomedical applications. Firstly, the development of a conceptual multi material powder deposition system for biomedical applications. Secondly, the validation of multi material DMLS Ti6Al4V-Cu structures to serve as an antibacterial implant interface. The study aims to lay a foundation for further work in the field of advanced medical implants.

1.3. The scope of the project

This research study is concerned with elaboration of a multi material powder deposition system, which can be applied not only for manufacturing multi material DMLS objects for biomedical applications, but for other industries where multi material objects are required.

1.4. Research methodology

The methodology for the study is summarized in the following schematic diagram (Figure 1.4.1):

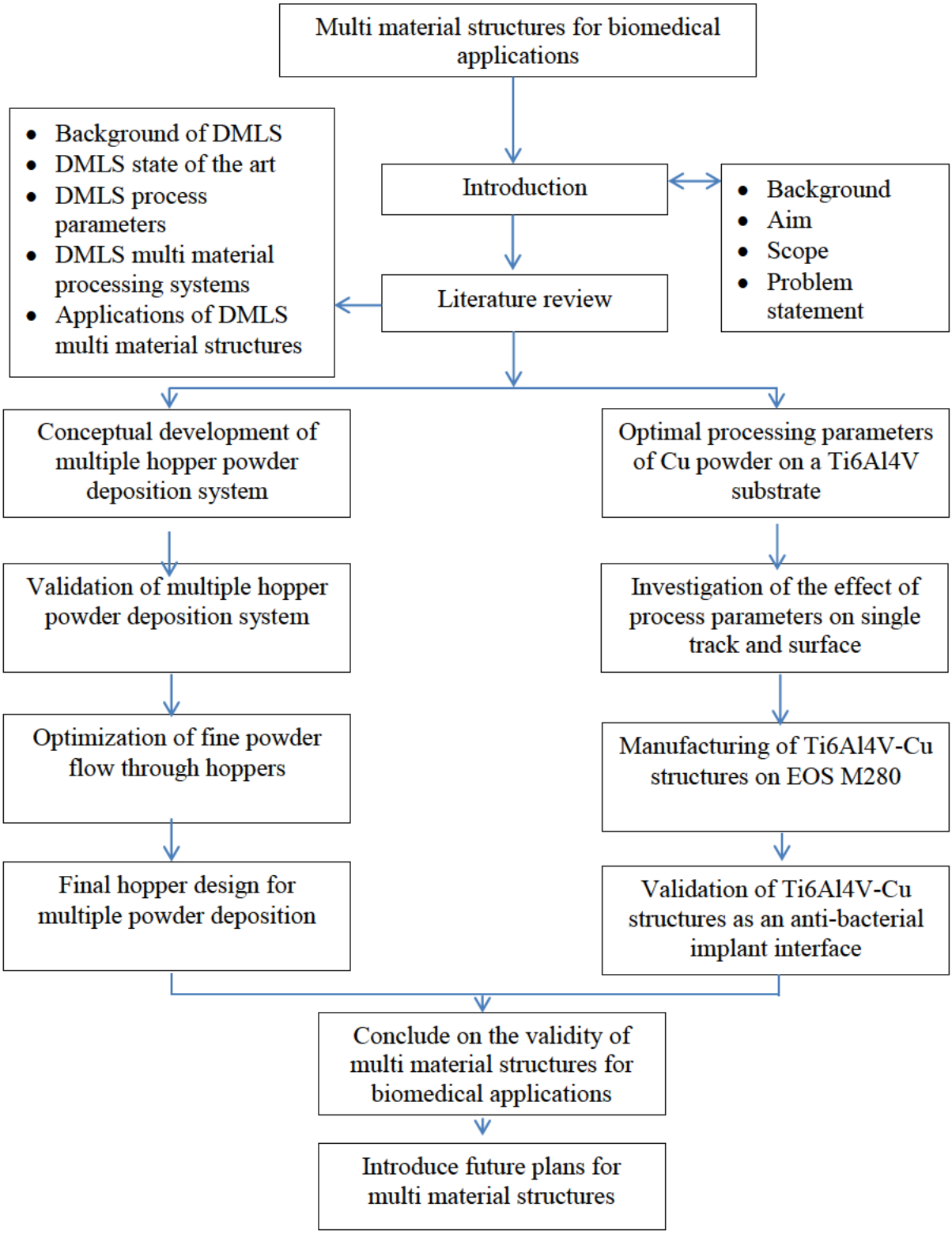

Figure 1.4.1. Schematic of research methodology for the study

1.5. An overview of the dissertation

The following outline defines the dissertations structure:

- Chapter1 gives an introduction and background to the study. In this chapter the aim, scope and methodology of the study are elaborated.
- Chapter 2 gives an account of the literature reviewed. In this chapter an in depth review is conducted on the background and state of the art of DMLS, processing of DMLS parts and comparison of existing multi material powder deposition systems.
- Chapter 3 describes the materials utilized in the study.
- Chapter 4 highlights the conceptualization, validation and optimization of a multiple hopper powder deposition system.
- Chapter 5 describes the research conducted on the processing and validating of Ti6Al4V-Cu structures as a multi material implant interface that can reduce the risk of bacterial infection.
- Chapter 6 concludes the study. Summarizing and discussing the investigation as well as highlighting future work.

1.6. Expected contributions

This study validates the concept of multi material powder deposition system and DMLS multi material structures for biomedical applications. The experimental procedures and preliminary results received in this study will act as a guide for a future in depth study of Ti6Al4V-xCu structures for biomedical application and final development of a multiple hopper powder deposition system for DMLS.

1.7 References

Fraunhofer institute., 2003. Generative Manufacturing Methods : Selective Laser Melting. Available at: http://www.ipk.fraunhofer.de [Accessed April 12, 2015].

Vaezi, M., Chianrabutra, S., Mellor, B. & Yang, S., 2013. Multiple material additive manufacturing – Part 1: a review. Virtual and Physical Prototyping, 8(1), pp.19–50.

Wehmöller, M., Warnke, P.H., Zilian, C. & Eufinger, H., 2005. Implant design and production-a new approach by selective laser melting. Proc. International Congress Series, 1281, pp.690–695.

Chapter 2. REVIEW OF DMLS AND MULTI MATERIAL STRUCTURES

2.1. Direct metal laser sintering technology

2.1.1. Evolution of DLMS systems

Laser sintering of powder dates back to 1979, where R.F Housholder, a private inventor, was the first to suggest selective sintering/melting of powders to form functional objects. The stated object of the invention was "to provide a new and unique molding process for forming three dimensional articles in layers and which process may be controlled by modern technology such as computers". In one embodiment "fusible particles are employed to form each layer which is then selectively fused by a laser beam to fuse an area in each layer which defines that portion of the article in the layers".

In the abstract of the patent it is written: “A molding process for forming a three-dimensional article in layers. In one embodiment, a matrix comprising a planar grid-like member having a plurality of openings formed there through is employed. In an initial layer, casting material and mold material are deposited in selected openings to form a portion of the article in that layer with the casting material surrounded by the mold material. The matrix is located sequentially in adjacent layers and in each layer, the selective deposition of casting and mold material is repeated whereby the article is formed layer by layer from the casting material held in place by the mold material. The casting material is solidified and the mold material is removed. In another embodiment, “planar layers of material are sequentially deposited. In each layer, prior to the deposition of the next layer, a portion of its area is solidified to define that portion of the article in that layer. Selective solidification of each layer may be accomplished by using heat and a selected mask or by using a controlled heat scanning process” (Figure 2.1.1). Housholder never constructed the invention due to the high cost of the laser.

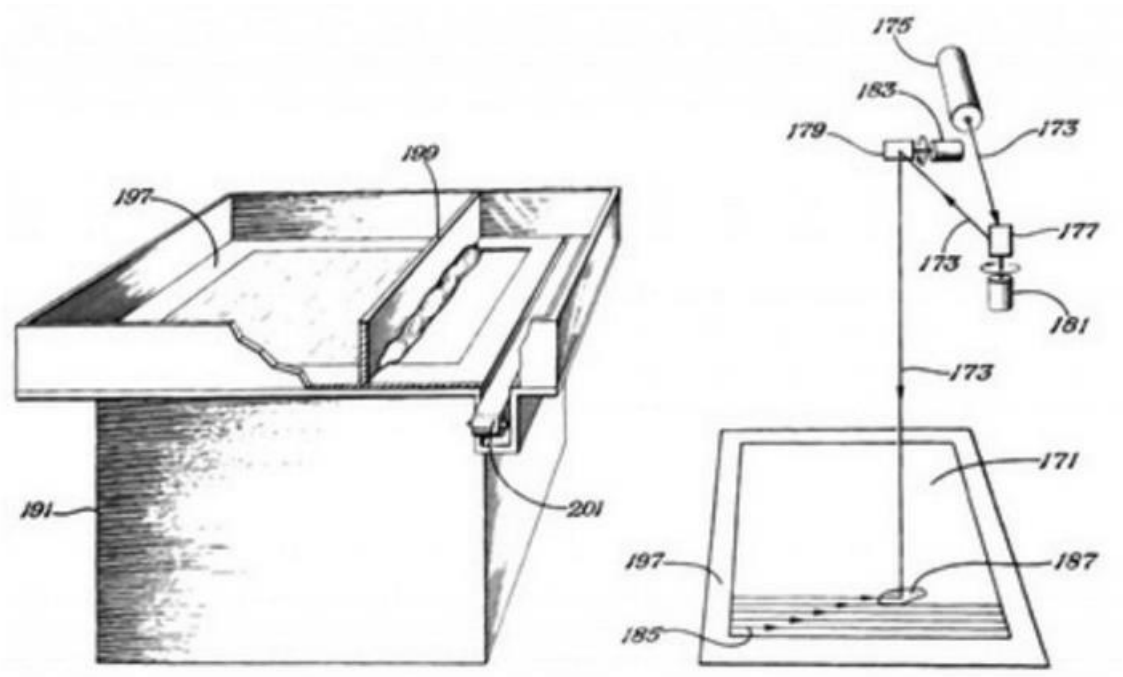

Figure 2.1.1. Schema of the Housholder patent (1979)

In 1986 Carl Deckard, a master's student at the University of Texas at Austin, sponsored by the National Science Foundation (NSF), described an apparatus similar to Housholder's idea. Instead of making a part by cutting away at a larger chunk of material, it was proposed to build an object up layer by layer (Figure 2.1.2). Deckard describes in the patent "A method and apparatus for selectively sintering a layer of powder to produce a part comprising a plurality of sintered layers. The apparatus includes a computer controlling a laser to direct the laser energy onto the powder to produce a sintered mass. The computer either determines or is programmed with the boundaries of the desired cross-sectional regions of the part. For each cross-section, the aim of the laser beam is scanned over a layer of powder and the beam is switched on to sinter only the powder within the boundaries of the cross-section. Powder is applied and successive layers sintered until a completed part is formed. The powder can comprise of plastic, metal, ceramic, or polymer substance. In the preferred embodiment, the aim of the laser is directed in a continuous raster scan and the laser turned on when the beam is aimed with the boundaries of the particular cross-section being formed" (Deckard 1989). Experimentation was done using a 100 W Nd:YAG laser in continuous mode with ABS polymer powder. The invention was not restricted to plastics materials only. He suggested that the process could also allow the use of metallic, ceramic or

polymer powders. Deckard's process manufactured three-dimensional objects by using laser beam to fuse powder into solid prototypes, one layer at a time. Initially he called his method Part Generation by Layer wise Selective Sintering (PGLSS), later changing the name to Selective Laser Sintering (SLS).

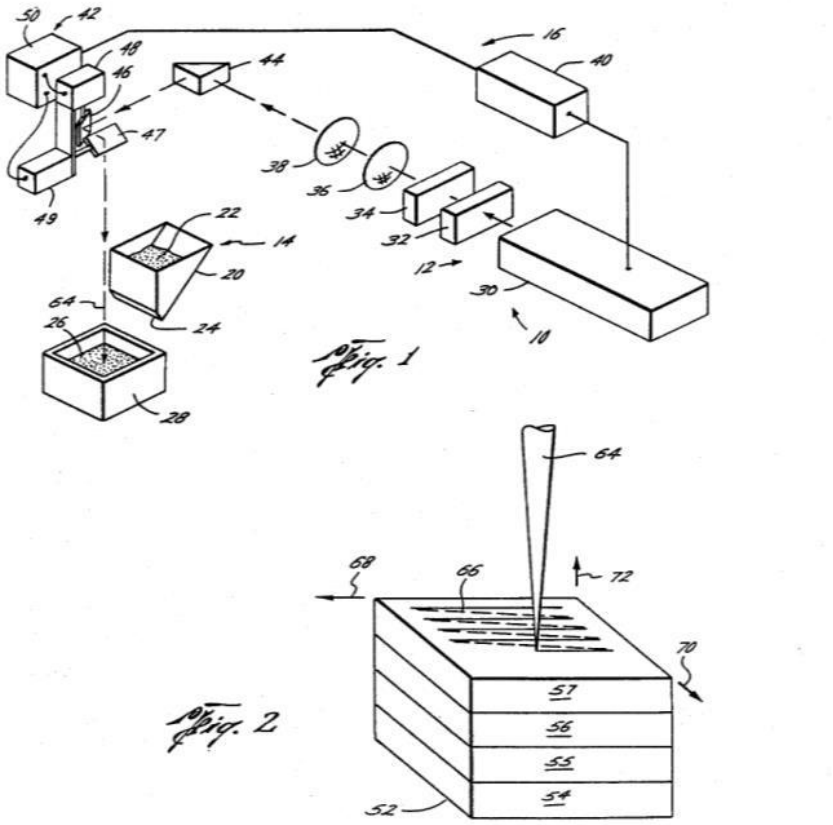

Figure 2.1.2. Deckard's invention (1986)

The DMLS process was first patented in 1996 by inventors Dr Wilhelm Meiners, Dr Konrad Wissenbach and Dr Andres Gasser at the Fraunhofer Institute for Laser Technology (ILT) in Germany. In the patent Meiners *et al.* (1996) described the DMLS process as a method for manufacturing a moulded body in accordance with three-dimensional (3D) Computer Aided Design (CAD) data. Metallic material is deposited layer by layer in powder form. Several layers of powder are successively deposited one on top of the other. Each layer of powder is heated to a specified temperature by means of a focused laser beam to a given area, before the next layer of powder is deposited. The produced part is immediately ready to be used as a prototype or final product (Figure 2.1.3).

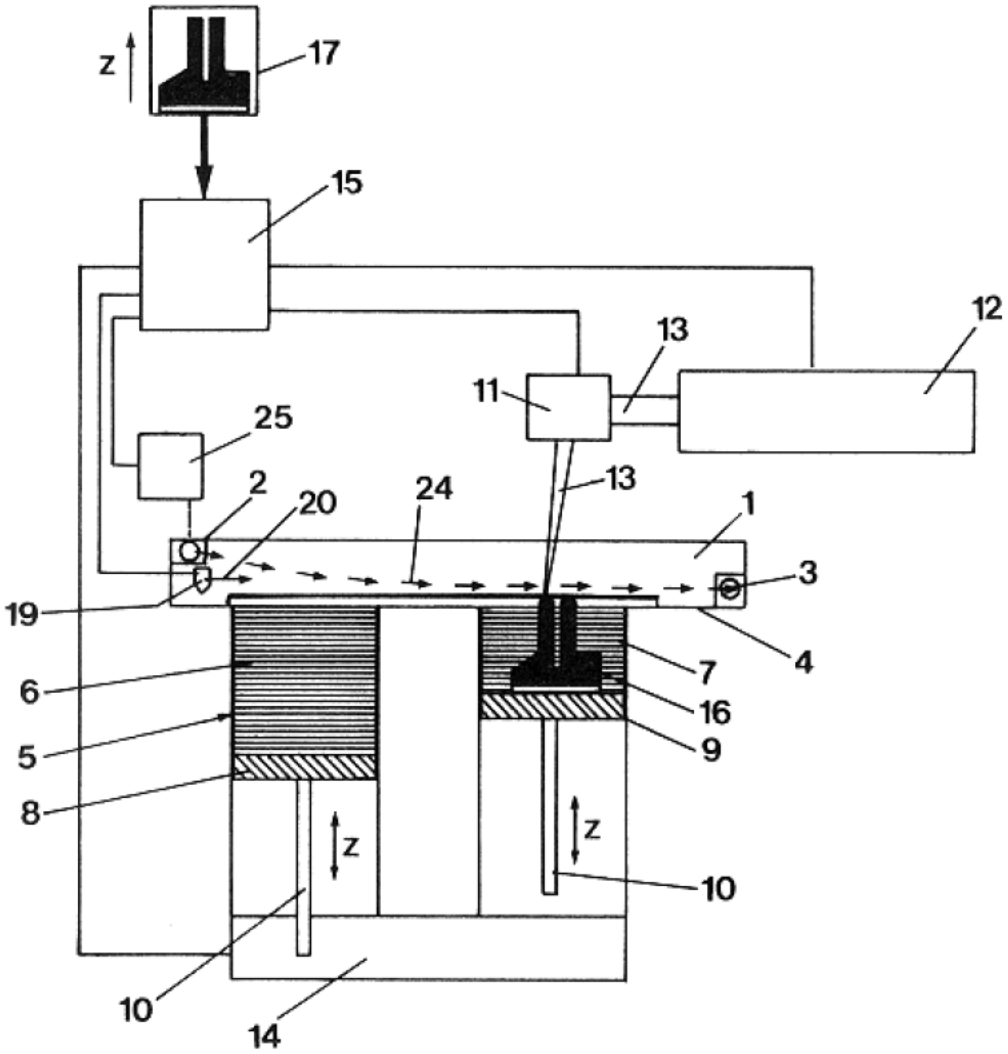

Figure 2.1.3. Meiners *et al.* (1996) patent schematic

In 2013 the American Society for Testing and Materials (ASTM) defined Selective Laser Melting (SLM) or Direct Metal Laser Sintering (DMLS) as "a powder bed fusion process used to make metal parts directly from metal powders. Powder bed fusion is described as an additive manufacturing process in which thermal energy selectively fuses regions of a powder bed" (ASTM International, 2013)

The DMLS process starts with a CAD design on programs such as SolidWorks, Pro-engineer or Inventor (Figure 2.1.4). The CAD file is saved as .STL format. An STL file is a triangular representation of 3D surface geometry. The file is sliced into 2D sections where the slice thickness is the same as the powder delivery thickness. The layer thickness plays a major role on

the quality and definition of the produced object. In most commercial applications a layer of powder is deposited and a laser melts the cross section as pre-determined by the slice data. By processing layer by layer a 3D object is formed. Parameters such as layer thickness and powder material grain size and shapes are associated with the deposition of the powder layer. Laser power and spot size, scanning speed and deposition time determine the processes productivity.

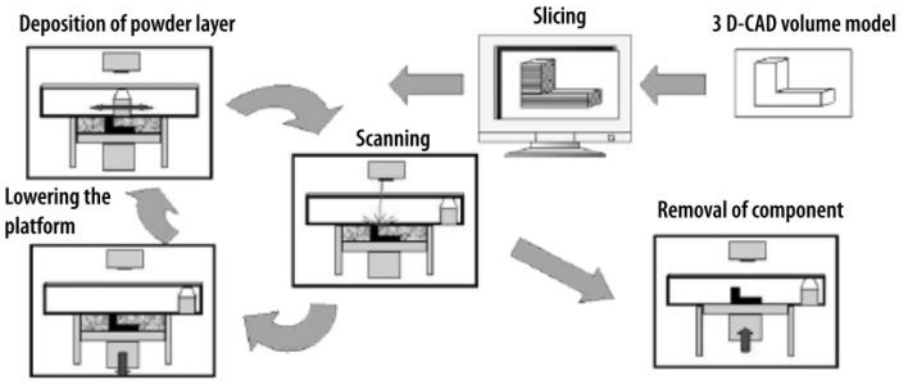

Figure 2.1.4. DMLS process (Bremen & Meiners, 2012)

2.1.2. State-of-the-art

The new and innovative manufacturing technique of DMLS has seen massive sales growth in the past ten years (Figure 2.1.5). According to the 2014 Wohler's Report there was a 78.5% growth in the market alone between 2012 and 2013.

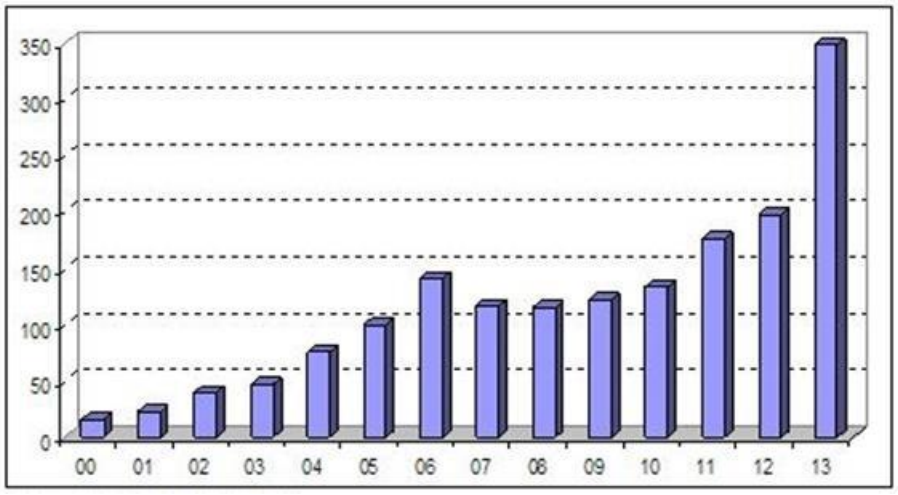

Figure 2.1.5. Growth in DMLS (Wohler's Report, 2014)

Electro Optical Systems (EOS), SLM solutions, 3D systems, Renishaw and Concept Laser produce commercial DMLS machines.

EOS M280 has a 200 W or optional 400 W Yb-fiber laser and a build platform volume of 250x250x325 mm. EOS also produces the M290 that comes standard with a 400 W fibre laser. Their large industrial machine, the M400 has a 400x400x400 mm build platform volume. Productivity is increased with a 1000 W fibre laser and a dual recoating system. Dual recoating refers to powder deposition from both sides of the powder delivery platform reducing non-productive machine time (EOS GmbH, 2013).

Phenix systems, which was taken over by 3D Systems in middle 2013 have three DMLS machines in thier range namely PXS, PXM and the PXL. The PXM machine has 300 W fiber laser with 1070 nm wavelength with a build platform volume of 140x140x100mm. The PXM is the upgrade to the PM100 that had a 50 W fiber laser, 1075 nm wavelength and a maximum scanner speed of 3 m/s. The PXS has a 50 W laser and a 100x100x80 mm build volume. The PXS is suggested for dental applications while the larger PXL with a 500 W fiber laser is better suited for applications in the medical, tool making and prototyping areas (3D Systems, 2013).

The Renishaw AM250 has a 200 W fiber laser with an optional 400 W fiber laser and a build volume of 250x250x300 mm. The AM250 also features a vacuum chamber evacuation followed by high purity argon gas in order to create a high quality atmosphere, crucial when building in reactive materials such as titanium (Ti). The high quality atmosphere is ideal for the production of medical implants (Renishaw, 2012; Andreas & Schwarze, 2014).

SLM Solutions 500HL has a 500x280x320 mm build platform and utilizes double laser beam technology to melt the powder. In this high-performance system, four 400 W fiber laser or two 400 W and 1000 W lasers melt metallic powder via an optical 3D scanning unit (SLM Solutions GmbH, 2013). SLM solutions also supply smaller machines such as the SLM250HL and the SLM125HL. These machines only employ a singular laser system with lasers ranging between 100 W and 1000 W. Concept Laser's M2 cusing machine also employs a multi laser system that consists of two 200 W fiber lasers or an optional two 400 W lasers to decrease process time.

2.1.3. DMLS process

At the core of the DMLS process is a laser beam scanning over the surface of a thin powder layer. As the laser beam melts material along a row of powder particles it forms a molten pool. Each layer of the part is sequentially filled with elongated tracks of melted powder lines referred to as single tracks (Figure 2.1.6a). Single tracks or the continuous formation of the molten pool is the most basic building block in the DMLS process. The previously re-melted layer or the substrate forms the platform for the new layer of powder to be deposited and the process repeats. Layers are formed by applying multiple single tracks next to one another or also known as track-by-track formation of the molten pool boundaries (Figure 2.1.6c). Objects are formed by placing multiple single tracks layer by layer upon one another (Figure 2.1.6b). Thus the optimization of the molten pool and single track formation plays a major role in the quality and properties of the produced 3D object.

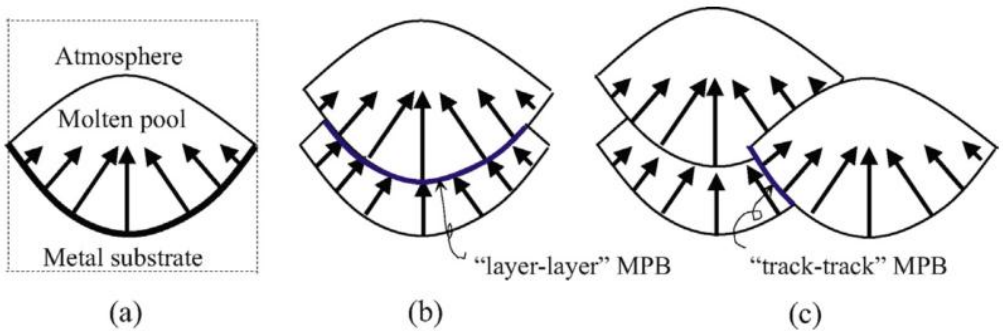

Figure 2.1.6. Schematic diagram molten pool configuration during the DMLS process: (a) single molten pool (b) layer–layer (c) track–track (Shifeng *et al.*, 2014)

Characteristics of the produced DMLS object such as porosity, microstructure and mechanical properties are influenced by the parameters of DMLS. Parameters of the DMLS process can be divided into three distinct sections namely machine-based, material-based and process input parameters (Figure 2.1.7).

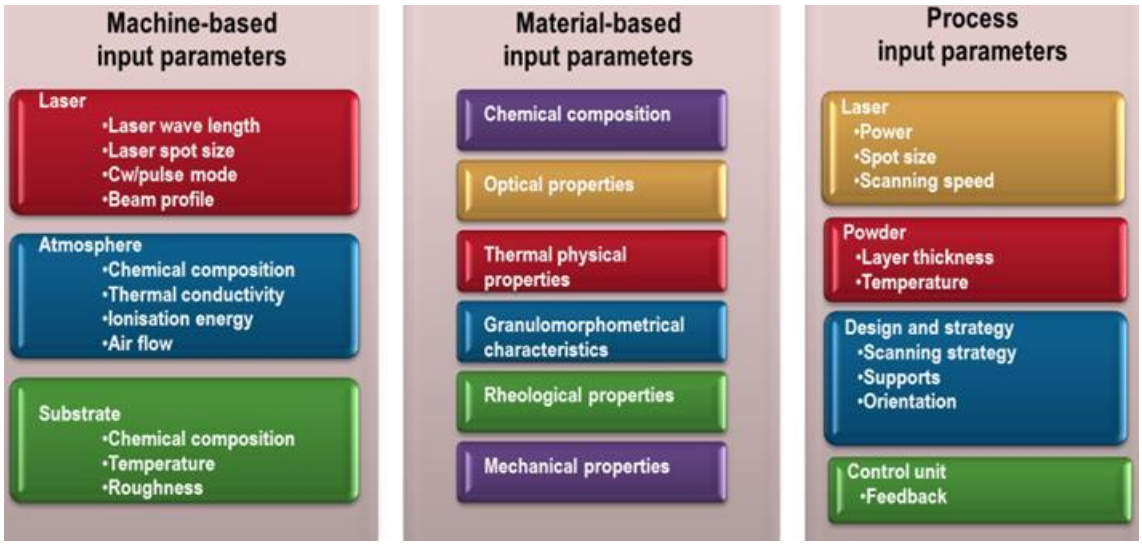

Figure 2.1.7. DMLS parameters (Yadroitsev, 2009)

A DMLS machine has three main areas of interest when considering machine based input parameters: the laser or heat source, the atmosphere in which the process takes place and the substrate or base on which the objects are manufactured. Absorption of the energy from the laser beam causes the powder particles to melt. These melting particles form the molten pool. The wavelength directly affects the percentage radiation absorbed and depends on the specific material (Figure 2.1.8). Laser spot size, mode and beam intensity profile define input energy density. The build atmosphere and the material composition of the substrate also influence the quality of parts produced by DMLS. Materials such as Ti6Al4V need to be produced in an argon atmosphere to eliminate the formation of oxides. The formation of oxides negatively affects the mechanical properties of the produced DMLS parts.

Growth in fields of AM powder technologies such as DMLS, electron beam melting and direct metal deposition have put emphases on metal powder production. Two main types of powder are used, master alloy and pre-alloy powders. Pre-alloy are formed by utilizing atomized material that is of the exact composition as the final part. Meanwhile master alloys are formed by utilizing alloy enriched atomized powders that are mixed and only forms the final composition after the laser melts the compound powder mixture during the DMLS process. Investigations showed that pre-alloyed powders are more preferable for AM (Davies & Dunstan, 2004).

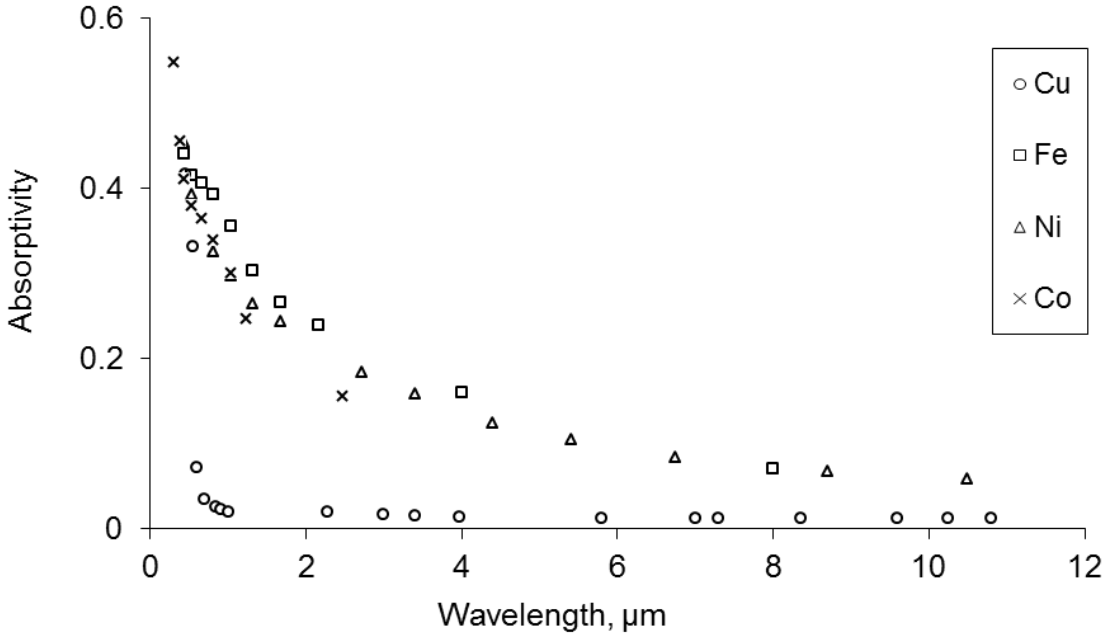

Figure 2.1.8. Absorptivity of different pure metals *versus* wavelengths (Yadroitsev, 2009)

There are three types of atomizing of the powder: water, gas and centrifugal atomizing. Gas atomizing is the more commonly used process for producing metal powders for DMLS. Molten metal is sprayed while being cooled using gas. The rapidly cooling fine spray of molten material solidifies to form the metallic powder (Figure 2.1.9). The rate of cooling and composition of the fluid used in the atomizing process influences the powder properties directly. By using water the material is cooled faster but greater oxidation occurs, while an increase of water pressure induces a decrease in particle size (Achelis & Uhlenwinkel, 2008; Dhokey *et al.*, 2014). Chemical composition and the method used in producing the powder have a major effect on the material properties (Table 2.1.1).

Powder properties directly influence the depositing of powder onto the substrate and formation of the molten pool. The distribution of powder is majorly effected by properties such as powder size and morphology of powder particles.

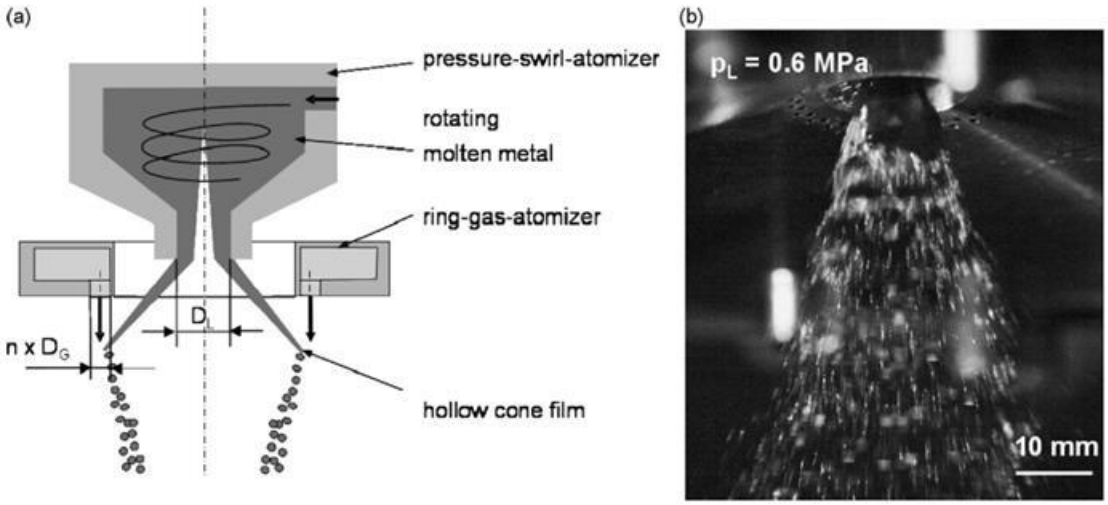

(a) (b)

Figure 2.1.9. (a) Scheme of the gas atomizer process. (b) Photograph of pressure-swirl atomization (Achelis & Uhlenwinkel, 2008)

Table 2.1.1. Material-based input parameters (Yadroitsev, 2009)

Optical properties	Reflection/absorption Optical penetration
Granulomorphometric characteristics of powder grains	Particle size Particle size distribution Particle shape Particle roughness
Thermal properties	Thermal conductivity Specific heat Latent heat Melting temperature Thermal expansion
Chemical properties	Reaction enthalpy Chemical solvency
Metallurgical properties	Oxidation potential Alloy composition Diffusion coefficients Liquid-solid range
Rheological properties	Viscosity Surface tension
Mechanical properties	Elastic modulus Yield point Tensile strength

Powder consists of statistical distribution of particles with different sizes also referred to as particle size distribution. Particle size distribution defines a powder layer thickness and homogeneity of delivered powder layer which, in turn, influences porosity and mechanical properties of DMLS parts (Yadroitsev, 2009; Liu *et al.*, 2011; Spierings *et al.*, 2011).

Particle shape or powder morphology refers to the shape of the individual powder particles. The shape of powder particles determines how the particles position themselves or pack together. A powder with spherical particles has a higher random packing density over more irregular shaped particles. In the DMLS process particle shape is an important factor in creating a optimal layer thickness for fully dense objects. Spherical shaped particles are preferred for the DMLS process as they flow easily to form a homogenous powder layer and have higher pack density, which is beneficial for molten pool formation. Particle shape has an influence on powder layer formation and the absorptivity of powder bed. The larger the absorptivity the more energy from the laser beam will be absorbed by powder bed. Particle shape and particle size distribution are parameters effecting powder flowability. Powder flowability is the ability of powder to flow in a desired manner in a specific piece of equipment. It is important to have good powder flowability when depositing a thin powder layer. More spherical shaped powder particles flow better than irregularly shaped particles that have sharp rugged edges. Larger sized powders particles with a narrow particle size distributions flow better than powders with wide particle size distributions. Cohesive forces between the fine powder particles lead to agglomeration and the formation of a non-homogenous powder layer. An optimal powder layer thickness has to be selected for employed powders (Yadroitsev *et al.*, 2012).

The density of powder is measured in terms of the apparent/bulk density and tap density. The apparent density and tap density are indicators of powder flow properties. Apparent density is the actual volume occupied by a mass of loose powder. Apparent density is influenced by particle size shape and roughness. Apparent density decreases with a decrease in particle size and when particles are more irregularly shaped or have an increase in surface roughness. Tap density is the density (mass per unit volume) of a specific powder after exposure to vibration under specified conditions. Vibrating a loose powder lowers the friction between the powder particles resulting in more effective powder packing reducing the space between particles. Therefor tap density will

be greater than the apparent density. Particle shape, particle porosity, and particle size distribution are powder properties that most affect tap density.

The powders most suitable for DMLS are powders produced by inert gas atomization because of their spherical shape producing better flowability and non-cohesivity. Pre-alloyed powders perform best for the DMLS process because of their rapid solidification and homogeneous chemical composition. When considering the particle size, the maximum diameter of the particles should be less than the laser spot size.

Machine-based input parameters define the scope of the process parameters for a specific material. There are three main areas of focus concerning the process parameter of the DMLS process namely the laser, powder and manufacturing strategy parameters (Figure 2.1.7). These three parametric areas have a large influence on the single track geometrical characteristics which contributes to the final quality and properties of the DMLS part (Figure 2.1.10).

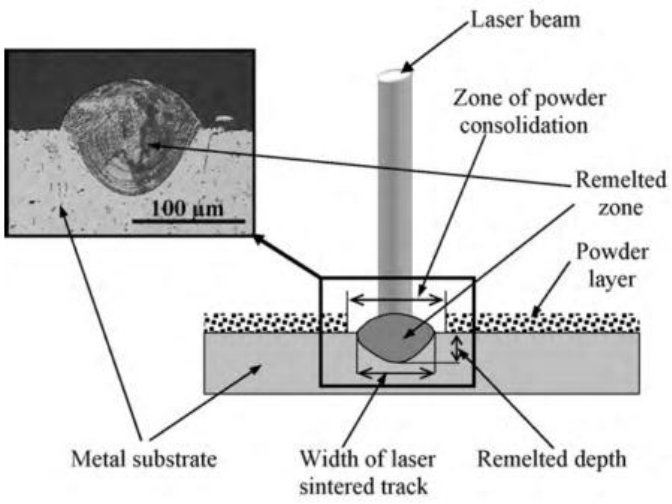

Figure 2.1.10. Geometrical characteristics of the single DMLS track (Yadroitsev, 2009)

Yadroitsev (2009) conducted numerous investigations on the effect of process parameters on single track formation utilizing a Phenix Systems PM 100 machine (max 50W YLR-50 cw Ytterbium fiber laser, 1075 nm wavelength, 3 m/s max scanning speed and 70 µm laser spot size). Experiments showed a definite correlation between process parameters and the quality of single track formation. By comparing different laser powers, scanning speeds and layer thickness optimal process parameters were investigated for 316L stainless steel. Powder was delivered in

such a way to vary from 0-400 µm on the substrate while the laser power remained constant at 50 W. The scanning speed was varied between 0.04-0.28 m/s to form the diagram seen in the Figure 2.1.11. From the diagram it is clear that definite stable (continuous single tracks) and unstable zones (not continuous single tracks) are formed. The study showed that irregularity, distortion and formation of drops indicated unstable single track formation due to energy input and layer thickness. It is also noted that the range of layer thickness and scanning speed for producing continuous single tracks increases with the increase in laser power. Although for each laser power there is a maximum and minimum limits of the powder layer thickness. Concluding that low scanning speed tends to form distortions and irregularities while excessively high scanning speed tends to form drops (balling effect). The stability of the single track formation is not only depend on the laser power, scanning speed and layer thickness but also the substrate material, physical properties and morphology of the material (Yadroitsev *et al.*, 2009, 2010).

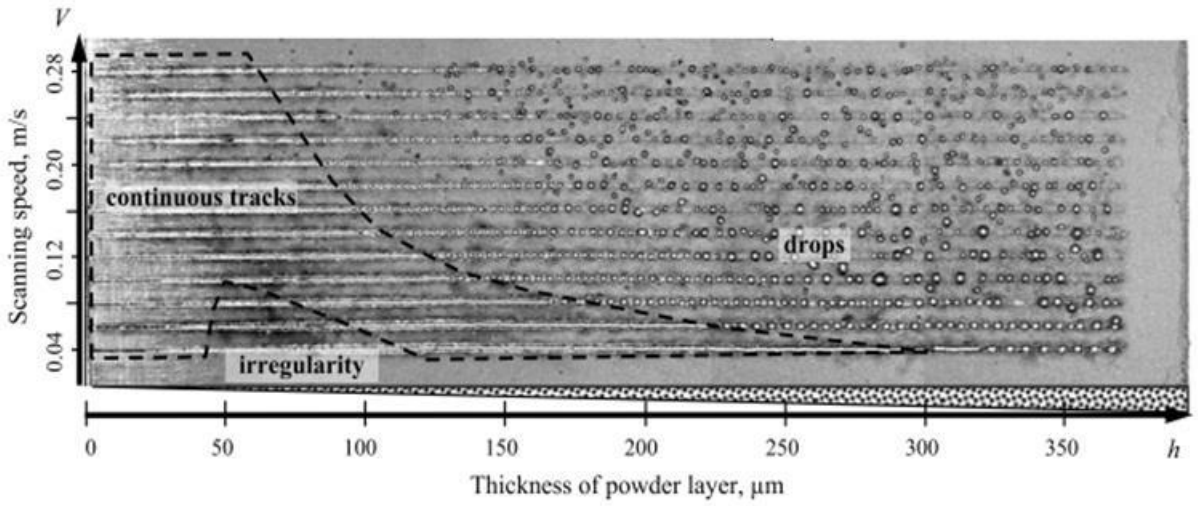

Figure 2.1.11. Influence of powder layer thickness and scanning speed on stability of DMLS single tracks (Yadroitsev& Smurov, 2010)

Yadroitsev *et al.* (2015) developed a multi iteration algorithm to assist in selecting optimal process parameters to produce a high-quality DMLS product. Laser power, spot size, scanning speed as well as material temperature-dependent properties are utilized to select initial parameters at different powder layer thickness.

Part orientation on the build platform has an effect on the mechanical properties of the produce DMLS part. Shifeng *et al.* (2014) investigated model orientation and slip theory between track-track and layer-layer molten pool boundaries to estimate model failure. Tensile testing was used to compare the mechanical properties at difference orientations. Tensile test samples were manufactured using vertical and horizontal orientation as well as different angles between the tensile loading direction and the laser scanning direction (Figure 2.1.12) thus changing the model orientation. A HRPM-II DMLS machine with a 200 W continuous wave fiber laser, 1068–1095 nm wavelength and 20 µm layer thickness was utilized to manufacture test samples. Samples were grown from 316L stainless steel powder. Results of the tensile test indicated that the average tensile strength of the vertical specimens (669 MPa) was higher than that of the horizontal specimens (624 MPa). The tensile strength of the samples manufactured from the DMLS process had higher tensile strength than that of conventional forging (450 MPa) of the same material. On other hand, the average percentage elongation of the vertical specimens (49.6%) was higher than that of the horizontal specimens (15.6%). A clear trade-off of tensile strength (horizontal) and ductility (vertical) is noticed. The reason for the difference in tensile properties between the horizontal and vertical specimens can be explained from the molten pool boundary characteristics on the stress cross sections of the molten pool at different tensile directions (Figure 2.1.13). Failure is due to slipping/separating of the single tracks either in the track-track or layer-layer directions because of the stress applied to the molten pool cross section.

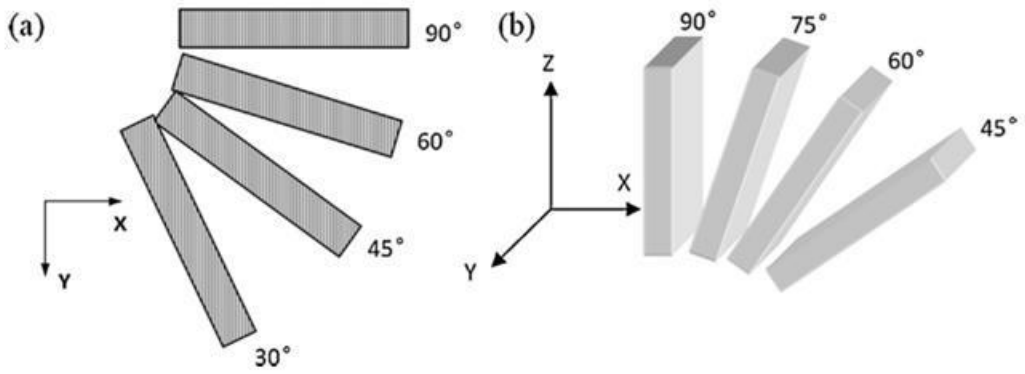

Figure 2.1.12. Tensile specimen orientation on build platform (a) horizontal processing; (b) vertical processing (Shifeng *et al.*, 2014).

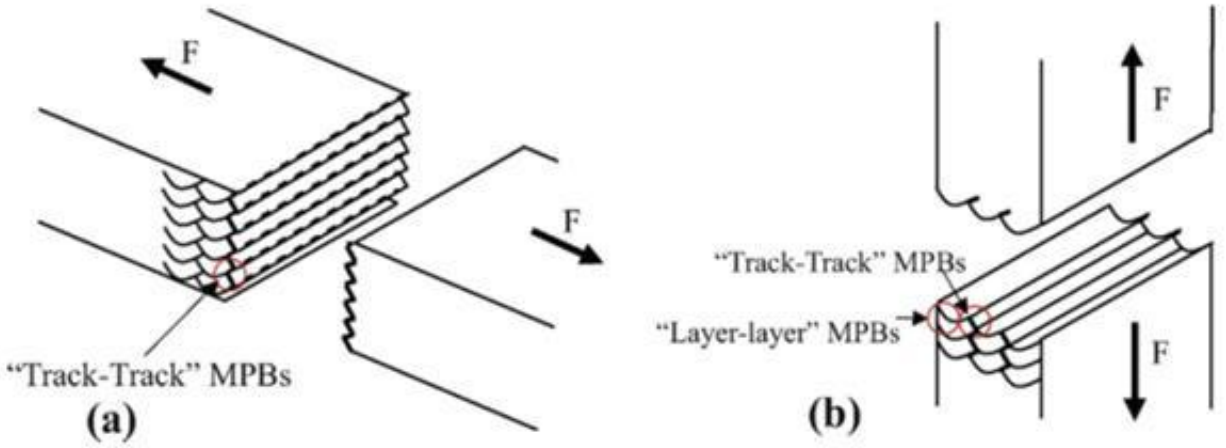

Figure 2.1.13. Failure by (a) track-track and (b) layer-layer molten pool boundaries (Shifeng *et al.*, 2014)

Geometrical features such as sharp corners, down-facing surfaces and overhangs often have bad surface finishes due to unstable molten pool formation. The main reason for these inadequate results is that the laser parameters are set to melt powder on top of a previously melted layer of powder. The heat energy is conducted to the previous melted layers and is also used to form the molten pool. If powder is melted on a previously non sintered powder layer, the thermal conductivity is decreased; the molten pool then becomes unstable unless the parameters are changed to suit the new conditions. By adding a feedback system to the DMLS process the molten pool formation can be monitored. By changing the parameters of the molten pool formation according to the feedback data the molten pool size remains stable and operates at optimal processing parameters (laser power, scanning speed etc.). Kruth *et al.* (2007) modified a DMLS-machine developed at K.U. Leuven-PMA with a high-speed CMOS camera and a photodiode in an attempt to monitor constant molten pool formation. After conducting case studies with titanium and stainless steel powder of overhanging structures it was concluded, that there was a significant improvement in quality when using a feedback system (Figure 2.1.14).

Reinarz *et al.* (2010) optimized the formation of difficult geometry features by changing the CAD data to compensate for the change in conductive heat transfer (Figure 2.1.15). Though this process is time consuming and in most cases unpredictable, case studies showed improvements in formation of the geometrical features.

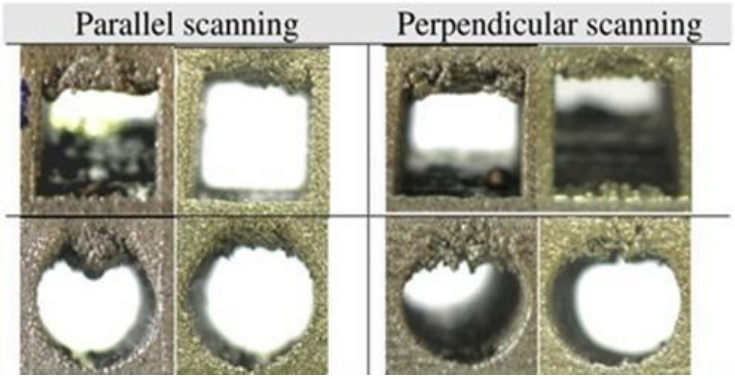

Figure 2.1.14. Comparison of overhanging structure without and with feedback (Kruth *et al.*, 2007)

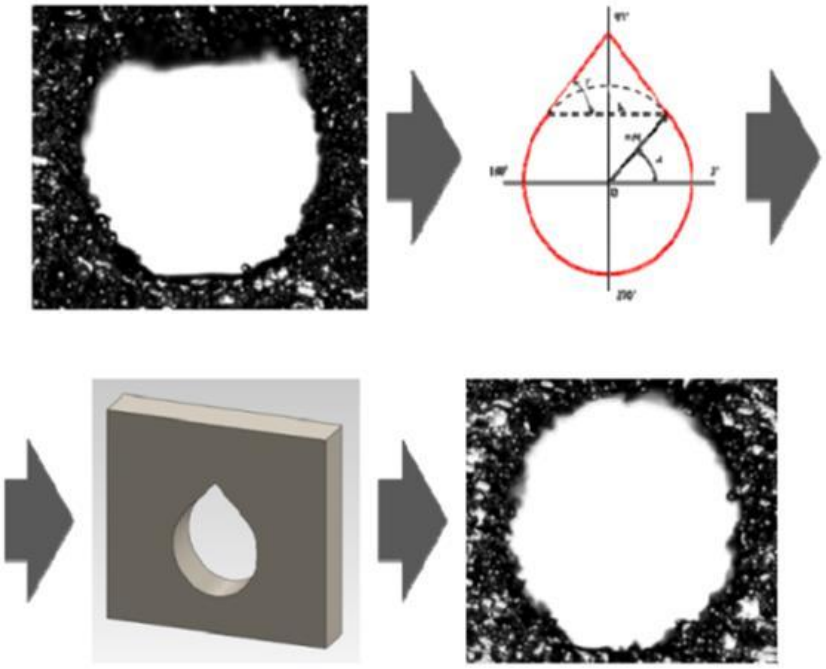

Figure 2.1.15. Geometry optimization by CAD (Reinarz *et al.*, 2010)

Manufacturing strategies will also play a major role when processing multi materials with DMLS. The laser will react differently to varies materials and at the interface where materials interlock. Parameters such laser power and scanning speeds will need to be changed as the laser moves from one material to the next. Part orientation and design intent will become increasingly important to manufacture models with suitable density, mechanical properties and surface quality.

2.2. Multi material structures by DMLS

Growth in the DMLS field has produced the need for objects containing multiple materials for applications in the medical, tool making, aerospace and other hi-tech industries. Multi material layered manufacturing refers to a process of fabricating an object consisting of more than one material in a single manufacturing process. By depositing multiple materials, regions with different mechanical properties, thermal conductivity zones or corrosion-resistant coatings can be achieved in a single manufacturing cycle utilizing the DMLS process.

With the DMLS process metals that were previously unable to bond now can be (Figure 2.2.1). Physical bonds are formed from creating an interlocking interface of rapid solidification of different molten materials (Figure 2.2.2).

	W	Ta	Mo	Cr	Co	Ti	Be	Fe	Pt	Ni	Pd	Cu	Au	Ag	Mg	Al	Zn	Cd	Pb	Sn
W																				
Ta																				
Mo																				
Cr		P																		
Co	F	P	F	G																
Ti	F			G	F															
Be	P	P	P	P	F	P														
Fe	F	F	G			F	F													
Pt	G	F	G	G		F	P	G												
Ni	F	G	F	G		F	F	G												
Pd	F	G	G	G		F	F	G												
Cu	P	P	P	P	F	F	F	F												
Au	–	–	P	F	P	F	F	F												
Ag	P	P	P	P	P	F	P	P	F	P		F								
Mg	P	–	P	P	P	P	P	P	P	P	P	F	F	F						
Al	P	P	P	P	F	F	P	F	P	F	P	F	F	F	F					
Zn	P	–	P	P	F	P	P	F	P	F	F	G	F	G	P	F				
Cd	–	–	–	P	P	P	–	P	F	F	F	P	F	G		P	P			
Pb	P	–	P	P	P	P	–	P	P	P	P	P	P	P	P	P	P	P		
Sn	P	P	P	P	P	P	P	P	F	P	F	P	F	F	P	P	P	P	F	

Excellent
G Good
F Fair
P Poor

Figure 2.2.1. Laser weldability of dissimilar metal combinations (Steen, 2003)

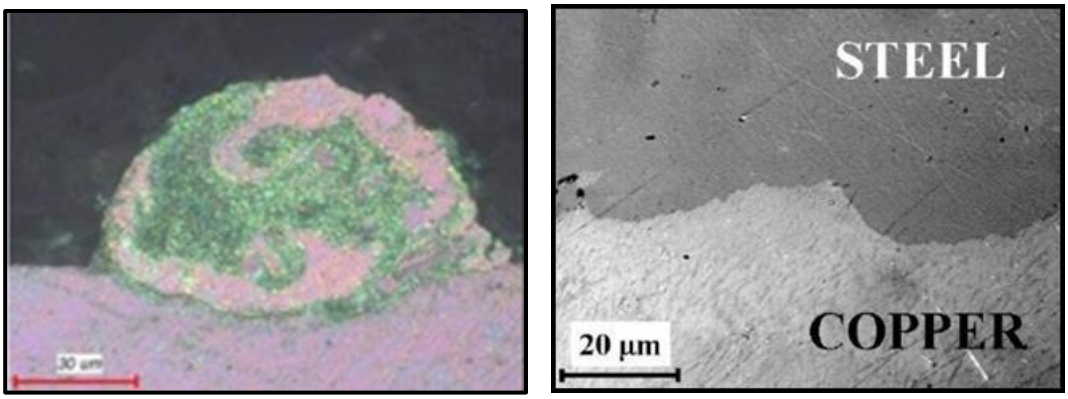

Single track Interface steel-Cu

Figure 2.2.2. DMLS track of interlocking stainless steel and Cu and interface of cross-section of the 3D Cu-steel DMLS specimen (Yadroitsev, 2009)

2.2.1. Multi material powder deposition

Powder deposition plays a major role in the DMLS process. The DMLS process requires a thin powder layer to be deposited on the substrate before the powder is melted. The layer thickness as well as the powder bed surface quality affects the density of the produced part and the surface roughness directly. During DMLS, powder is delivered in varies way to create a thin (20-200 µm) layer of powder material. With the current DMLS process, multi material objects are possible but only with material differences between layers (Z-axis). The current DMLS powder delivery system limits the process to a single material per layer. New approaches are needed to produce multi material parts not only in the building direction (Z-axis), but also allows material differences on a single layer (X-Y axis) (Figure 2.2.3). The “ideal” multi material process will dispense multiple material powders on a single layer and between layers.

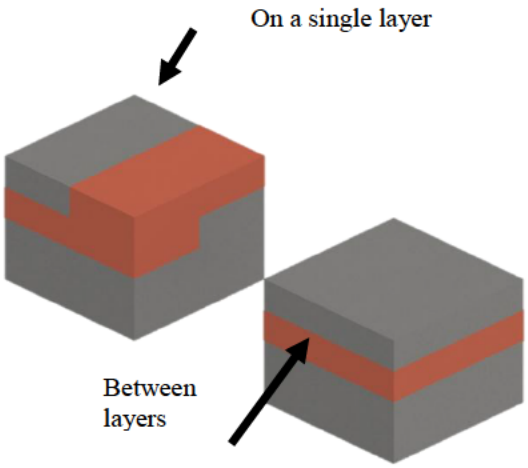

Figure 2.2.3. Multi material parts (Ott & Zaeh, 2010)

Conventional DMLS powder delivering systems

Commercially there are three main powder recoating mechanism to form a powder layer on the build platform namely roller, stiff blade and hopper.

Phenix systems utilized a roller to deposit the powder from the powder delivery platform to the build platform (Figure 2.2.4) with powder layer thicknesses of 10-50 µm (3DSystems, 2013).

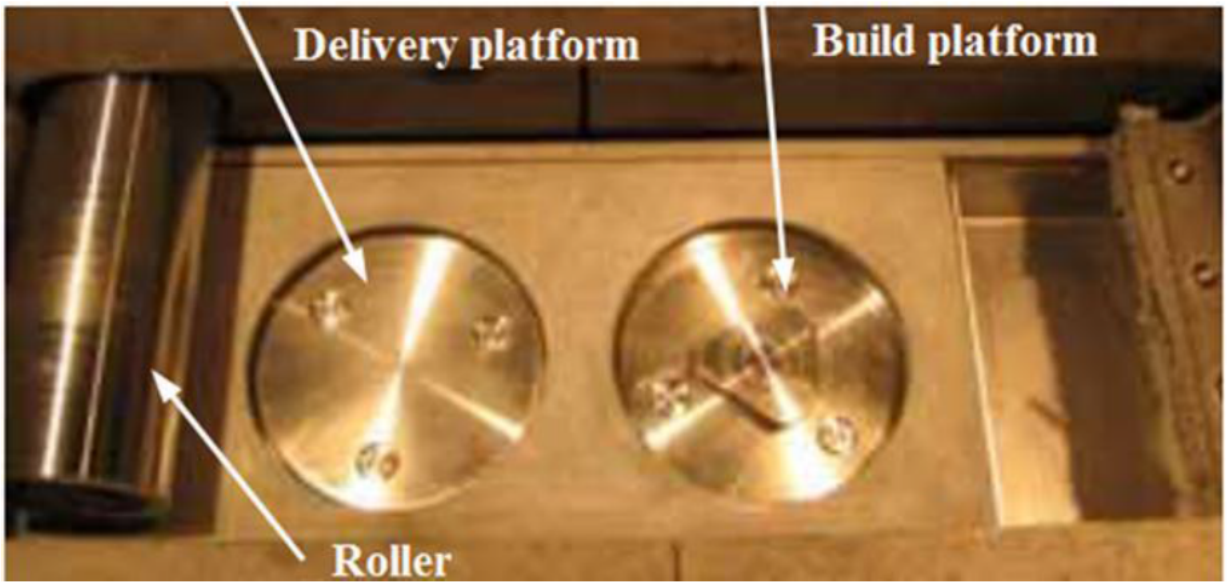

Figure 2.2.4. Phenix powder recoating system

EOS M280 DMLS machine deposits the powder with a recoating blade (Figure 2.2.5). Powder is shifted from the dispenser platform to the build platform by means of stiff tool steel blade or soft carbon fibre brush. The blade creates an even layer of powder that the laser selectively melts. The build platform is lowered by a layer thickness and the dispensing platform is raised by one layers volume.

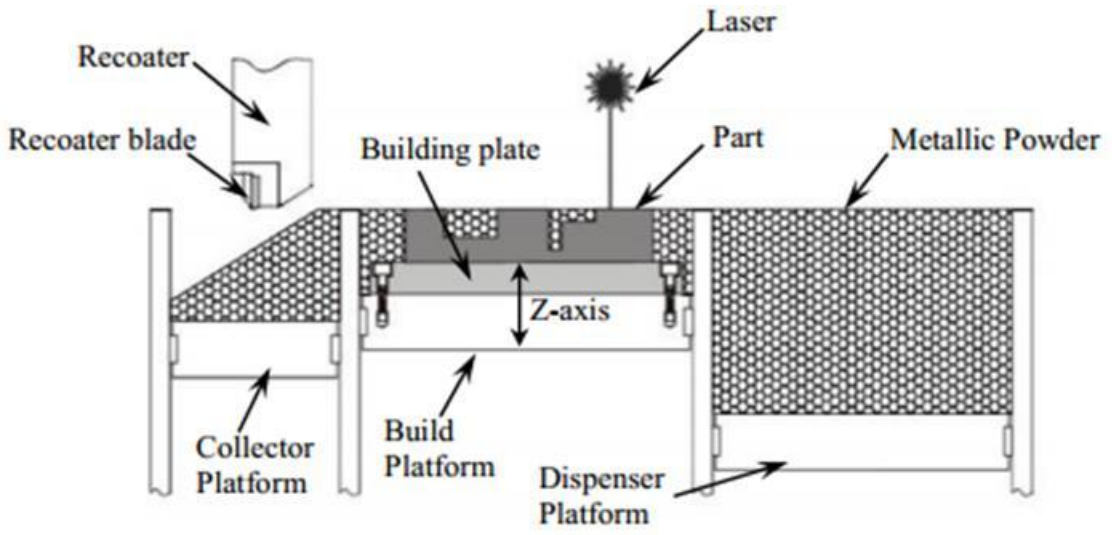

Figure 2.2.5. Blade recoating system of EOS (Gong *et al.*, 2013)

The Renishaw AM250 and SLM Solutions use a hopper and blade to deposit the powder onto the powder bed with layer thicknesses of 20-100 µm (Figure 2.2.6). The hopper and blade method eliminates the need for a dispenser platform. According to the Renishaw website "The AM250 features an external powder hopper with valve interlocks to allow additional material to be added whilst the process is running. It is possible to remove the hopper for cleaning or to exchange with a secondary hopper for materials change, using the universal lift. The powder overflow containers are outside the chamber and feature isolation valves so that unused materials can be sieved and reintroduced to the process via the hopper while the system is running". This also allows the hopper to be removed while the process is running to allow a second material to be introduced on the build platform. The difference in material will be between layers and not on the same layer.

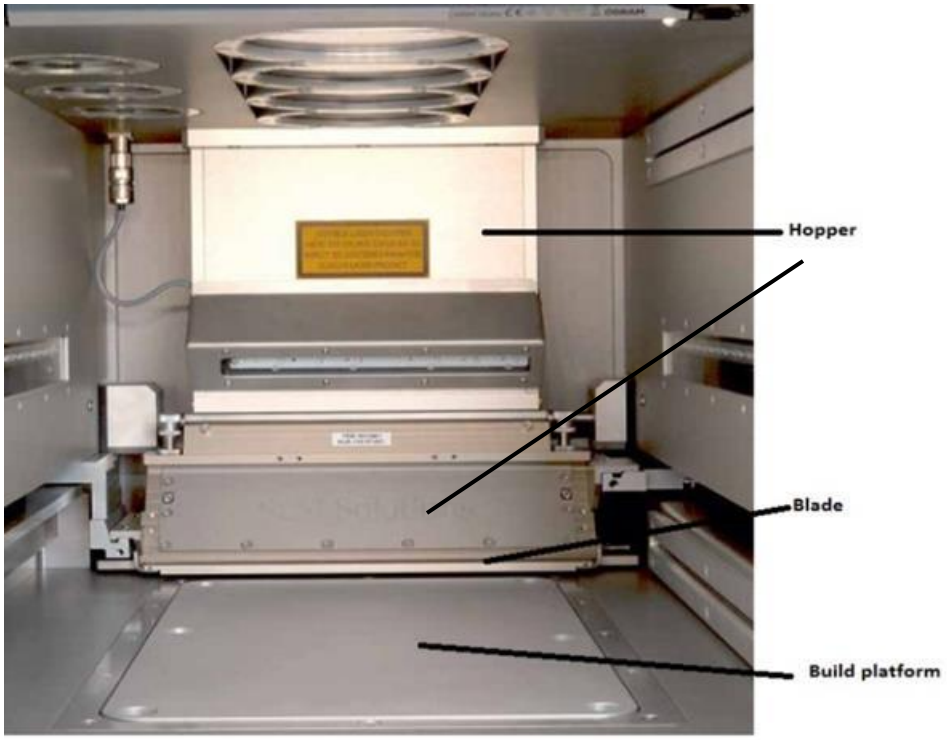

Figure 2.2.6. SLM Solutions hopper recoating system

In essence all three recoating systems are similar, each pushes an even powder layer over the build platform. The disadvantage of the current DMLS recoating systems is that only one powder can be dispensed per layer due to the pushing nature of the mechanisms.

Systems for multi material structures in the building direction

With modification current conventional DMLS delivering system have the ability to produce multi material models but with material difference between layers. Yadroitsev *et al.* (2007, 2009) utilized a PM-100 machine with a two-step manufacturing process to demonstrate the potential of producing multi material cooling systems using the DMLS process. "Sandwich" samples containing stainless steel 316L, Cu and Inconel 625 were successfully manufactured and validated the possibility of multi material parts (Figure 2.2.7). Proving that with the DMLS process bonds between different materials could be formed that would usually not occur.

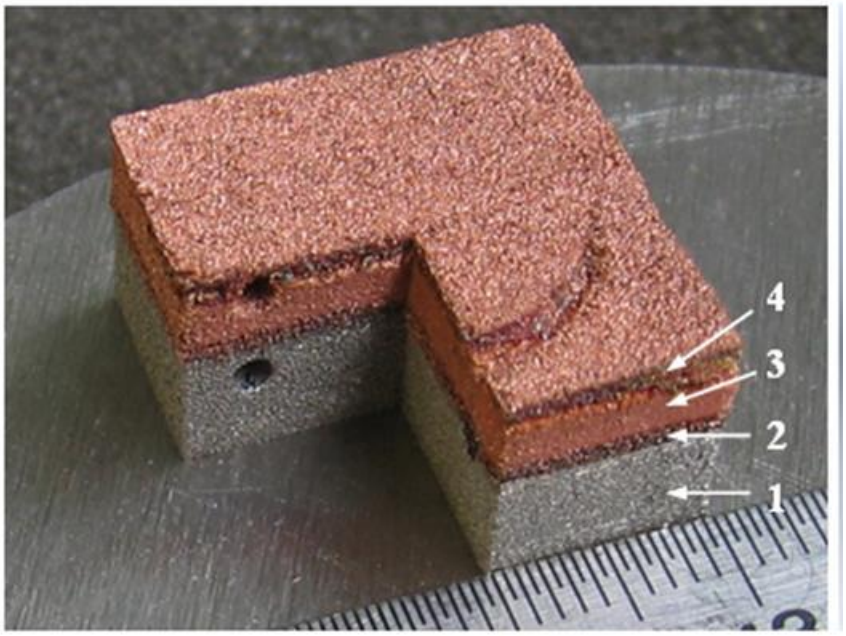

Figure 2.2.7. Sandwich" sample with cooling channel: 1– SS grade 316 L, 2 – 50% Cu + 50% In625; 3 – Cu; 4 – 50% Cu + 50% In625 (Yadroitsev *et al.*, 2009)

Liu *et al.* (2014) conducted further experiments with multi material DMLS samples containing 316L stainless steel and Cu alloy. Validating the possibility of multi material parts while also investigating the bonds at the interface of the two materials (Figure 2.2.8). Utilizing a SLM250HL machine with a modified recoater, two different materials were dispensed independently on the substrate. This recoater allows different powders to be dispensed between layers. Tensile tests indicated that the stainless steel/Cu specimens showed lower tensile stress than that of the stainless steel specimens but higher than that of Cu specimens. Thus indicating that good metallurgical bonds were formed between the two materials.

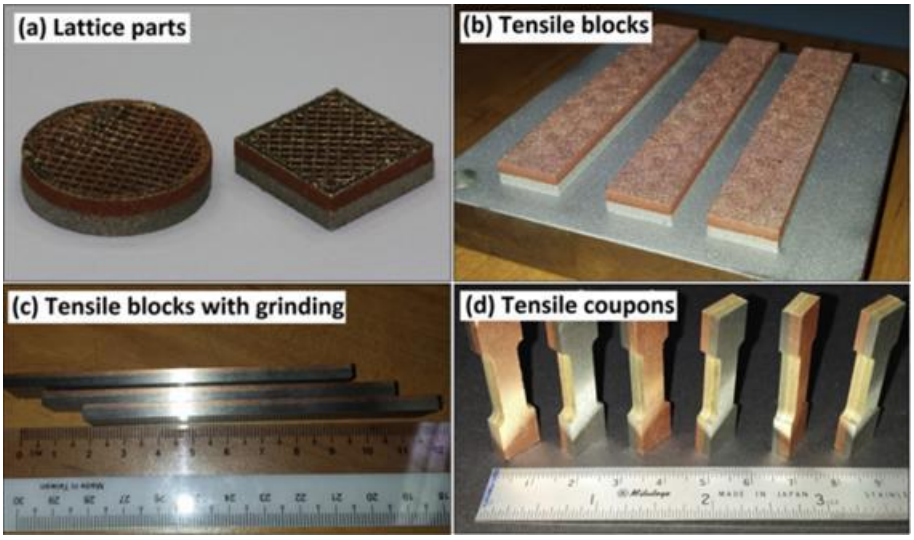

Figure 2.2.8. (a) Lattice steel/Cu DMLS parts (b) steel/Cu tensile blocks (c) side profile of tensile blocks showing no delamination (d) tensile coupons produced from the tensile blocks (Liu *et al.*, 2014)

Systems for functionally graded materials

Functionally Graded Material (FGM) refers to a multi material structure where two or more materials have continuously varying volume fractions in a specific direction. Varied material gradients are produced to suit a specific application and achieve higher levels of performance than parts produced from a single material. For example, protective coatings and interfacial zones can be produced to reduce mechanical and thermally induced stresses caused by inadequate material properties. Functionally graded materials are ideal candidates for applications that experience severe thermal, mechanical and biological gradients. Due to the layer by layer nature of DMLS, the composition of the material can be controlled within each layer and precise regulation variation of the different materials can be deposited. Gradually changing the composition of material from a metal to ceramic or from metal to metal to create varied thermal and mechanical regions (Aboudi *et al.*, 1999; Mahamood *et al.*, 2012).

Mumtaz *et al.* (2007) produced functionally graded Waspaloy and Zirconia samples (Figure 2.2.9). Waspaloy is a high temperature super nickel alloy used in the aerospace industry. Zirconia is a ceramic that is typically used to create thermal barrier coatings. Powder layers were deposited by means of a hopper that moved over the powder bed. This allowed for a variation in material composition in between layers (Z-axis). The powder was selectively melted using a

550 W Nd:YAG pulsed laser. Samples of increasing compositions of 1-10% Zirconia functionally graded with Waspaloy were successfully manufactured. The Zirconia within the layers showed to be embedded amongst the solidified Waspaloy. Good physical bonding occurred, while achieving part density of 99.66%.

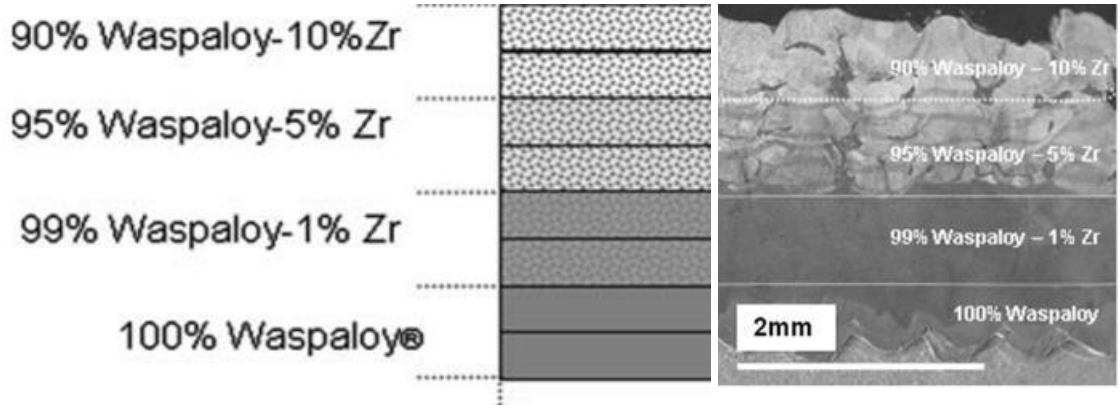

Figure 2.2.9. Layers of functionally graded composition in the z-axis (Mumtaz *et al.*, 2007)

Beal *et al.* (2004) manufactured functionally graded material from H13 tool steel and Cu powder. The experiment was conducted to prove the viability of functionally graded injection moulding tools. Variations of the powder mixture were deposited on a single layer (x-axis). The pre-mixture powders were placed in the compartments of the hopper according to the desirable composition design. The hopper moved over a platform spreading the powder mixtures into interlocking stripes (Figure 2.2.10). This resulted in a material gradient on a single layer. A high power Nd:YAG laser in a argon atmosphere was used to selectively melt the powder. An average powder layer thickness of 300 µm was used. Samples of H13 and Cu showed good bonds between the two materials. However, a cross-sectional image showed the formation of cracks in the H13 and Cu samples. Optimized laser processing parameters are needed to moderate the cooling rate of the material to reduce or eliminate the crack formation in the samples.

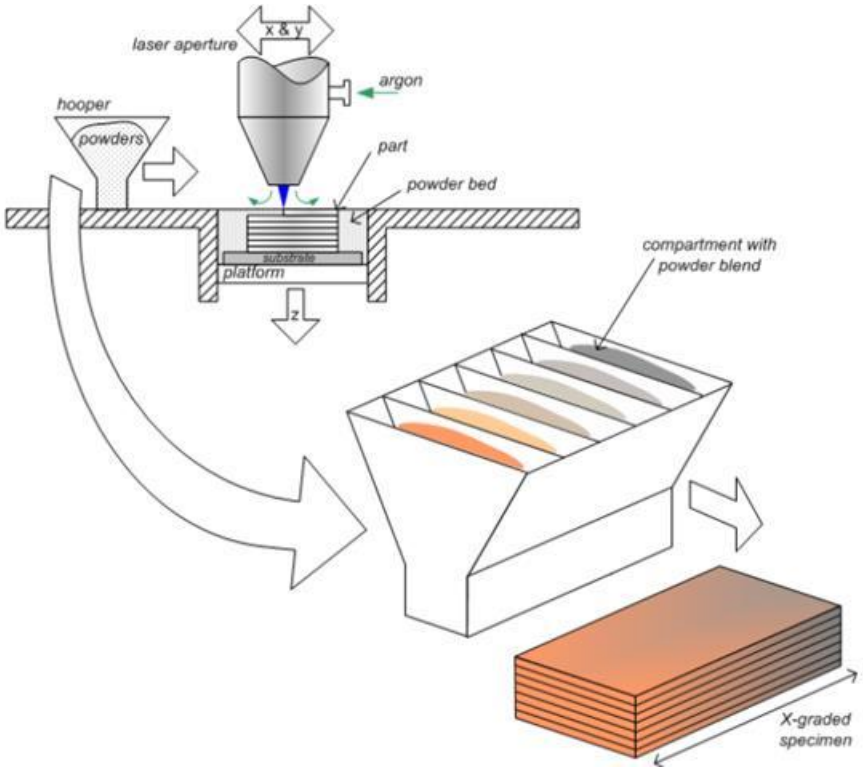

Figure 2.2.10. A schematic diagram of x-axis recoater (Beal *et al.*, 2004)

Multiple powder feeders for a single layer

Lappo *et al.* (2003) developed a system where a complete layer of the first material is dispensed with a roller. Selective removal of areas where the second material should be applied is done with electrostatic or vacuum methods. A nozzle is used to deposit the second material into the removed areas. A 2.5 mm diameter air pressurize (0.1 psi) nozzle was utilized to induce flow of the fine powder (Figure 2.2.11).

Meiners *et al.* (1996) describe a patented process for multi material model production where powder is deposited onto the build platform and selectively removed so to introduce a second material (Figure 2.2.12). A layer of the first powder is deposited on to the substrate. The areas of the first material are selectively melted and the un-melted material is removed (suction or electrostatic attraction). A nozzle system then deposits the second powder on to the desired areas and a laser beam melts the specific regions.

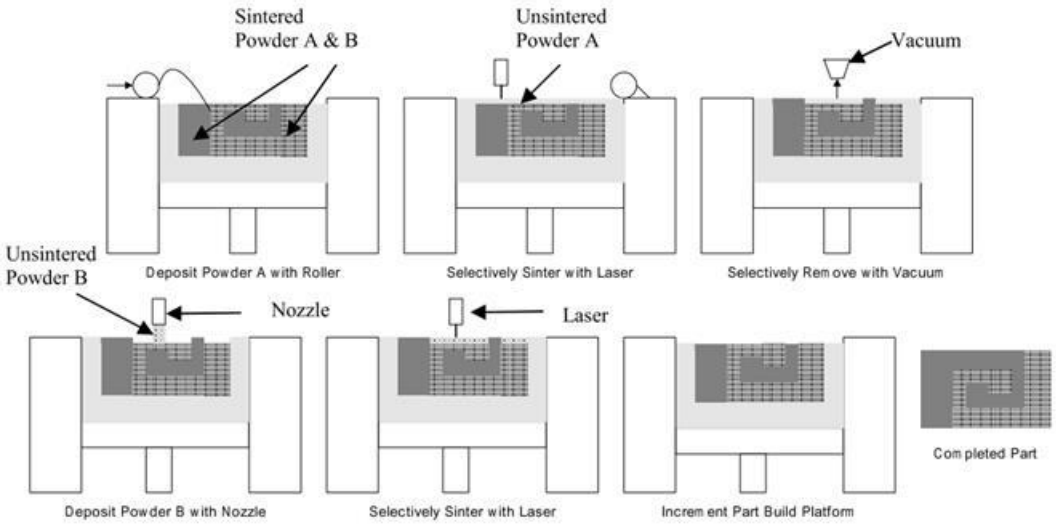

Figure 2.2.11. Multi material process schematic applied by Lappo *et al.* (2003)

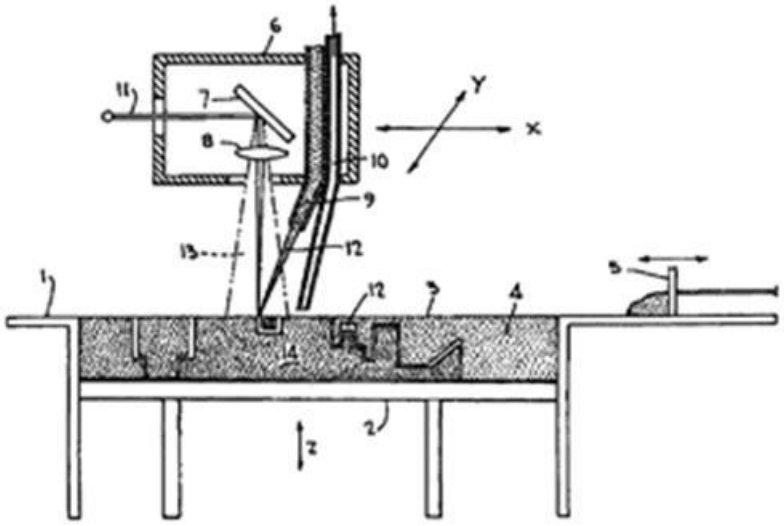

Figure 2.2.12. Patent schematic of Meiners *et al.* (1996)

Hovel *et al.* (2011) proposed a concept where the first material is deposited in powder form on to the substrate and is selectively melted by a laser or electron beam. Thereafter the second material is applied in the form of a tape, sheet, foil, or three-dimensional pre-form where after it is selectively melted to produce the desired shape (Figure 2.2.13).

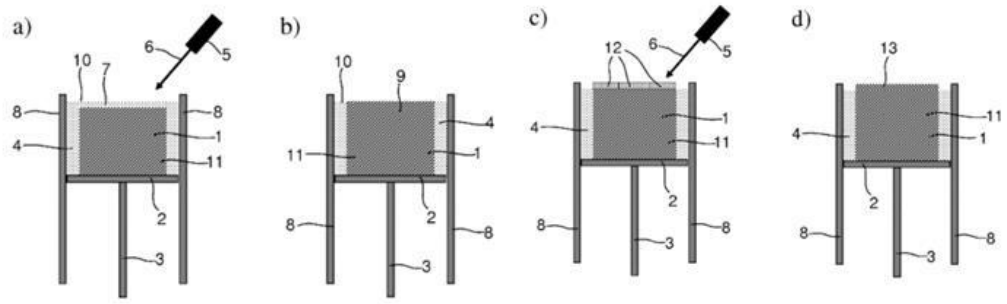

Figure 2.2.13. Hovel *et al.* (2011) multi material process

Micro feeding of fine powder through a capillary tube with a vibration to induce flow is a common approach to dispensing powder on the build platform to create multi material parts. Matsusaka *et al.* (1995) proved that continuous controlled discharge (0.2 mg/s) of fine powder (about 10 µm in size) through a vibrating capillary tube (0.4-1.6 mm diameter) was possible. It was concluded that a thin layer of micro vibrating powder particles forms on the inner wall of the tube and act as lubrication to the powder flow.

Li *et al.* (2002) made use of piezoelectric transducers to produce an ultrasonic vibration (20 kHz) applied to the capillary tube (125 µm) to control the powder flow rate. Continuous discharge of the Cu and stainless steel powders was achieved at a flow rate of approximately 5-10 g/s with a line of width (127 µm). In 2004 Li *et al.* patented the idea of vibration induce micro powder flow through a capillary tube to produce small scale models (Figure 2.2.14). The patent mentions that the apparatus had multi material applications.

Chianrabutra *et al.* (2014) dispensed fine powder particles by a vibration-assisted system using a glass nozzle (250 µm nozzle diameter with a nozzle angle of 75°), know as dry powder printing. Powder is discharged directly from the dispenser. Particles form a stable arch structure across the outlet, thus no flow occurs. Powders are dispensed through the outlet by breaking the arch structure by vibration from a piezoelectric transducer attached to the dispenser. Successfully depositing single strips of powder less than 100 µm in width. Vibration assisted deposition is a valid concept form multi material deposition. Also noting that there are some clear drawbacks to this accurate powder dispensing system. Firstly, due to the small resolution it is a time consuming process. Secondly, external vibrations (e.g. movement from the CNC table) make the process somewhat unpredictable.

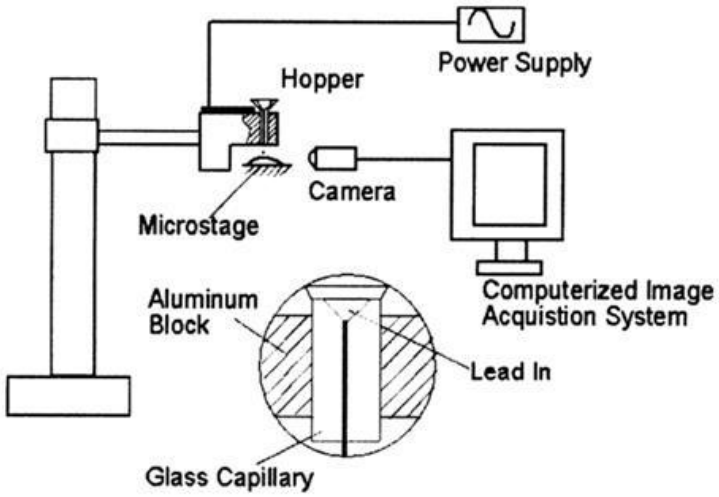

Figure 2.2.14. Micro-feeding experimental setup (Li *et al.*, 2002)

Yang & Evans *et al.* (2003) experimented with acoustic vibration to control the flow rate of dry powders in open capillaries. H13 tool steel powder (212 µm particle size) was dispensed through a glass capillary tube (450 µm inner diameter). The vibration was induced by a sub-woofer loudspeaker (40 Hz to 4 kHz frequency range). The study concluded that acoustic vibration is a valid approach for delivering powder to the build platform and that a difference in waveform, frequency and amplitude had an effect on the flow rate. A vibrating tube offers accurate powder dispensing (60 µm -0.5 mm spatial resolution), but at small flow rates (≤1 mg/s). A vibrating capillary tube is one of the better approaches to solve the complex design problem of applying multiple materials on a single layer in the DMLS process (Yang & Evans, 2007).

Al-Jamal *et al.* (2008) deposited multiple materials (Cu-H13 tool steel) on a single layer to investigate the bond between the specific materials. Variation in the hardness over the interface area proved that there is a distinct region where the material join and not a sharp dividing line. This was further proved by a tensile test on the specimen where the interface had a larger tensile stress than the weaker of the two materials. To obtain the results a Nd:YAG laser and modified 3-axis table were utilized. Powder was fed to the build platform via four hoppers. Each hopper contained its own material. Powder flow was induced with a 0.4 mm nozzle and a piezoelectric translator to cause vibration.

Gu & Giuliani (2009) patented the use of multiple powder feeders to a central dispensing hopper on a 3-axis system to manufacture multi material parts. The powder feeder comprises of a feed hopper and feed screw. Each feed hopper is filled with a different powder and is feed to the build platform via the dispensing hopper (Figure 2.2.15).

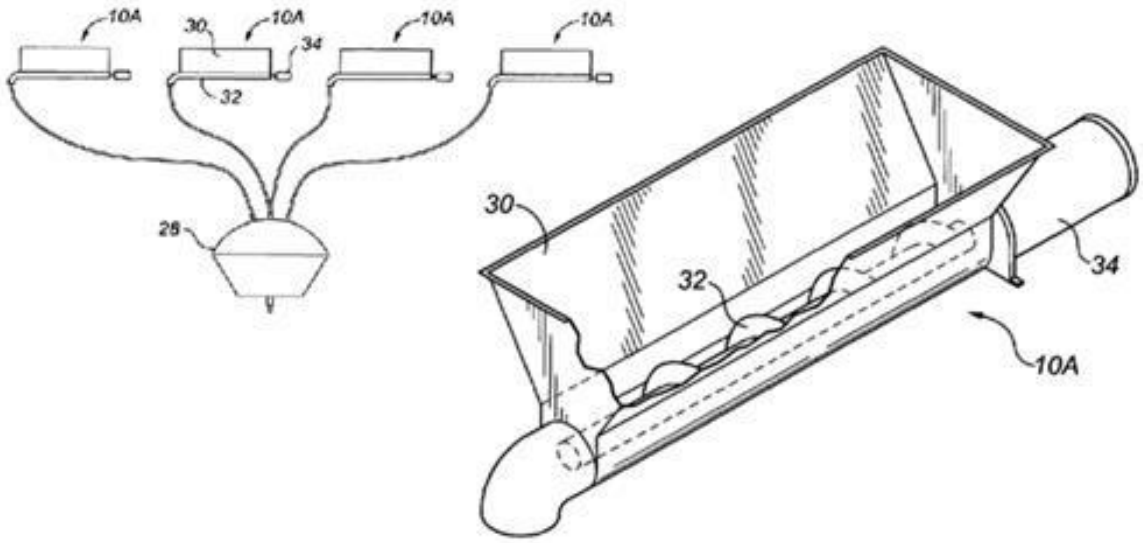

Figure 2.2.15. Schematic of multiple powder feeders (Gu & Giuliani, 2009)

Van der Eijk *et al.* (2004) suggests a process using the laws of electrostatic charge to produce the layers. A photoreceptor is charged to a specified charge density using a scorotron. An electrostatic image of the part slice is created on the photoreceptor by light exposure, using a computer controlled LED printer head. The light exposure causes the photoreceptor to retain the electrostatic charge only for the image of the slice. The photoreceptor plate is aligned horizontally over the powder reservoir where the electrostatic force causes the powder to be attracted to the plate in the exact image of the part slice. The layer of powder is then deposited on the build platform by discharging the electrostatic charge of the photoreceptor (Figure 2.2.16). The process is repeated for multiple powder till a complete layer is formed. The entire layer is then selectively melted. By placing layer upon layer a 3D part is formed.

Phenix Systems (2012) patented a concept of producing multi material parts utilizing a mask to deposit different powders onto selected regions of the build platform (Figure 2.2.17). To form the mask, a fine mesh with binder material (resin or polymer) is used. A laser beam selectively bonds the binder material to the mesh and creates a desired geometry, i.e. “mask”. The mask is

placed over the build platform. A powder layer is deposited over the mask so that the powder flows through the opened mesh cells onto the build platform in the desired regions. The mask is removed. The powder is then selectively melted by a laser beam. The remaining powder of the first material is removed from the mask and the used mesh is removed. Then a new mask for the second powder is created and the process repeats, till a complete layer is formed. Placing layers upon each other forms a dense 3D part.

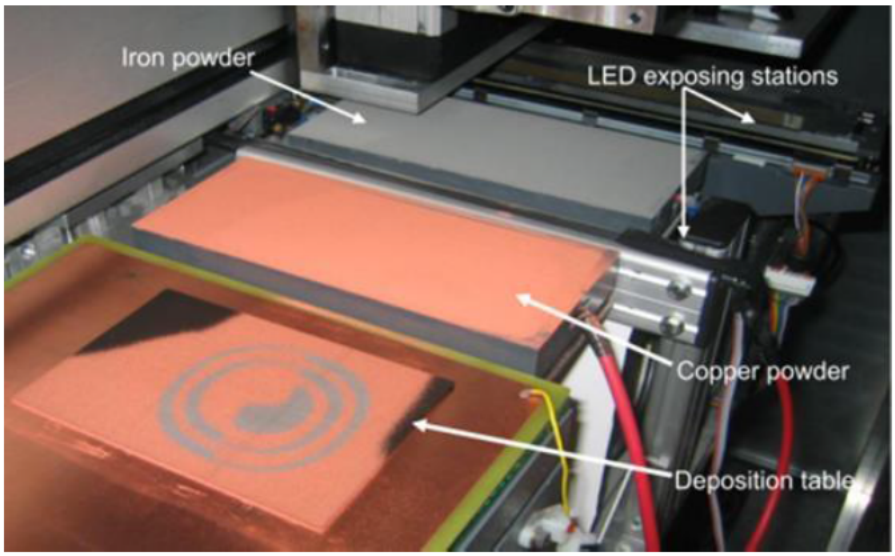

Figure 2.12.16. Electrostatic powder dispenser (van der Eijk *et al.*, 2004)

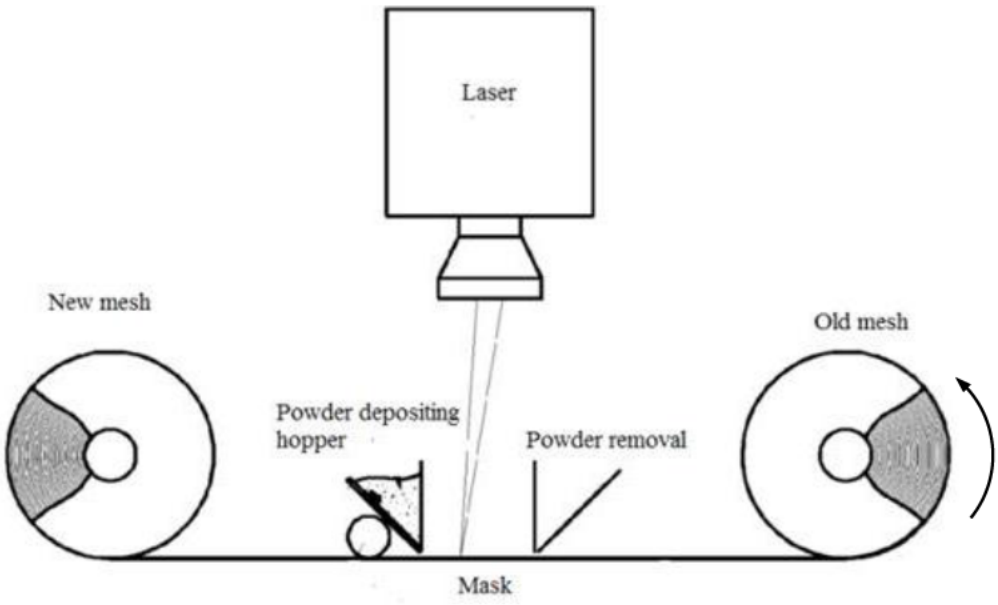

Figure 2.2.17. Phenix Systems (2012) multi material process

The problem with multi material powder dispensing is to create a smooth, consistent powder thickness layer. Dispensing powder through a nozzle or capillary tube especially has this problem due to the extruding nature of single tracks of powder onto the build platform. As single tracks are positioned next to each other they cause a ridge between the two single tracks as seen in Figure 2.2.18. These ridges lead to an uneven powder bed surface which has a direct negative effect on the laser single track formation. Inadequate laser single track formation leads to rough surface finishes and less dense 3D DMLS parts (Ott & Zaeh, 2010).

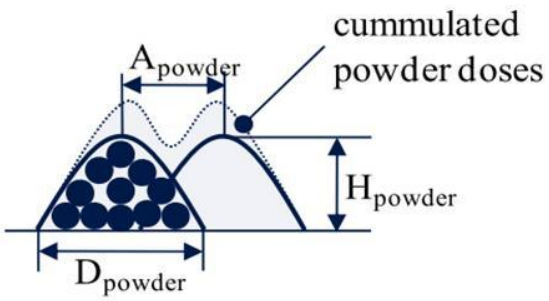

Figure 2.2.18. Powder ridge between tracks (Ott & Zaeh, 2010)

An "ideal" multi material process should have a high resolution of accuracy, while producing a homogeneous surface morphology and create a sharp inter-locking interface between the different materials. To ensure that the process is economically viable a time efficient process is needed. Table 2.2.1 compares various methods of producing multi material structures on a single layer as described above, highlighting the advantages and disadvantages.

Table 2.2.1. Methods of producing a multi material structures on a single layer

Method	Reference	Advantages	Disadvantages
Selective removal and deposition	Lappo *et al.* (2003) Meiners *et al.* (2005) Hovel *et al.* (2011)	High resolution	Re-melted interface Time consuming
Vibration controlled powder flow	Yang *et al.* (2003) Al-Jamal *et al.* (2008)	High resolution Interlocking interface	Time consuming Bad surface morphology
Mask controlled deposition	Phenix Systems (2012)	High resolution	High cost of processing Time consuming Re-melted interface
Electro-static attraction	Van der Eijk *et al.* (2004)	High resolution Time effective Sharp interlocking interface	Bad surface morphology

Method	Reference	Advantages	Disadvantages
Multiple powder feeders with central dispensing hopper	Gu & Giuliani (2009)	High resolution Sharp interlocking interface Functionally graded composition	Inhomogeneous powder layer Feeder blockages

2.2.2. Application of multi material structures

Direct manufacturing of multi material implants by DMLS

Failure of medical implants can cause great pain and discomfort to patients, is very expensive to repair and has a small chance of full recovery. According to Kurtz *et al.* (2009), the total number of hip repair surgery is expected to increase by 137% and knee repair surgery by 607% between the years 2005 and 2030.

Dumbleton (1977) presented the variation of probability of removal as a function of time of implantation (Figure 2.2.19) Removals may be required due to fracture of the femoral component, infection, excessive wear, or loosening of the prosthesis. Geetha *et al.* (2009) conducted an in depth review on the reasons for implant failure. It was indicated that the main causes of implant failure that leads to revision surgery: 1) inflammation (rejection); 2) wear/corrosion of the interface material may have toxic effects on the surrounding tissue; 3) fibrous encapsulation (results in nonbonding with the surrounding tissue); 4) low fracture toughness or low fatigue strength; 5) mismatch in modulus of elasticity between bone and implant. Though medication helps to cure this, by utilizing better biocompatible material and materials having antibacterial properties the chances of rejection can be dramatically lowered. Loosening of the implant is caused by a mismatch of modules of elasticity which leads to stress shielding. Material selection has a major effect on the life span of the medical implant.

Materials used for implants especially for load bearing applications should have excellent biocompatibility, superior corrosion resistance in body environment, a combination of high strength but low modulus mechanical properties, high fatigue and wear resistance, high ductility and should not be toxic to the surrounding tissue. Failure of implants can be reduced by selecting property specific bio-materials. Research continues to improve bio-materials to reduce failure.

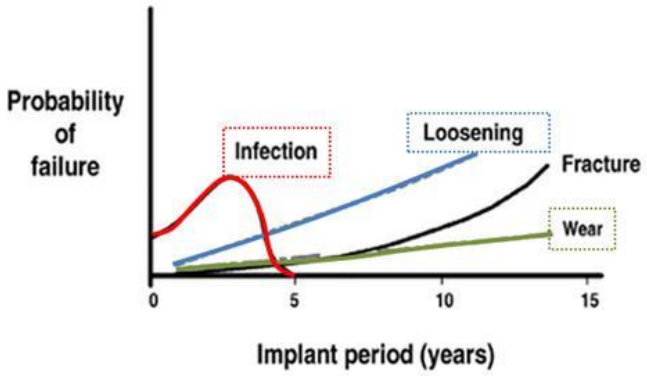

Figure 2.2.19. Timeline of implant probable failure (Dumbleton, 1977)

Using multiple biocompatible materials on a single medical implant has the opportunity to greatly increase the quality of medical implants. Implants can be constructed to have different mechanical, chemical and physical properties in desired areas of the implant. A bone where the middle section is made from a material with a higher young's modules and the outer parts from a material with less hardness to improve the functionality of the implant and reduce stress shielding on the bone. Screw connections or weld joints can be avoided when considering the joint connections of different material in current implants.

There are various material available for the production of biocompatible medical implants. Lodererova *et al.* (2009) produced multi material samples of Ti6A14V and CoCr. Experiments conducted on the mechanical properties and the biocompatibility of the two materials concluded that the materials could be used in medical implants due to their biocompatibility, corrosive and abrasive resistance properties. Habijan *et al.* (2013) conducted experiments with both dense and porous Ni–Ti shape memory alloys (NiTi-SMA) coated with human mesenchymal stem cells (hMSC). NiTi has an elastic modulus (28 GPa) similar to bone (0.3–20 GPa). The study showed that NiTi reduces the stress difference between the bone and the implant decreasing the chance of the implant loosening. NiTi supports the application of hMSC to the implant which enhances bones growth at the implant interface.

Typical examples of multi material biomedical implants are dental implants. Implants composing of titanium and hydroxyapatite (HAP) satisfy both mechanical and biocompatible property requirements of dental implants. Watari *et al.* (1997) studied implants composing of Ti and HAP

that were implanted into Wister strain rats. The implant consisted of higher percentages of Ti for the upper part where biting force is directly applied and more HAP for the lower part which is implanted inside the jaw bone to improve biocompatibility and reduce stress shielding (Figure 2.2.20). Results showed superior biocompatibility with new bone formation and no inflammation was observed throughout the implantation period. By combining different materials, property specific regions can be formed. The introduction of multi material implants will improve the quality, functionality and life span of biomedical implants.

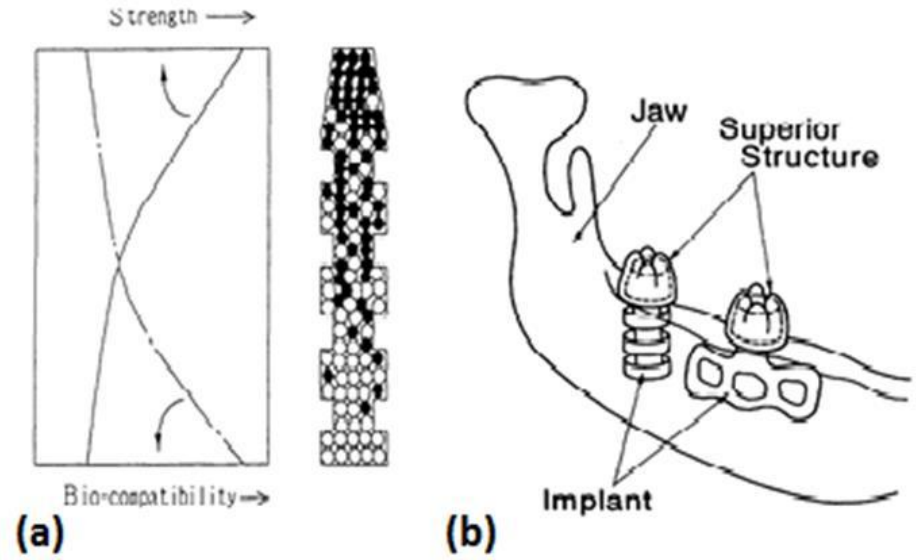

Figure 2.2.20. Dental implants: (a) functionally graded implant properties; (b) dental implant in jaw (Watari *et al.*, 1997)

Tool making

Injection moulding, die casting and blow moulding use moulds to mass produce parts. The process requires a molten material to be injected into a cavity inside a mould, where after the part is cooled and ejected. The moulding process contains three stages namely filling, cooling and ejection. Process parameters such as cycle time and warping/shrinkage are directly affected by the temperature of the mould. By increasing the heat flow (ability of the mould to reject the heat), parts of better quality can be produced in shorter cycle times. Currently DMLS is being utilized to produce moulds with higher heat flow by growing internal cooling channels that conform to the surface of the mould. By utilizing conformal cooling channels the cooling water is closer to the heat source on the surface of the mould (Figure 2.2.21), therefor the heat transfer

is more effective. Studies have shown that Ni/Cu moulds with conformal channels led to productivity improvements of approximately 70% when compared to a similar mould made with conventional steel with drilled cooling channels (Dimla *et al.*, 2005).

By combining the mechanical and thermal properties of multiple materials on a mould, an increase in productivity and quality of the plastic parts produced can be expected. These multi material moulds are known as hybrid moulds. Cu is an ideal material for heat transfer within injection moulds due to its high heat transfer coefficient. The disadvantage of using Cu in moulds is that it has low wear resistances so the mould lifespan is shortened. Hybrid moulds have Cu insides and a protective maraging tool steel shell, producing a mould with improved heat transfer and adequate lifespan (Houtekier & Gent, 2006; Beal *et al.*, 2004).

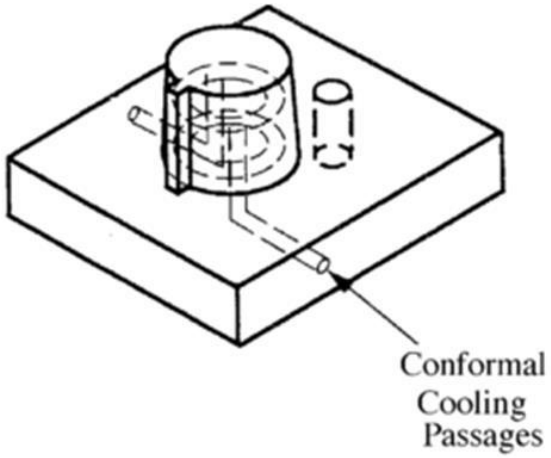

Figure 2.2.21. Conformal cooling (Dimla *et al.*, 2005)

By using multiple materials in the mould design and integrating conformal cooling, the heat flow of a mould can be further improved. Materials such as Cu that have higher thermal conductivity, in conjunction with conformal cooling produce an effective heat sink. Such a mould would contain for example a steel outer shell with a Cu inside with conformal cooling to reject the heat. This approach would lower the mould temperature considerably due to the increase heat rejection. The multi material DMLS process is the only technology that will have the capability of producing such moulds due to its layer by layer manufacturing (Ott & Zaeh, 2010).

Other applications

Subramanian *et al.* (2014) describes a patent for multi material gas turbine blades (Figure 2.2.22). The blade consists of three different materials. Firstly, a structural metal like titanium to provide mechanical strength and to maintain the shape of the airfoil blade. Secondly, a bond coat on the surface of the blade to protect the blade and thirdly a thermal barrier. The thermal barrier consists of a material with a higher heat capacity to increase the heat reject from the surface of the blade using 3D cooling channels.

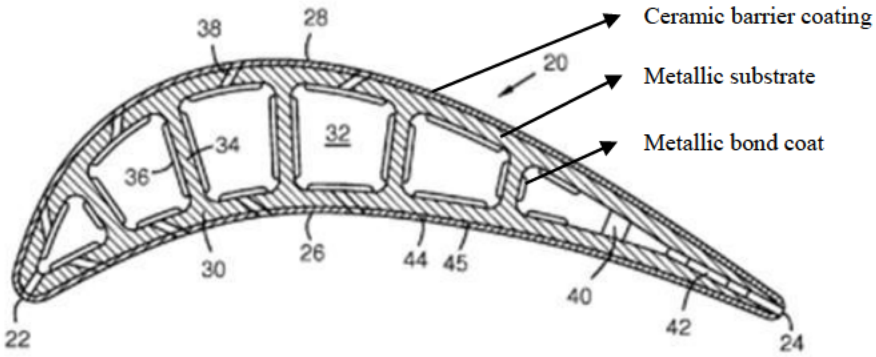

Figure 2.2.22. Multiple material turbine blade (Subramanian *et al.*, 2014)

2.3. Conclusion

This chapter gives an overview of the relevant literature concerning DMLS technology and systems for multi material processing. DMLS has evolved over the past 30 years into a competitive manufacturing process. With a large range of commercial DMLS machines available, majorly influencing the medical, tool making, aerospace and prototyping industries. Commercial DMLS machines can however, only produce parts from one material on a specific layer. Literature indicates a few prototypes of multi material systems but all of them are conceptual developments. There is no concrete solution to multi material manufacturing yet.

Multi material layer manufacturing can improve the performance and life span of biomedical implants. Implant failure is almost always caused by inadequate material properties. Multi material implants contain property specific regions to prevent failure and increase the life span of the implant. To produce multi material implants with the correct surface quality, mechanical properties and accuracy the optimal parameters for the DMLS process need to be determined.

Processing multi material on a single layer will increase the already complex task of producing high quality parts. Multi material layer processing with DMLS will allow implants to be manufactured that previously were not possible with conventional manufacturing.

Modern commercial DMLS machines can produce complex parts from one material on a specific layer. Currently there are two experimental approaches to create multi material objects utilizing DMLS.

- A powder is deposited on the building platform in the appropriate regions and the material is selectively melted by a laser. Non-sintered powder is removed by vacuum, electrostatic or mechanical methods. The second powder is delivered and selectively melted. Additional modification to this approach uses a tape, sheet, foil or three-dimensional pre-forms to introduce the second material.
- Different powders are deposited on the building platform i) by hoppers with different cells for the powders; ii) by special nozzles (capillaries) with acoustic vibration to facilitate application of the powder; or iii) by electrostatic methods to deposit different materials before melting. A multi material powder layer is selectively melted by a laser beam. The process is repeated thus creating a 3D object.

Literature indicates a few prototypes of multi material systems, but all of them are conceptual. Original solutions for multi material delivering systems are a vital task for future progress in DMLS.

2.4. References

3DSystems, 2013. Phenix PX Brochure. Available at: http://www.3dsystems.com [Accessed January 7, 2015].

Aboudi, J., Pindera, M.J. & Arnold, S.M., 1999. Higher-order theory for functionally graded materials. Composites Part B: Engineering, 30, pp.777–832.

Achelis, L. & Uhlenwinkel, V., 2008. Characterisation of metal powders generated by a pressure-gas-atomiser. Materials Science and Engineering A, 477, pp.15–20.

Al-Jamal, O.M., Hinduja, S. & Li, L., 2008. Characteristics of the bond in Cu-H13 tool steel parts fabricated using SLM. CIRP Annals - Manufacturing Technology, 57, pp.239–242.

Andreas, D. & Schwarze, D., 2014. Multi-Laser Selective Laser Melting. Proc. 8th International Conference on Photonic Technologies, Fürt, Germany.

ASTM International, 2013. F2792-12a - Standard Terminology for Additive Manufacturing Technologies, pp.10–12.

Beal, V.E., Erasenthiran, P., Hopkinson, N., Dickens, P. & Ahrens, C.H., 2004. Fabrication of x-graded H13 and Cu powder mix using high power pulsed Nd: YAG laser. Proc. Solid Freeform Fabrication Symposium, Austin, TX, USA.

Bremen, S. & Meiners, W., 2012. Selective Laser Melting. A manufacturing technology for the future. Laser Technik Journal, 9(2), pp.33–38.

Cooke, A. & Slotwinski, J., 2012. Properties of metal powders for additive manufacturing: a review of the state of the art of metal powder property testing. US Department of Commerce, National Institute of Standards and Technology.

Davies, P.A. & Dunstan, G.R., 2004. Comparison of master alloy and pre-alloyed 316l stainless steel powders for metal injection molding (mim). Proc. Pm2tec world congress, Chicago, IL.

Deckard, C., 1989. Method and apparatus for producing parts by selective sintering. Patent US4863538.

Dhokey, N.B., Walunj, M.G. & Chaudhari, U.C., 2014. Influence of water pressure and apex angle on prediction of particle size for atomization of Cu powder. Advanced Powder Technology, 25(2), pp.795–800.

Dimla, D.E., Camilotto, M. & Miani, F., 2005. Design and optimisation of conformal cooling channels in injection moulding tools. Journal of Materials Processing Technology, 164-165, pp.1294–1300.

Dunkley, J. J., 2013. Advances in atomisation techniques for the formation of metal powders. Advances in Powder Metallurgy, 1, pp.3-18

Dumbleton, J. H., 1977. Elements of hip joint prosthesis reliability. Journal of Medical Engineering & Technology, 1(6), pp.341-346

EOS GmbH, 2013. EOSINT M280 Brochure. Available at: http://ip-saas-eos-cms.s3.amazonaws.com [Accessed January 7, 2015].

Fraunhofer institut, 2003. Generative Manufacturing Methods : Selective Laser Melting. Available at: http://www.ipk.fraunhofer.de [Accessed April 12, 2015].

Geetha, M., Singh, A.K., Asokamani, R. & Gogia, A.K., 2009. Ti based biomaterials, the ultimate choice for orthopaedic implants–a review. Progress in Materials Science, 54(3), pp.397–425.

Gong, H., Rafi, K., Karthik, N., Starr, T. & Stucker, B., 2013. The Effects of processing parameters on defect regularity in Ti-6Al-4V parts fabricated by Selective Laser Melting and Electron Beam Melting. Proc. 24th Annual International Solid Freeform Fabrication Symposium – An Additive Manufacturing Conference, Austin, TX, USA.

Gu, P. & Giuliani, V., 2009. Multisource and multi material freeform fabrication. Patent US007572403B2.

Habijan, T., Haberland, C., Meier, H., Frenzel, J., Wittsiepe, J., Wuwer, C., Greulich, C., Schildhauer, T.A. & Köller, M., 2013. The biocompatibility of dense and porous Nickel-Titanium produced by selective laser melting. Materials Science and Engineering, 33(1), pp.419–426.

Hautekier, R., Cardon, L., Moerman, M., Ragaert, K., Voet, A., Van Pee, B. & Mingneau, J., 2006. The effect of multiple material moulds on the thermal behaviour and mould design strategy. Proc. Rapid Product Development, Marinha Grande, Portugal.

Housholder, R.F., 1979. Molding process. Patent US4247508.

Hövel, S., Stankowski, A. & Rickenbacher, L., Hoevel Simone, 2011. Method of applying multiple materials with selective laser melting on a 3d article. Patent US 20110106290A1.

Krauss, H. & Zaeh, M.F., 2013. Investigations on manufacturability and process reliability of selective laser melting. Physics Procedia, 41, pp.815–822.

Kruth, J.P., Mercelis, P., Van Vaerenbergh, J. & Craeghs, T., 2007. Feedback control of Selective Laser Melting. Proc. 3rd International Conference on Advanced Research in Virtual and Rapid Prototyping, Leiri, Portugal.

Kurtz, S.M., Lau, E., Ong, K., Zhao, K., Kelly, M. & Bozic, K.J., 2009. Future young patient demand for primary and revision joint replacement: National projections from 2010 to 2030. Clinical orthopaedics and related research, 467, pp.2606–2612.

Lappo, K., Jackson, B., Wood, K., Bourell, D.L. & Beaman, J.J., 2003. Discrete multiple material selective laser sintering (M2SLS): Nozzel design of powder design. Proc. Solid Freeform Fabrication Symposium, Austin, Texas, pp.93–108.

Li, X., Choi, H. & Yang, Y., 2002. Micro rapid prototyping system for micro components. Thin Solid Films, 420-421, pp.515–523.

Li, X., Yang, Y. & Choi, H., 2004. Apparatus and method of dispensing small-scale powders. Patent US 20040012124A1.

Liu, B., Wildman, R., Tuck, C., Ashcroft, I. and Hague, R., 2011. Investigation the effect of particle Size distribution on processingpParameters optimisation in selective laser melting process. Proc. Solid Freeform Fabrication Symposium, Austin, TX, USA.

Liu, Z.H., Zhang, D.Q., Sing, S.L., Chua, C.K. & Loh, L.E., 2014. Interfacial characterization of SLM parts in multi-material processing: Metallurgical diffusion between 316L stainless steel and C18400 Cu alloy. Materials Characterization, 94, pp.116–125.

Lodererova, M., Rybnicek, J., Steidl, J., Richter, J., Boivie, K., Karlsen, R. & Åsebø, O., 2009. Biocompatibility of metal sintered materials in dependence on multi-material graded structure. Proc. 13th International Conference on Biomedical Engineering, Heidelberg, Berlin.

Mahamood, R.M., Akinlabi, E.T., Shukla, M. and Pityana, S., 2012. Functionally graded material : An overview. Proc. World Congress on Engineering , London, UK.

Matsusaka, S., Urakawa, M. & Masuda, H., 1995. Micro-feeding of fine powders using a capillary tube with ultrasonic vibration. Advanced Powder Technology, 6(4), pp.283–293.

Meiners, W., Wissenbach, K. & Gasser, A., 1996. Selective laser sintering at melting temperature. Patent US006215093b1.

Mumtaz, K.A. & Hopkinson, N., 2007. Laser melting functionally graded composition of Waspaloy and Zirconia powders. Journal of Materials Science, 42(18), pp.7647–7656.

Ott, M. & Zaeh, M.F., 2010. Multi-material processing in additive manufacturing. Proc. 21th Annual International Solid Freeform Fabrication Symposium, Texas, Austin, pp.195–203.

Phenix systems, 2012. Method for creating an object, by means of laser treatment, from at least two different powder materials, and corresponding facility, Patent US20120228807A1.

Reinarz, B., Karlheinz, P. J. H. & Gerd, W., 2014. Optimization of media feed channels in laser beam melting. Proc. American Society for Precision Engineering, Raleigh, North Carolina, USA, pp.13-19.

Renishaw, 2012. Brochure: The power of Additive Manufacturing. Available at: http://resources.renishaw.com [Accessed January 9, 2015].

Shifeng, W., Shuai, L., Qingsong, W., Yan, C., Sheng, Z. & Yusheng, S., 2014. Effect of molten pool boundaries on the mechanical properties of selective laser melting parts. Journal of Materials Processing Technology, 214(11), pp.2660–2667.

SLM Solutions GmbH, 2013. SLM 500 HL Brochure. Available at: http://stage.slm-solutions.com [Accessed January 6, 2015].

Spierings, B., Herres, N. & Levy, G., 2011. Influence of the particle size distribution on surface quality and mechanical properties in additive manufactured stainless steel parts. Proc. Solid Freeform Fabrication Symposium, Austin, Texas, pp.397-406.

Steen, W.M., 2003. Laser material processing—an overview. Journal of Optics A: Pure and Applied Optics, 5(4), pp 3.

Subramanian, R., Ott, M., Thomaidis, D., Sadovoy, A. & Münzer, J., 2014. Additive manufacture of turbine component with multiple materials. Patent US 20140099476A1.

Vaezi, M., Chianrabutra, S., Mellor, B. & Yang, S., 2013. Multiple material additive manufacturing – Part 1: a review. Virtual and Physical Prototyping, 8(1), pp.19–50.

Van Der Eijk, C., Mugaas, T., Karlsen, R., Åsebø, O., Kolnes, Ø. & Skjevdal, R., 2004. Metal printing process - development of a new Rapid Prototyping process for metal parts. Proc. World PM Conference, Vienna.

Watari, F., Yokoyama, A., Saso, F., Uo, M. & Kawasaki, T., 1997. Fabrication and properties of functionally graded dental implant. Composites Part B: Engineering, 28(96), pp.5–11.

Wehmöller, M., Warnke, P.H., Zilian, C. & Eufinger, H., 2005. Implant design and production-a new approach by selective laser melting. International Congress Series, 1281, pp.690–695.

Wohlers, T., 2014. *Wohlers report 2014: Global reports: Belgium*. Wohlers Associates.

Yadroitsev, I. & Smurov, I., 2010. Selective laser melting technology: From the single laser melted track stability to 3D parts of complex shape. Physics Procedia, 5(2), pp.551–560.

Yadroitsev, I., 2009. Selective laser melting: Direct manufacturing of 3D-objects by selective laser melting of metal powders. LAP Lambert Academic Publishing, Saarbrücken, Germany.

Yadroitsev, I., Bertrand, P. & Smurov, I., 2007. Parametric analysis of the selective laser melting process. Applied Surface Science, 253, pp.8064–8069.

Yadroitsev, I., Bertrand, P., Laget, B. and Smurov, I., 2007. Application of laser assisted technologies for fabrication of functionally graded coatings and objects for the International Thermonuclear Experimental Reactor components. Journal of nuclear materials, 362(2), pp.189-196.

Yadroitsev, I., Krakhmalev, P. & Yadroitsava, I., 2015. Hierarchical design principles of selective laser melting for high quality metallic objects. Additive Manufacturing, 7, pp.45-56.

Yadroitsev, I., Yadroitsava, I., Bertrand, P. & Smurov, I., 2012. Factor analysis of selective laser melting process parameters and geometrical characteristics of synthesized single tracks. Rapid Prototyping Journal, 18(3), pp.201-208.

Yang, S. & Evans, J.R.G., 2003. Computer control of powder flow for solid freeforming by acoustic modulation. Powder Technology, 133, pp.251–254.

Yang, S. & Evans, J.R.G., 2007. Metering and dispensing of powder; the quest for new solid freeforming techniques. Powder Technology, 178(1), pp.56–72.

Chapter 3. MATERIALS

3.1. Ti6Al4V (ELI) powder

Ti and its alloys have a wide range of applications in industries, which require high levels of reliable performance such as biomedical, aerospace, automotive, chemical plant, power generation and oil and gas extraction industries. Ti and its alloys have high mechanical strength, low weight ratio and outstanding corrosion resistive properties (Donachie, 2000).

Ti is available in several different grades. Most grades are of alloyed type with various additions of Al, V, Ni, Mo, Cr or Zr. These elements are added to change the mechanical characteristics, heat resistance, conductivity, microstructure, creep, ductility and corrosion resistance properties of pure Ti. Ti6Al4V is one of the most widely used Ti alloys. It is an alpha-beta alloy containing 6 wt% Al and 4 wt% V. Ti6Al4V has a good combination of strength and toughness while exhibiting excellent corrosion resistance properties. The properties of this alloy originate from the refinement of the grains upon cooling and subsequent low-temperature aging to decompose martensite structures formed upon quenching (Donachie, 2000).

Ti6Al4V has numerous applications in the aerospace, automotive and marine industries because of its mechanical and corrosive resistant properties. Its superior biocompatibility makes it an excellent biomaterial. Ti6Al4V ELI (Grade 23) is very similar to Ti6Al4V (Grade 5), except that Ti6Al4V ELI contains reduced levels of oxygen, nitrogen, carbon and iron. “ELI” refers to extra low interstitials. These lower interstitials improved ductility and increase fracture toughness of the Ti6Al4V ELI material. The improved mechanical properties of extra-low-interstitial grades compared to standard grades of Ti alloys are the result of reduced oxygen levels (Donachie, 2000). Generally, Ti6Al4V is used in applications up to 400 °C. It has a density of roughly 4420 kg/m^3, Young's modulus approximately 110 GPa, and ultimate tensile strength about 1 GPa (Table 3.1.1). By comparison, annealed type 316 stainless steel has a density of 8000 kg/m^3, elastic modulus of 193 GPa, and tensile strength of only 570 MPa (ASM Aerospace, 2015).

Table 3.1.1. Typical physical and mechanical properties for wrought Ti6Al4V alloy (AZO materials, 2015; ASM Aerospace, 2015)

Property	Typical Value
Density	4420-4430 kg/m^3
Melting Range	1649±15°C
Solidus	1604 °C
Liquidus	1660 °C
Beta transus	999±15°C
Specific heat capacity	526.3-560 J/kg.°C
Volume electrical resistivity	170 ohm.cm
Thermal conductivity	6.7-7.2 W/m.K
Mean coefficient of thermal expansion 0-100°C /°C	8.6x10^{-6}
Mean coefficient of thermal expansion 0-300°C /°C	9.2x10^{-6}
Electrical resistivity	0.000178 ohm-cm
Magnetic permeability	1.00005
Magnetic susceptibility	3.3e-006
Tensile strength, ultimate (varies with heat treatment)	950 MPa
Tensile strength, yield (varies widely with heat treatment)	880 MPa
0.2% Proof stress	910 MPa
Elongation at break	14 %
Reduction in area	36%
Elastic modulus	114 GPa
Hardness, Vickers	349
Compressive yield strength	970 MPa
Notched tensile strength	1450 MPa
Ultimate bearing strength	1860 MPa
Bearing yield strength	1480 MPa
Poisson's ratio	0.342
Charpy impact	17 J
Fatigue strength	240 MPa
Fatigue strength	510 MPa
Fracture toughness	75 MPa-m½
Shear modulus	44 GPa

A chemical composition of the employed spherical argon-atomized Ti6Al4V (ELI) –45 µm powder from TLS Technik is shown in Table 3.1.2, Figure 3.1.1. The 10th, 50th and 90th percentiles of equivalent diameter (weighted by volume) of the powder were d_{10}=12.64 µm, d_{50}=22.93 µm and d_{90}=37.03 µm, respectively (Figure 3.1.2). Powder particles were highly spherical in shape.

Table 3.1.2. Chemical composition of Ti6Al4V ELI powder (in weight %)

Ti	Al	V	O	N	H	Fe	C
ASTM standard Ti grade 23							
88.1 - 91	5.5-6.5	3.5-4.5	≤0.13	≤0.030	≤0.0125	≤0.25	≤0.080
Employed powder							
89.263	6.31	4.09	0.12	0.009	0.003	0.20	0.005

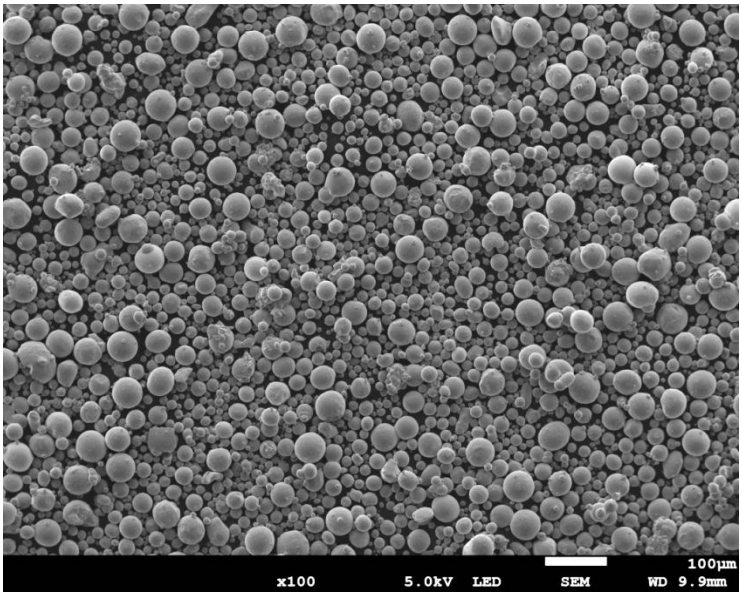

Figure 3.1.1. SEM photo of the employed Ti6Al4V ELI powder

Figure 3.1.2. Particle size distribution of employed Ti6Al4V powder

3.2. Copper powder

Pure, unalloyed Cu has high electrical and thermal conductivity as well as good corrosion resistance properties. Studies have also shown that Cu has strong antibacterial properties (Jung *et al.* 2014). Almost all alloying elements affect the electrical conductivity of Cu negatively. Commercially pure Cu is represented by UNS numbers C10100 to C13000. The most popular form of pure Cu is the standard electrical wire grade of Cu (C11000). The various grades of unalloyed Cu differ in the amount of impurities present. Pure Cu has a minimum Cu content of 99.3% Cu or higher (Everhart, 1975). Cu alloys often contain materials such as beryllium, cadmium, or chromium. Most Cu alloys retain the face-centered cubic structure of pure Cu. Therefore their physical properties remain similar to those of pure Cu. The main reason for alloying Cu is to produce higher mechanical strength and increase thermal stability (resistance to softening) (Davis, 2001). Typical physical and mechanical properties for oxygen-free pure Cu are shown in Table 3.1.3.

Table 3.1.3. Typical physical and mechanical properties for oxygen-free pure Cu (AZO materials, 2015; Davis, 2001; Everhart, 1975)

Property	Typical Value
Density	8890 - 8940 kg/m^3
Melting point	1083°C
Solidus/Liquidus	1065/1086°C
Specific heat	387 J/kg.°C
Volume electrical resistivity	1.68x10^{-8} ohm.m
Thermal conductivity	398-401 W/m.K
Mean coefficient of thermal expansion 0-100°C /°C	15.94e^{-6}
Mean coefficient of thermal expansion 0-300°C /°C	17.49e^{-6}
Tensile strength, ultimate (varies with heat treatment)	221 - 455 MPa
Tensile strength, yield (varies widely with heat treatment)	69.0 - 365 MPa
0.2% Proof stress	50-340MPa
Elongation at break (in 101.6 mm (4 in.))	55.00%
Reduction in area	51%
Elastic modulus	115 GPa
Hardness, Vickers	75.0 - 105
Compressive yield strength	221 - 455 MPa
Notched tensile strength	0.517 MPa
Poisson's ratio	0.310
Charpy impact	130.15N m
Fatigue strength	117 MPa
Shear modulus	44.0 GPa

A chemical composition of the employed spherical Cu (–45 µm) powder from TLS Technik shows 99,9 % pure Cu (Figure 3.1.3). The 10^{th}, 50^{th} and 90^{th} percentiles of equivalent diameter (weighted by volume) of the powder are d_{10}=9.45 µm, d_{50}=21.9 µm and d_{90}=37.54 µm, respectively (Figure 3.1.4).

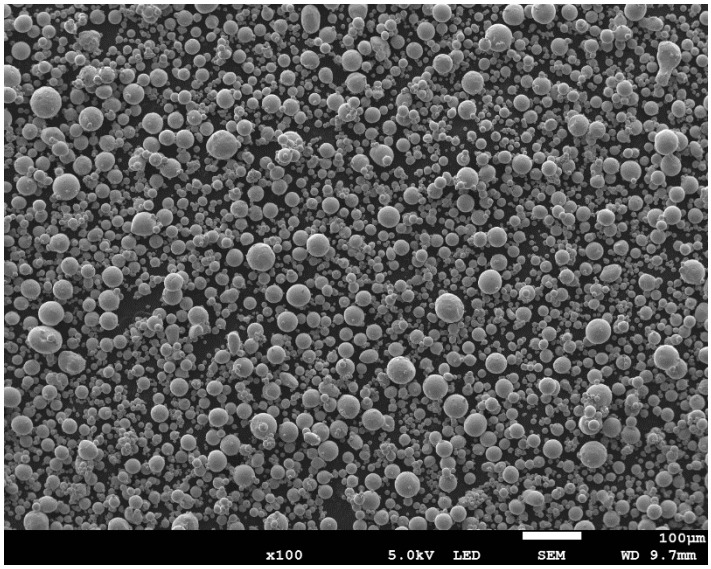

Figure 3.1.3. Spherical particles of the employed Cu powder

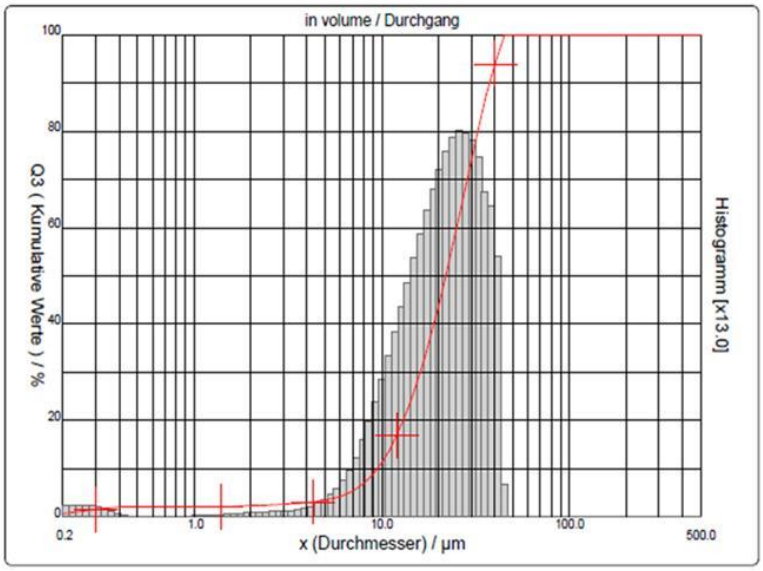

Figure 3.1.4. Particle size distribution of employed Cu powder

3.3. References

Arcam, 2015. Ti6Al4V ELI powder boucher. Available at: http:// http://www.arcam.com/ [Accessed May, 2015].

ASM Aerospace, 2015. Ti technical data sheet. Available at: http://www.aerospacemetals.com/ [Accessed May, 2015].

AZO materials, 2015. Grade 23 Ti-6Al-4V ELI (UNS R56401) data sheet. Available at: http://www.azom.com/ [Accessed May, 2015].

Davis, J.R., 2001. ASM Specialty Handbook: Copper and copper Alloys. Materials Park, OH : ASM International, pp.3-6.

Donachie Jr, M.J., 1982. Introduction to titanium and titanium alloys. American Society for Metals, Titanium and Titanium Alloys Source Book, p.7.

Everhart, J.L., 1975. Copper and copper alloy powder metallurgy: Properties and applications. Metal Powder Industries Federation. Available at: http:// www.copper.org/resources /properties/ [Accessed May, 2015].

Jung, C., Straumann, L., Kessler, A., Pieles, U. and de Wild, M., 2014. Antibacterial Cu deposited onto and into the oxide layer of titanium implants. BioNanoMaterials, 15, pp.110.

Chapter 4. MULTI MATERIAL HOPPER POWDER DEPOSTION

4.1. Introduction

In this chapter an original concept of multi material powder deposition system will be investigated. The chapter is split into two main sections; firstly the development of a conceptual design for a multi hopper powder deposition system is described. The second half of the chapter establishes parametric data for powder flow through hoppers to establish optimal design specifications. Finally a hopper design is described.

As stated in Chapter 2, a multi material system must be time efficient, form a sharp interlocking powder interface, homogeneous powder surface with a high resolution. It is important to note that for biomedical application there are very few internal structures, however contour dimensions need to be highly accurate. For medical implants it is highly critical to have fully dense part or lattice structures with controllable porosities. For this, a homogenous powder layer needs to be delivered.

To form multi material objects by DMLS, multiple materials need to be deposited on to the build platform. The flow behaviour of powder first needs to be understood before an accurate concept of a multi material deposition system can be achieved. Powder flow is defined as a relative movement of particles among neighbouring particles, or along the wall surface of a container. To deposit a smooth thin layer of powder two main aspects need to be addressed, firstly powder flow properties and secondly powder flowability.

Flow properties of powder refer to the behaviour of the bulk material which results from the external forces acting on individual powder particles. Powder properties include compressibility, cohesive strength, and wall friction of the powder particles. Powder flowability is the ability of powder to flow in a desired manner in a specific piece of equipment. Thus, powder properties refers to the flow of material independent to the apparatus handling the powder while power flowability take into account the apparatus handling the powder. The same powder will flow differently in varies pieces of equipment; this is due to external factors caused by the equipment. External factors influencing powder flow include: compacting condition caused by the shape or mechanisms of the apparatus, vibration and temperature caused by the apparatus/surroundings,

electro-static charge and friction caused by the apparatus's surfaces such as container walls or depositing scrappers (material, shape, surface roughness, etc.), as well as the humidity that the powder is processed in.

For multi material powder deposition a free flow hopper is a well-considered concept. Powder flowability has a major influence when considering flow of powder in a hopper. The wall angle, outlet dimensions, material composition and surface finish have an effect on the ability of the material to flow freely. As noted, flowability is not only a function of the material properties, but also the equipment used for handling, storing, or processing the material. Equal consideration must be given to both the material characteristics and the equipment. The same powder may flow well in specific hopper but poorly in another; likewise, a given hopper may handle one powder well but cause another powder to stop flowing freely.

4.2. Multiple hopper powder deposition system

To deposit multiple materials on a single layer of the DMLS process, a multi hopper system is proposed. Each material has its own specific hopper. By dynamically varying the outlet dimensions of the hopper a time efficient yet accurate powder deposition system is realized. However the accuracy of internal structures is limited to the critical flow conditions of the system. The scraping nature of the hopper implies homogeneous powder surfaces and sharp interlocking powder interfaces. The hoppers outlet dimensions are varied by changing the outlet slot length. The slot length is varied mechanically.

The proposed process consists of a multi hopper system and a build platform (Figure 4.2.1). The Multi hopper system (Figure 4.2.1a) is attached to an X-Y CNC controlled table to position the hopper in the desired regions over the build platform. The hopper’s are interchanged to allow the next material to be deposited onto the build platform. The build platform (Figure 4.2.1b) is controlled to move in the Z axis, to allow for the next layer to be deposited. Each hopper has a variable slot length (Figure 4.2.1c). The slot refers to the outlet where the powder flows through onto the build platform. The slot length is varied by mechanically shifting the slider. Figure 4.2.1e shows the hopper when it is closed, by shifting the slider open powder can flow (Figure 4.2.1f). By varying the outlet dimensions of the hopper complex geometry can be produce in a time effective manner while still forming a homogeneous powder layer.

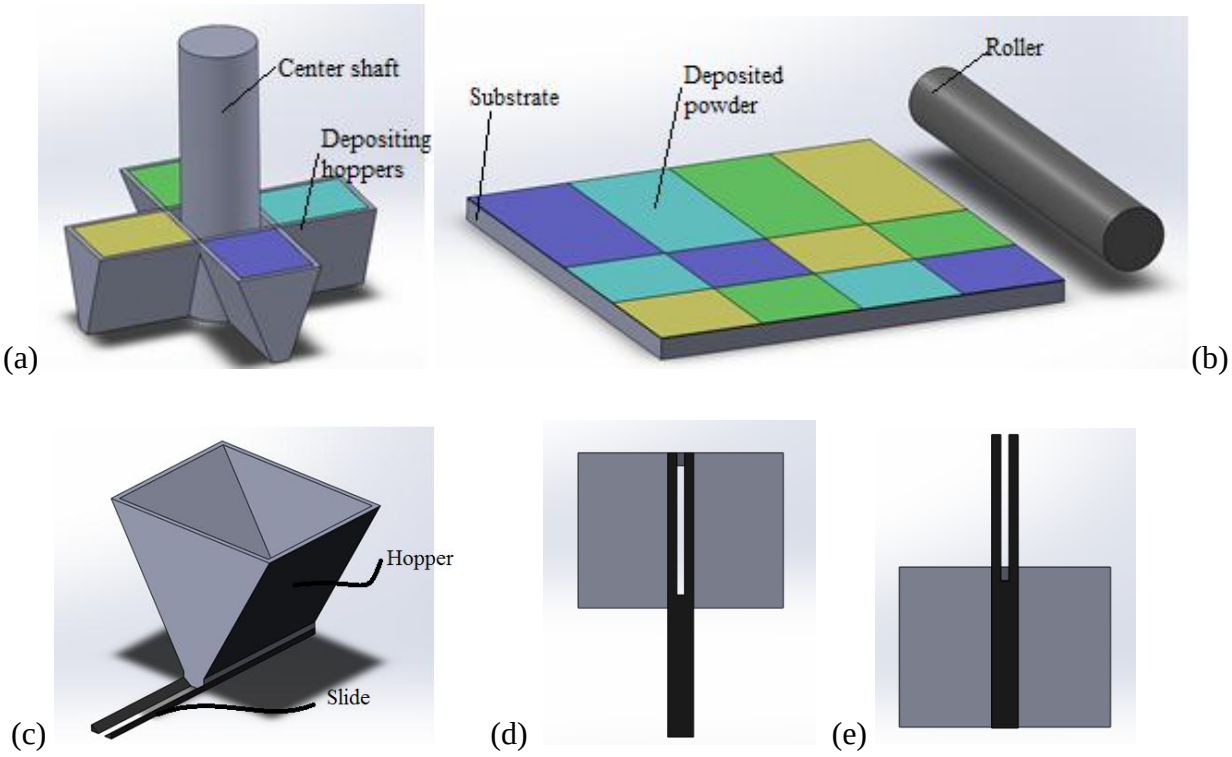

Figure 4.2.1. (a) Multi hopper system, (b) build platform, (c) hopper with variable slot length, (d) slot in open position and (e) slot in closed position

The process starts with a clean build platform (Figure 4.2.2a). The first hopper is moved into the desired position over the build platform. The hopper is controlled in the X and Y axis to allow for accurate movement over the build platform (Figure 4.2.2b). The first powder is deposited (Figure 4.2.2c). The flow is stopped by completely closing the slot. The hopper is positioned in the correct area and the powder is deposited. After the first powder is deposited the hopper is closed. The next hopper containing a different powder is position over the build platform (Figure 4.2.2d). Different powders are deposited in the desired regions till a full layer is formed (Figure 4.2.2e). The hopper has a variable slot length. By adjusting the slot length as the hopper is moving allows the formation of irregular shapes (Figure 4.2.2f). The variable slot length makes it possible to accurately deposit powder, yet time efficiently. A roller moves over the build platform to smooth out the layer to form a homogeneous surface (Figure 4.2.2g).The hopper then moves off the build platform. A laser beam selectively melts the desired regions (Figure 4.2.2h). The build platform moves a layer thickness downwards and the process repeats till a complete dense multi material object is formed.

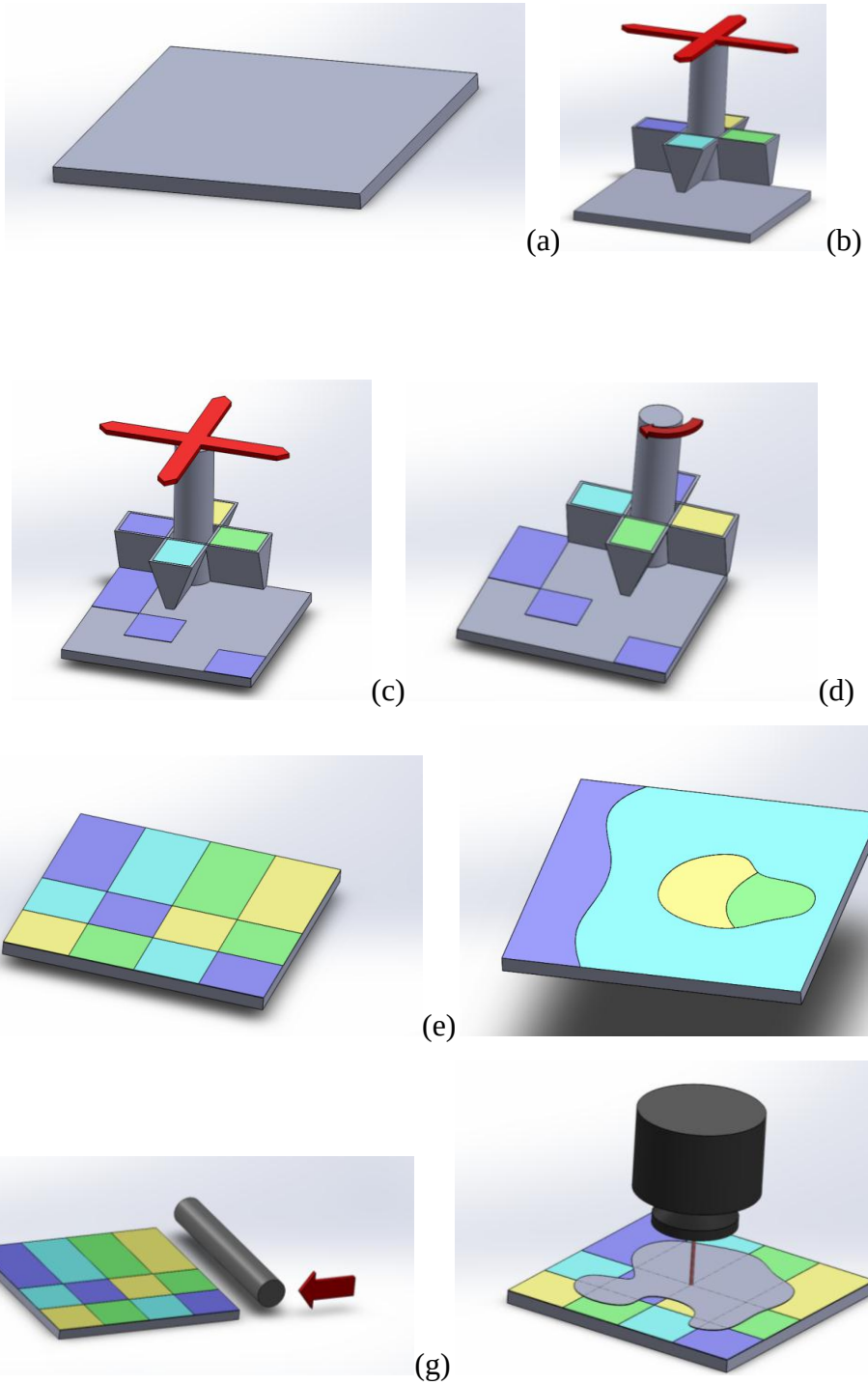

Figure 4.2.2. Multi material powder deposition process

4.3. Investigation of powder flow through hopper

Before a final design can be concluded, experiments should be done to determine the critical factors influencing powder flow and layer consistency. Flowability of a powder through a hopper is defined by the hopper designs. Factors such as surface finish, material composition of the powder and hopper wall, moisture content, hopper wall angle and outlet dimensions are all determining factors of flow conditions. Free flow of powder is important to induce a smooth thin layer of powder on the build platform. To determine the optimal flow parameters for fine powder through the hopper an experimental setup was developed. Results from this experimental setup will assist in making design decisions when selecting hopper dimensions for multi material deposition.

4.3.1. Powder flow in hoppers

Hoppers allow for accurate placement of the powder particles on the substrate while providing an effective storage area and continuous delivery of powder on to the build platform. There are two flow patterns that occur in powder hoppers, funnel flow (Figure 4.3.1a) and mass flow (Figure 4.3.1b) patterns.

Funnel flow occurs in hoppers when an active flow channel forms above the outlet while non-flowing powder stagnates on the hopper walls. Funnel flow forms when the hopper wall angles are too shallow or as result of rough hopper wall surface finishes. Rough hopper wall surface finishes increase the friction between the hopper wall and the powder particles, causing flow restriction. A mass flow pattern occurs when all the powder in the hopper is in motion, powder from the centre as well as from the hopper walls moves toward the outlet. The mass flow pattern provides steady, uniform well controlled discharge of powder, eliminating stagnant powder particles. The resulting flow pattern is a function of the powder properties and the interaction of the powder with the hopper wall. A hopper could exhibit mass flow with a specific powder and funnel flow with a different powder. The main factors influencing the type of flow pattern is the wall friction coefficients and the powder internal friction. Particle size and shape, moisture content as well as the wall surface influence the wall friction coefficient.

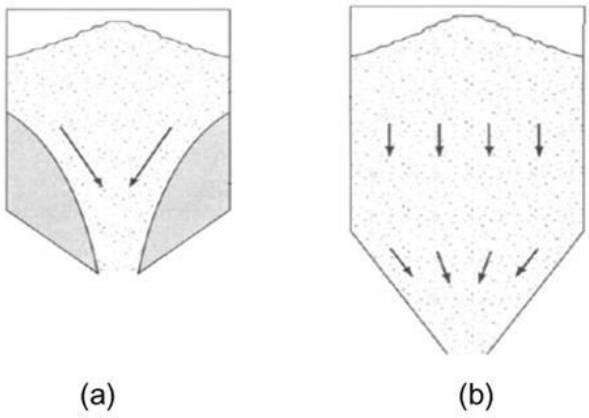

Figure 4.3.1. Flow patterns of hoppers (a) funnel flow (b) mass flow (Visagie & Smal, 2014)

Arching, rat-holing and segregation of the material are most common conditions causing powder to stop flowing in hoppers (Figure 4.3.2). Material properties (particle shape, size and size distribution) as well as hopper conditions (wall material, wall angle and outlet dimensions) influence the type and rate of flow. Fine powder flow is difficult to estimate due to the vast amount of factors influencing the flow rate and flow conditions. Smaller particles are greatly affected by inter-particle forces such as electrostatic and moisture which effect flow dramatically. Arching occurs when the outlet dimensions of a hopper are too small so that a stable arch forms above the outlet of the hopper. This happens because the forces between the powder particles cannot overcome gravity (Royal & Carson, 2000).

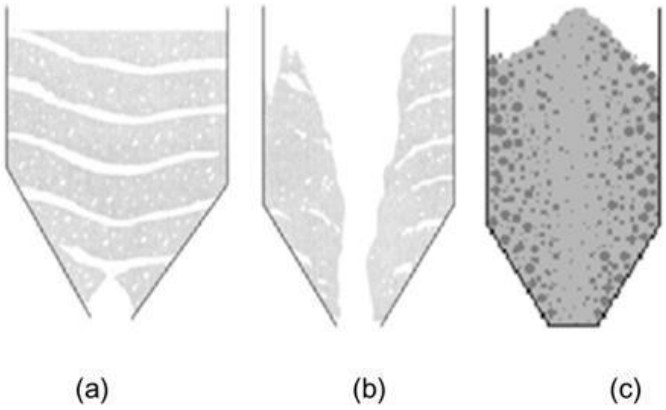

Figure 4.3.2. Conditions of non-flow in hoppers (a) arching (b) rat-holing and (c) segregation (Visagie & Smal, 2014)

Two forms of arching are found: interlocking and cohesive arching. Interlocking arching is when particles lock together mechanically; this is more applicable to larger sharp irregular shaped particles (Figure 4.3.3). Cohesive arching is caused by inter-particle forces (physical, chemical and electrostatic) that form between smaller powder particles. These forces cause the powder particles to bond together thus restricting the flow. Rat-holing is when there is only flow in a channel located above the outlet. As soon as the central flow channel has emptied, all flow from the hopper will stop flowing. Rat-holing occurs when the angles of the hopper wall are too high or if the wall friction is too large. Segregation occurs when the powder in the hopper has a large particle size distribution or if multiple powders are present in the hopper.

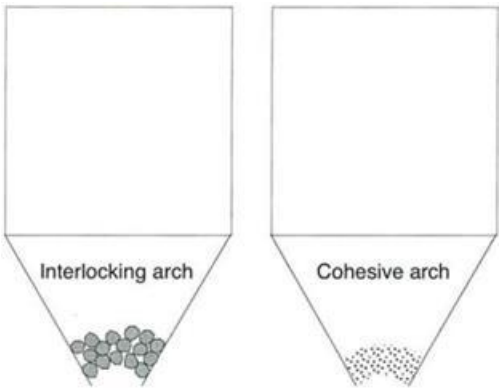

Figure 4.3.3. Interlocking and cohesive arching (Marinelli & Carson, 1992)

Visagie & Smal (2014) conducted an investigation on hopper design for powder delivery in additive manufacturing using a stainless steel hopper (Figure 4.3.4) with adjustable wall angles and slot opening sizes. The flowability powders such as Ti6Al4V, stainless steel 410, Inconel 718 and Haynes 31 powder alloy were investigated. Each powder's flow rate was recorded at different slot sizes and hopper wall angles. Concluding that powders with higher density and narrower particle size distribution had better flowability. The Ti6Al4V had an average particle size of d_{50} = 35 µm with particle sizes ranging from 20 – 60 µm (Figure 4.3.5). Finally concluding that flow rate is directly proportional to the outlet dimension if the hopper wall material is the same (Figure 4.3.6). The moisture, wall composition and surface roughness have an effect on the flow of powders (Lumay *et al.*, 2012).

According to Seville *et al.* (1997), the inter particle forces may potentially exceed particle weight for particles below 1 mm in size. Van der Waals force is an attractive force between atoms or nonpolar molecules caused by a temporary change in dipole moment arising from a brief shift of orbital electrons to one side of one atom or molecule, creating a similar shift in adjacent atoms or molecules. Surface structure or roughness was found to have a major impact on flowability in comparison to particle shape and size distribution in studies done by Popov *et al.* (1996) and Oshima *et al.* (1995). Not only the particle size, shape and size distribution of the powders display a large influence on the powder flowability but also particle surface properties such as roughness, chemical composition and the presence of liquid on the surface of the particles (Yablokova *et al.*, 2015).

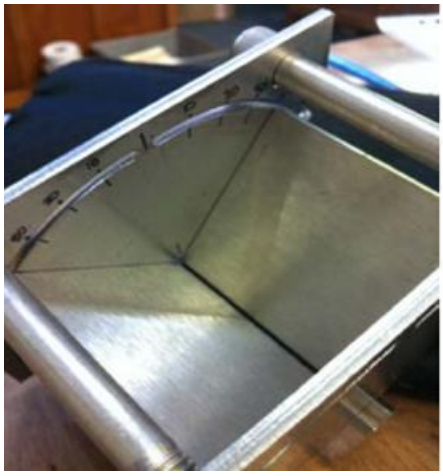

Figure 4.3.4. Top view of experimental hopper (Visagie & Smal, 2014)

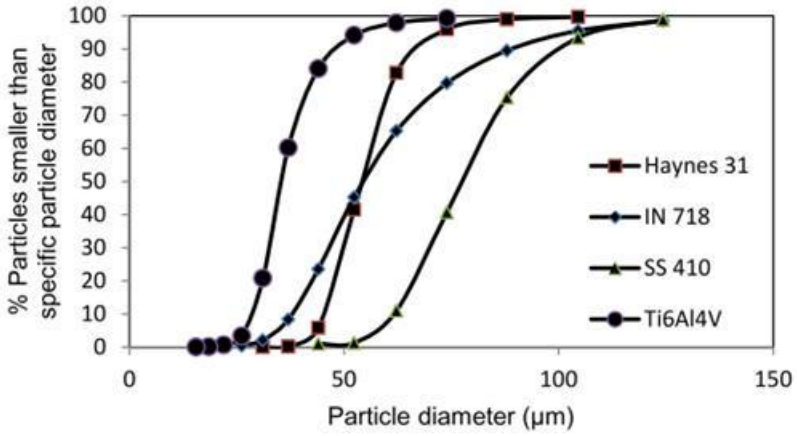

Figure 4.3.5. Particle size distributions of employed powders (Visagie & Smal, 2014)

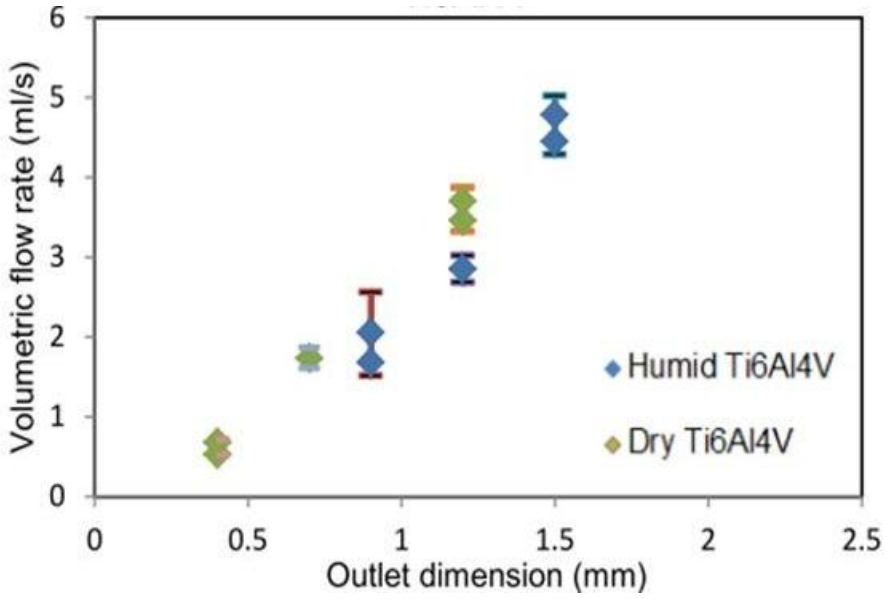

Figure 4.3.6. Volumetric flow rate of dried and humid Ti6Al4V powder at different slot sizes (Visagie & Smal, 2014)

4.3.2. Characterization of powder flow

To characterize powder flow, values such as Hausner's ratio, Carr index, angle of response and powder flow factor are used to numerically represent the flow of powder (Table 4.3.1). Other indicators of flow are particle size, particle size distribution and the shape of the particles.

Table 4.3.1. Characterization of powder flow (Carr, 1965; Hausner, 1967; Cain, 2002; Popov *et al.*, 2003)

Flow properties	Hausner ratio	Carr's index, %	Angle of repose, °	Flow factor
Excellent flowing	1-1.25	5-10	25-30	>10
Good (free-flowing)	1-1.25	11-15	30-38	>10
Fairly flowing	1.25-1.4	16-20	38-45	4-10
Passable flowing (cohesive)	>1.4	21-25	45-55	2-4
Poor, very cohesive (or non-flowing)	>1.4	26-31	>55	<2

In most cases the compressibility of a powder is a good indicator of powder flow and is often expressed numerically using the Hausner ratio and Carr index. Powders with higher compressibility exhibit stronger inter-particle forces which almost always result in poor flowability. Hausner ratio is the ratio between the tapped and bulk density of a specific powder.

A Hausner ratio of <1.25 indicates a powder that is free flowing while powder with values > 1.25 indicate weaker powder flow. Likewise Carr index refers to the difference between the tap density and the bulk density as a percentage of the tap density. Powders with smaller Carr index values have better flow properties, whilst powders with values <15% tend to be free flowing (Hassan & Lau, 2009).

$$Hausner\ ratio = \frac{\rho_{tap}}{\rho_{apparent}}$$

$$Carr\ index = \frac{\rho_{tap} - \rho_{apparent}}{\rho_{tap}} \times 100\%$$

The angle of response is a measure of cohesiveness of a specific powder to predict the flowability. Cohesiveness refers to particles being attracted to one another due to inter-particle forces. Angle of repose is defined as the angle between the horizontal and the slope of a heap of powder particles dropped from a predetermined height. Smaller angles (25°–38°) indicate better flow properties and lower cohesive forces while larger angles indicate poor flow properties (>55°). An increase in moisture content and electrostatic charge (from handling the material) result in higher angles of response. The angle of repose is determined experimentally by allowing a volume of powder to flow onto a flat surface, and then measuring the angle with respect to horizontal. Thalberg (2004) showed that the angle of repose is directly proportional to Hausner Ratio, thus indicating that both methods agree with each other and are relevant indicator of powder flow for fine powders (Figure 4.3.7).

Powders consisting of regularly shaped particles flow better than those consisting of irregularly shaped particles. Spherical shaped powder particles tend to be better for continuous powder flow. Course powder particles in most cases have better flow properties than fine powders (< 100µm). Fine particles tend to be more cohesive and therefore less free-flowing. Powders with narrow particle size distributions flow better than powders with wide particle size distributions (Yablokova *et al.*, 2015).

The Hall flow meter funnel described in ASTM B213-11 is a common method of characterizing different powders flow properties (Figure 4.3.8). The Hall flow meter funnel characterizes powder by the flow rate through a standard setup with a predetermined volume of powder. The flow rate is determined by timing the flow of powder through the opening (2.54 mm) once

opened and stop timing as soon as the last of the powder has exited the opening. ASTM specifies measuring the flow by volume instead of by mass thus eliminating the effect of powder density (Cooke & Slotwinski, 2012).

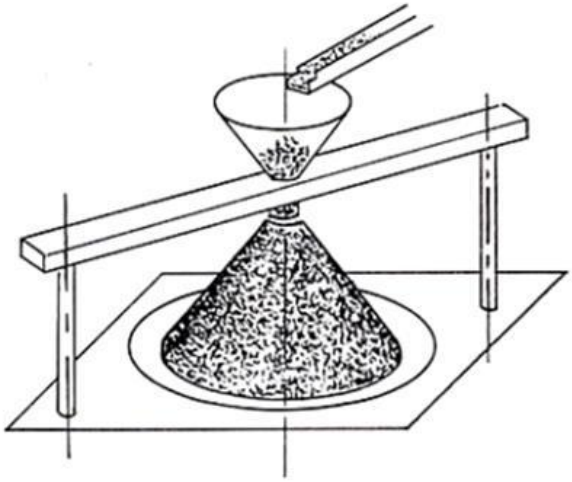

(a)

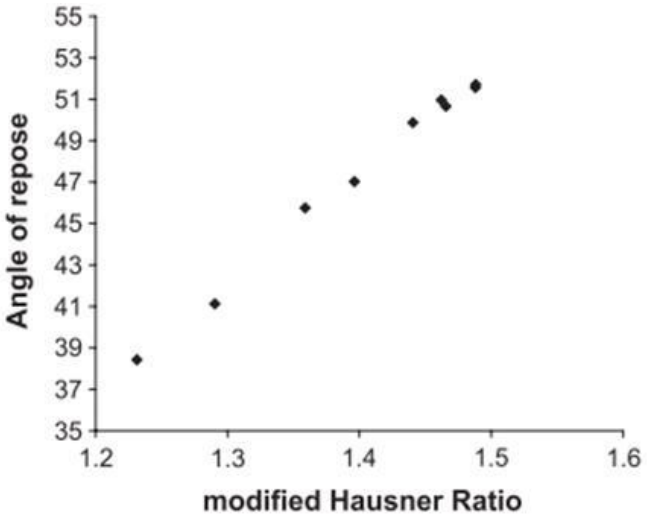

(b)

Figure 4.3.7. Setup for measuring angle of repose (a) and correlation between angle of repose and Hausner ratio (Thalberg *et al.*, 2004)

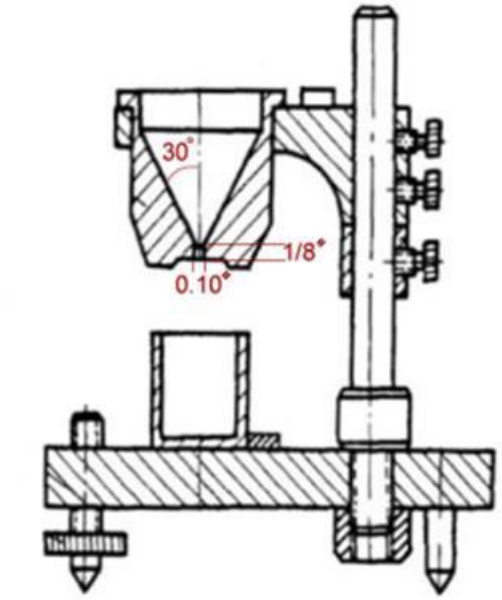

Figure 4.3.8. Hall flowmeter funnel (ASTM B213-11)

Jiang *et al.* (2009) developed a system for evaluating powder flowability based on a vibrating capillary tube. The system is based on the fact that powders with better flowability need less vibration to reach a predetermined flow rate. Different powders are compared by critical vibration acceleration. Powders with low values of critical vibration acceleration have greater flow properties. The vibration is controlled by a computer and the frequency of the capillary tube is measured with the non-contact vibration senor. The mass of the particles discharged from the capillary tube is measured with a digital scale. When comparing results from the vibration methods to the angle of repose of the same powders, the findings were similar but the vibration method had a higher level of accuracy.

A Jenike shear cell measures variation in shear stress between the powder particles. According to Bell (1999), Jenike's testing methods was proven to be a valid and repeatable method of comparing different powders flow properties. Behera *et al.* (2002) showed that the Jenike shear cell provides measurements of powder cohesive properties that can be used to design effective hoppers to prevent arching and rat-holing formation. The powder with greater cohesion forces require larger hopper openings to produces the same flow rate as powders with less cohesive forces.

The procedure outlined for the Jenike shear cell can be found in the ASTM standard D 6128-00. The apparatus consists of a base ring, upper shear ring and an applied normal force (Figure 4.3.9). The upper shear ring is fixed, whereas the lower base plate can move in a specific direction at a fixed shear rate which is controlled and monitored. A normal force is applied at the upper surface of the powder, allowing the shear behavior of the powder to be determined at various consolidating stresses.

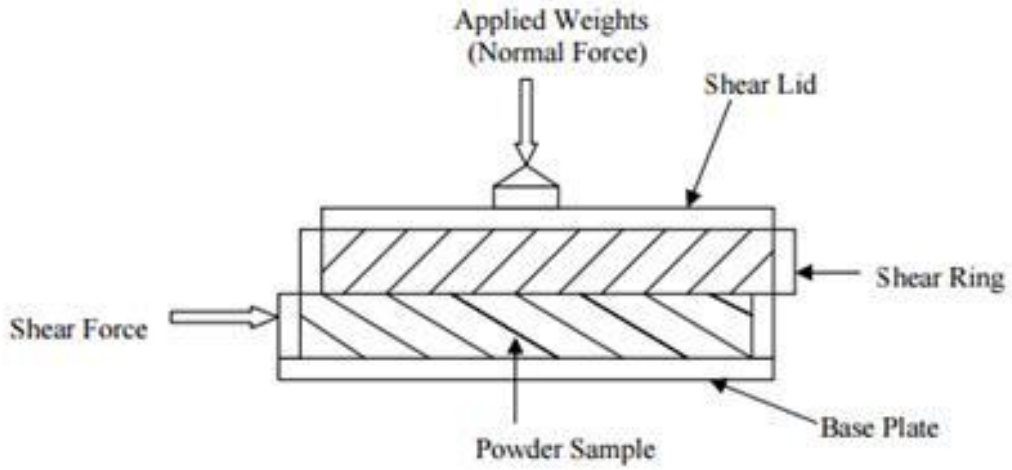

Figure 4.3.9. Janike shear cell (Bell, 1999)

4.4. Influence of the hopper geometrical characteristics on powder flow

4.4.1. Experimental setup

To determine the optimal hopper parameters for free flow condition an experimental hopper was designed. Due to the fact that powder flowability is directly influenced by the equipment it comes in contact with, the experimental hopper was manufactured to similar sizes and material composition as the hopper proposed for the multi powder deposition system. The experimental hopper was manufactured to have a variable slot width and adjustable wall angle. By comparing the powder flow rates at different slot widths and hopper angles the optimal parameters can be determined.

The experimental hopper is designed to be accurately adjusted to slot sizes ranging from 0-3 mm and wall angles of 10-100 degrees between the two wall faces (Figure 4.4.1). The hopper design was refined using SolidWorks (CAD). The hopper walls were manufactured from aluminium on an EDM wire cutter. The EDM wire cutter utilizes a spark erosion process to accurately cut through material. The 6 mm perspex side plates were manufactured on a CNC milling machine.

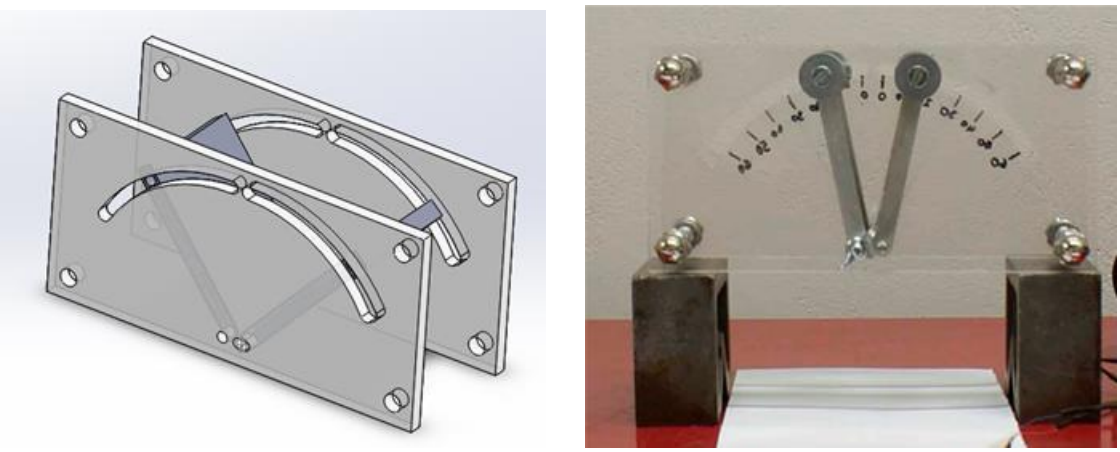

Figure 4.4.1. Experimental hopper with changeable wall angle

To produce accurate results the following experimental procedure was followed:

1. Clean work area so the there is no fine particles that can contaminate the employed powder.
2. Measure the temperature and humidity.
3. Measure the roughness of hopper wall surface.
4. Note particle size distribution and composition of powder.
5. Adjust hopper angle and slot size.
6. Place hopper on raise blocks.
7. Measure volume of powder.
8. Close outlet with stopper block.
9. Pour powder into hopper.
10. Start stop watch as soon as stopper block is removed.
11. Note if flow occurred.
12. Record the time taken for all powder to flow out the outlet.
13. Record flow rate.

14. Place powder into the becker again. Change the powder every third test to eliminate the electrostatic effect caused from handling the powder.
15. Blow the hopper clean with compressed air to remove left over powder.
16. Repeat experiment at the next hopper angle and slot size.

4.4.2. Results and discussion

Experiments were conducted at 23.3°C and 24% humidity of air for powder volume of 50 ml. The roughness of hopper wall surfaces was *Ra* = 2.63±0.1 µm and *Rz* =15.6±0.45 µm. Tests were conducted three times for each interval of hopper angle and slot width. Both Ti6Al4V and Cu powders experienced free flow for 2.5–3 mm slot size and 20°–60° hopper angles (Table 4.4.1). At 80°–100° powders left on the hopper (funnel flow, see Figure 4.4.2) since hopper wall angles are too shallow.

For a hopper angle of 30° flow had large deviations at 2.5 mm slot width for Ti6Al4V powder and 2 mm for Cu powder (Figure 4.4.3). These large deviations indicate unstable irregular flow. Probable reasons for this instability may include temporal arching or rat-holing. Mass flow was received for 60 degree hopper angle for both employed powders. Steady uniform well controlled powder flow occurred at this angle. Cu powder had a larger percentage of fine particles than that of Ti6Al4V powder (Figure 4.4.4.). Finer particles in most cases indicate weaker powder flowability. On the contrary, the results of the experiments indicated that Cu powder had higher volumetric flow rate than that of Ti6Al4V powder.

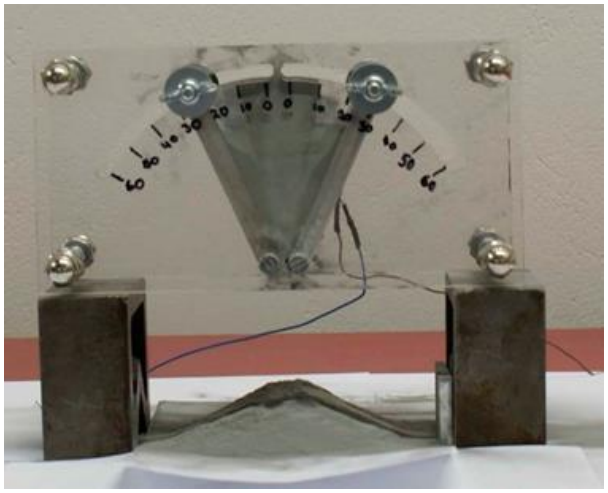

Figure 4.4.2 Experiment with powder flow

Table 4.4.1. Flow map and values of volumetric powder rates

Ti6Al4V powder

Slot width, mm / Angle, °	3	2.5	2	1.5	1
20	4.17	3.55			
	4.64	3.53			
	4.44	3.64			
30	5.88	2.99			
	5.78	4.43			
	5.81	3.50			
40	6.41	4.33			
	6.25	4.59			
	6.17	4.59			
60	8.62	6.17	3.82		
	8.47	6.06	3.31		
	8.62	5.75	3.03		
80	10.75	6.75			
	9.09	6.55			
	11.63	6.33			
100	12.59	10.10			
	13.12	8.93			
	14.93	10.73			

Cu powder

Slot width, mm / Angle, °	3	2.5	2	1.5	1
20	7.04	5.68	4.31		
	6.85	5.88	4.17		
	7.14	5.95	4.13		
30	7.46	5.75	4.63		
	7.25	5.43	3.65		
	7.14	5.68	4.35		
40	7.58	6.41	5.26		
	7.58	6.10	5.21		
	7.81	6.17	5.10		
60	9.09	7.14	5.38	2.78	
	8.93	7.25	5.21	2.86	
	9.26	6.94	5.15	2.73	
80	11.63	8.47	5.88	3.32	
	11.36	8.33	5.49	3.29	
	11.36	8.20	5.62	3.33	
100	15.63	9.62	7.14	5.07	
	12.82	10.42	6.76	5.05	
	15.63	10.20	6.41	5.15	

	No flow
	Powder left on hopper
	Free flow

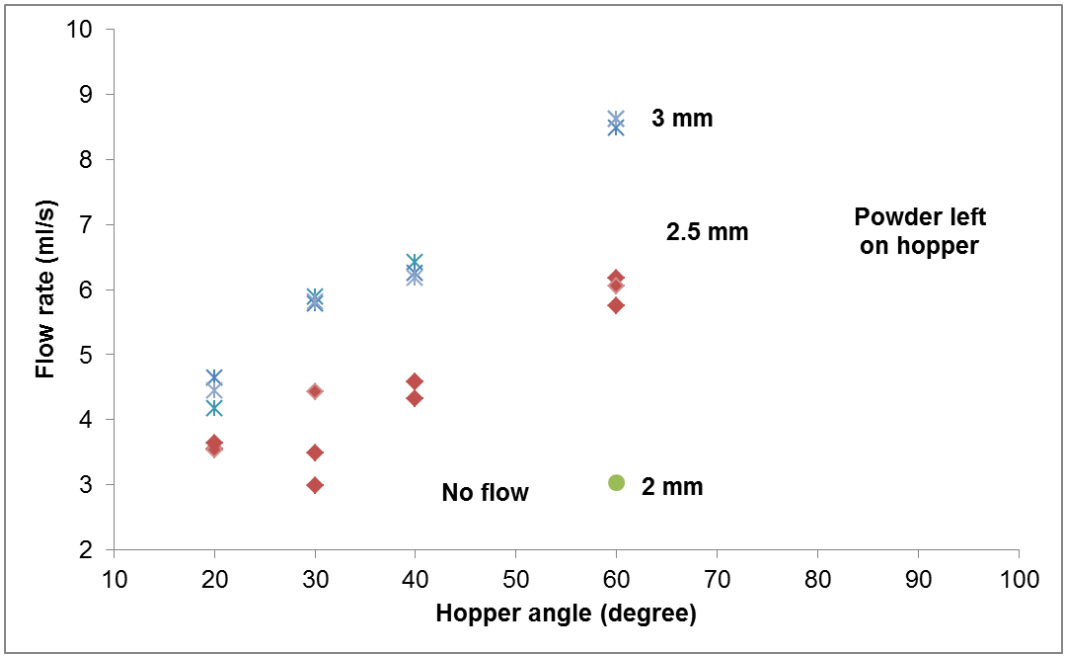

(a)

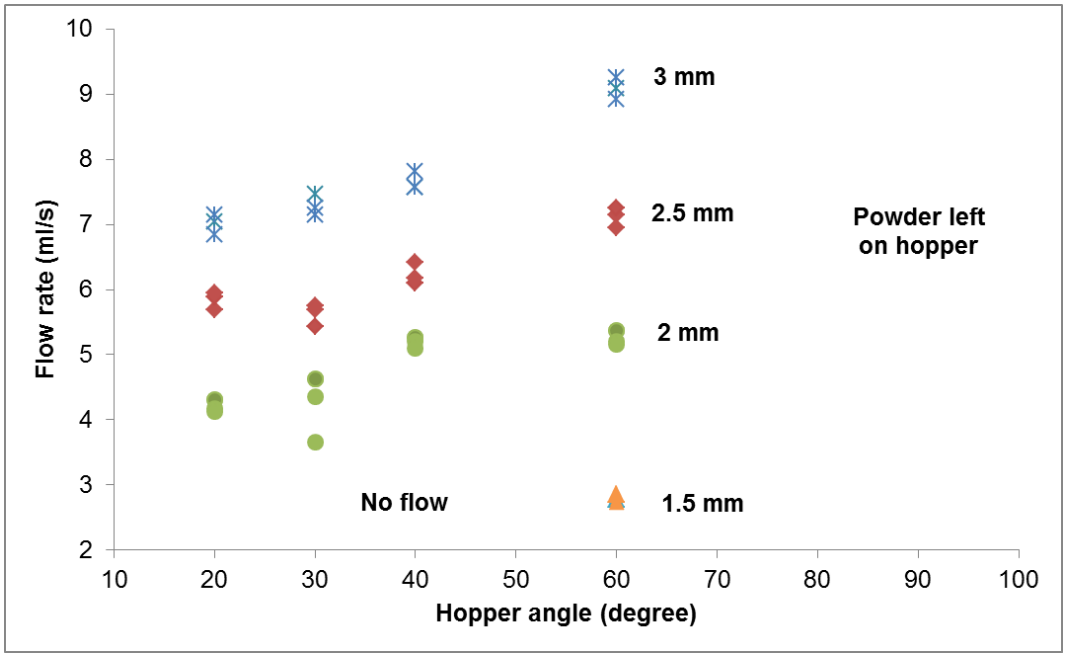

(b)

Figure 4.4.3. Flow rate of Ti6Al4V (a) and Cu (b) powders at different slot width and angles

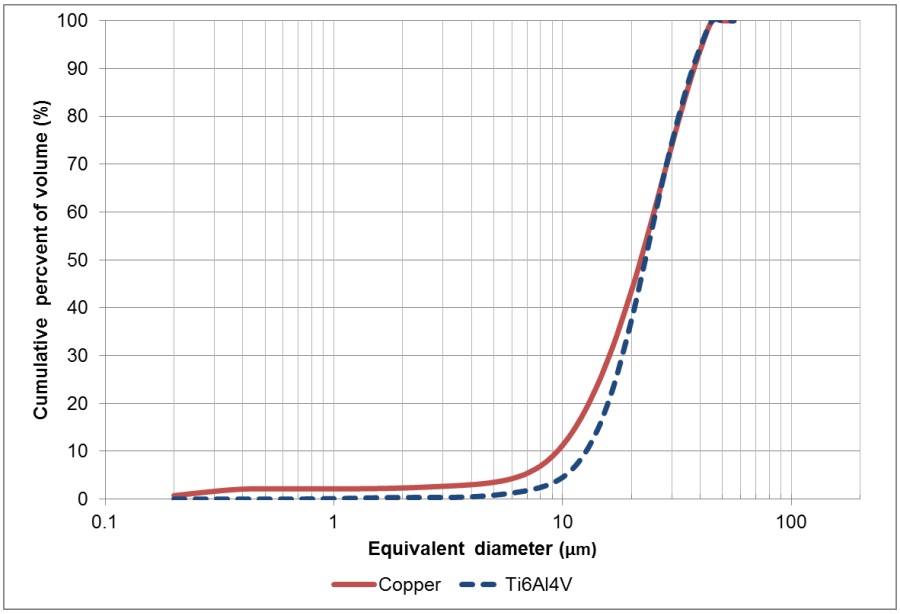

Figure 4.4.4. Particle size distribution for employed Cu and Ti6Al4V powders

Furthermore, the flow properties of the employed powders were compared. Hauser's ratio and Carr index were determined for each powder. To calculate Hauser's ratio and Carr's index the apparent and tap densities of the specific materials were obtained. Both employed powders showed good/excellent flow properties (Table 4.4.2). However, comparing the results of Cu to Ti6Al4V showed that they were very similar but Ti6Al4V indicated slightly better flow properties. This further implies that powder flow properties is not a good estimation of powder flow through hoppers. The hopper experiment indicated that Cu powder showed better results than Ti6Al4V powder, even though the powder size distribution and powder flow properties both indicated that Ti6Al4V powder would flow better than Cu powder.

Table 4.4.2. Powder flow properties of employed powders

Powder	ρ_{app}, g/cm^3	ρ_{tap}, g/cm^3	Hauser ratio	Carr index	Flow properties
Cu	4.76±0.06	5.39±0.02	1.13±0.02	11.6±1.4%	Good/Excellent flowing
Ti6Al4V (ELI)	2.51±0.01	2.79	1.11	10%	Excellent flowing

Possible reasons for Cu flowing better than Ti6Al4V may include oxidation, shape and morphology of particles as well as density of the material. The oxidation behaviour of the

employed materials may have an influence on powder flow rates (Figure 4.4.5). Oxide films can be formed during handling of the powders if a protective atmosphere is not utilized. A passive oxide film grows spontaneously on the surface of Ti and its alloy when the Ti is exposed to air at room temperature. These films are very thin (5-10 nm thickness). These films composes of 3 layers: 1) TiO – the first layer adjacent to metallic Ti, 2) an intermediary layer of Ti_2O_3, and 3) TiO_2 layer, which is in contact with the environment (Pouilleau *et al.*, 1997; Feng *et al.*, 2003; Cheng & Roscae, 2005). At room temperature, TiO_2 is the most important layer in protecting the Ti from further oxidation. The surface oxide film on Ti formed by air is so protective that the further oxidation of Ti is prevented in various circumstances and mediums. Even during sterilization in an autoclave under a saturated water vapor pressure at 120 °C for 1.8 ks, oxidation of Ti does not proceed (Gemelli & Camargo, 2007). For biomedical applications this TiO_2 layer is also responsible for the integration of human bone cell with the Ti implant interface.

White & Germar (1942) studied the rate of oxidation of Cu films at room temperature. It was shown that mass of oxidized Cu increased rapidly. A passive oxide film grows spontaneously on the surface of pure Cu at room temperature (Figure 4.4.5).

The presence of passive oxide films on Ti6Al4V and Cu powders can have an influence on electro charging of powders. Initially neutrally-charged powder particles are charged during the experiment, which may influence flow rates as the experiment progresses. Electrostatic charge can dissipate during time or inverse, to increase flowability of the fine powders (Freeman technology, 2014). Inter particulate forces are depend on the chemical composition of the particles, their shape and surface texture, bulk water content and processing history.

Both powders are similar in shape, both exhibiting spherical powder shapes (Figures 3.1.1 and 3.1.3). Taking into account all of the above mentioned factors it should be assumed that the better flowability of Cu powder was due to its higher density. The density of Cu powder is nearly twice as much as the density of Ti6Al4V powder. Density has a considerable effect on powder flow through free flow hopper since the particles of the powder fall freely due to gravity.

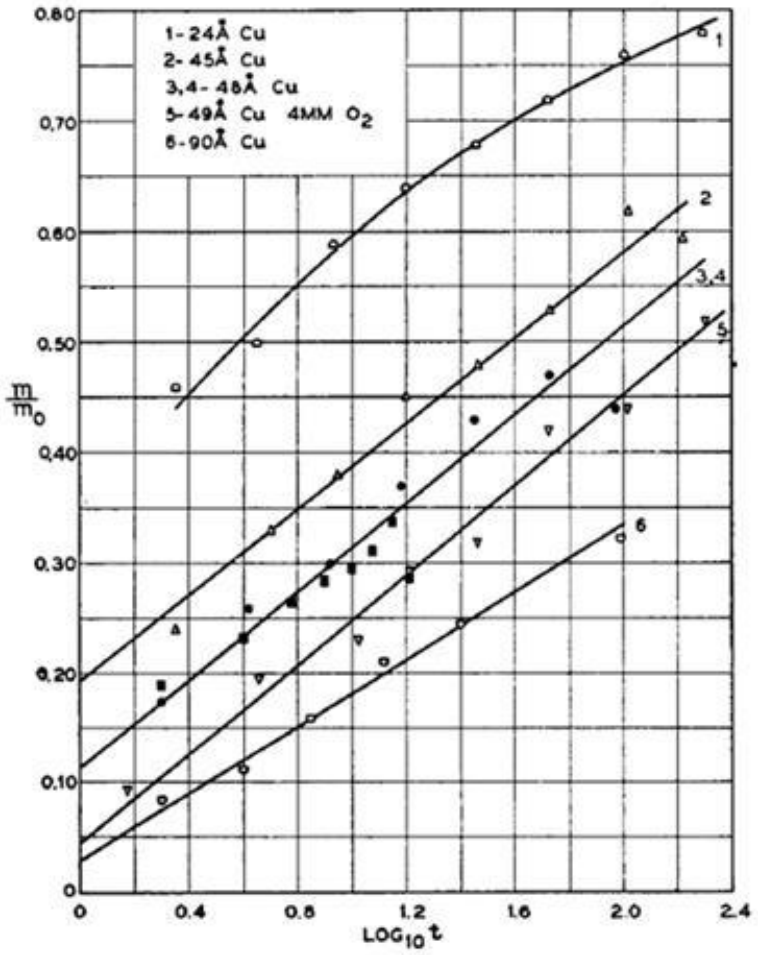

Log10t	0	0.4	0.8	1.2	1.6	2.0	2.4
min	1	2.5	6	16	40	100	250

Figure 4.4.5. Relation between the logarithm of the time of exposure (in minutes) of various Cu films to oxygen and the fraction, m/m_o, of the total amount of metal transformed to oxide, the pressure was 20 mm (White & Germar, 1942)

Materials with higher densities tend to have better flowability (Freeman technology, 2014). Both powders show stable and predictable flow rates at 3 mm slot width. At 60° hopper angle and 3mm slot width flow rates of Ti6Al4V and Cu powders had similar values (8.5-9 ml/s) (Figure 4.4.6). This may indicate that at a critical slot width (for a specific powder size distribution) external influences no longer have an effect on flow rate, and the only factor influencing the powders flow rate is the hoppers geometry (outlet dimensions and hopper wall angles).

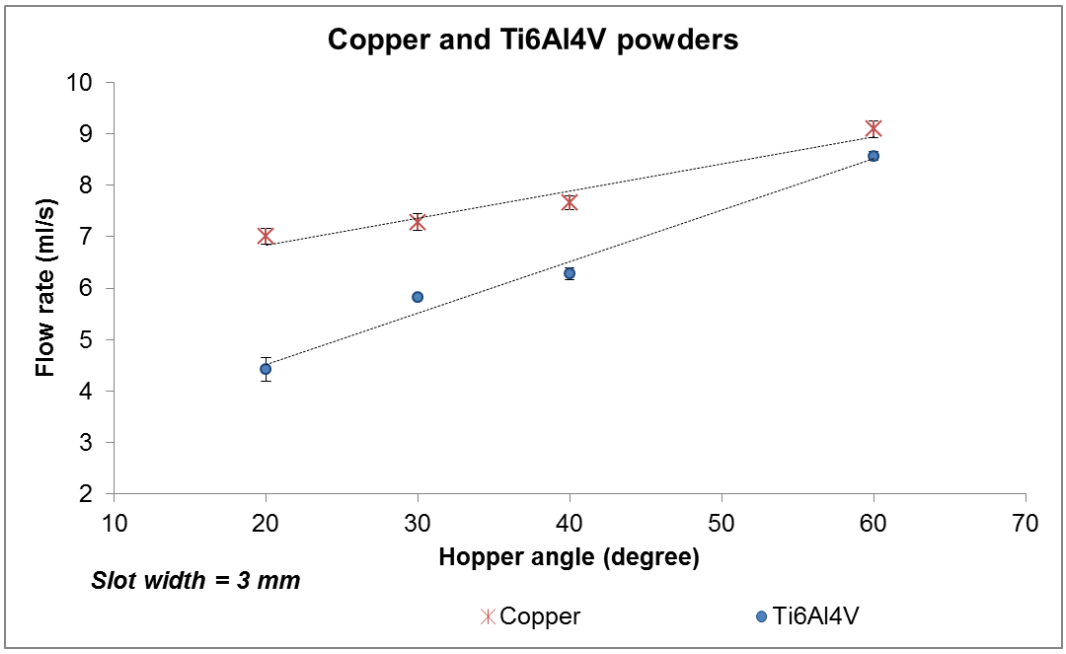

Figure 4.4.6. Particle size distributions of employed powders for hopper angle 60°

4.5. Validation of a hopper powder deposition system

4.5.1. Experimental setup

The aim of the second experiment was to verify the validity of the use of a multi hopper powder deposition system. Multiple materials were deposited onto a single layer to investigate the effect of different powder layer thickness and the interface where the two powders interchange.

Two prototype hoppers were designed on Solidworks (Figure 4.5.1). Both hoppers having a 3 mm slot width with a 50 mm slot length. The hoppers were manufactured on an EDM wire cutter from aluminium to have a 20° and 60° hopper angle. A steel 16 mm shaft was press fitted into the predetermined hole on the hopper. The shaft connects the prototype hopper to a X-Y controlled table (Figure 4.5.2). The X-Y controlled table allows the hopper to be moved accurately across the substrate at different speeds. A Magnum milling machine with an automated y-axis was adapted to be a setup X-Y controlled table. The milling machine has a Digital Read Out (DRO) that accurately determines the position. A Vertex 50 mm contact height gauge (Fig 4.5.2b) was used to position the hopper above the substrate. The Ti6Al4V substrate has a surface grinded finish with a surface roughness of Ra = 2.1±0.45 and Rz =12.1±0.8 µm.

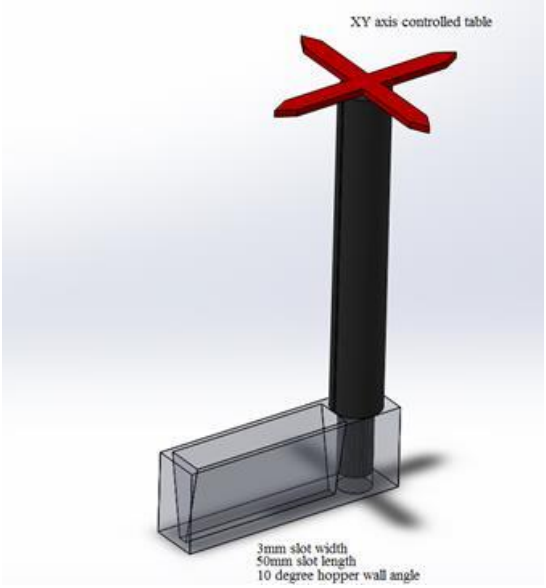

Figure 4.5.1 SolidWorks design of prototype hopper

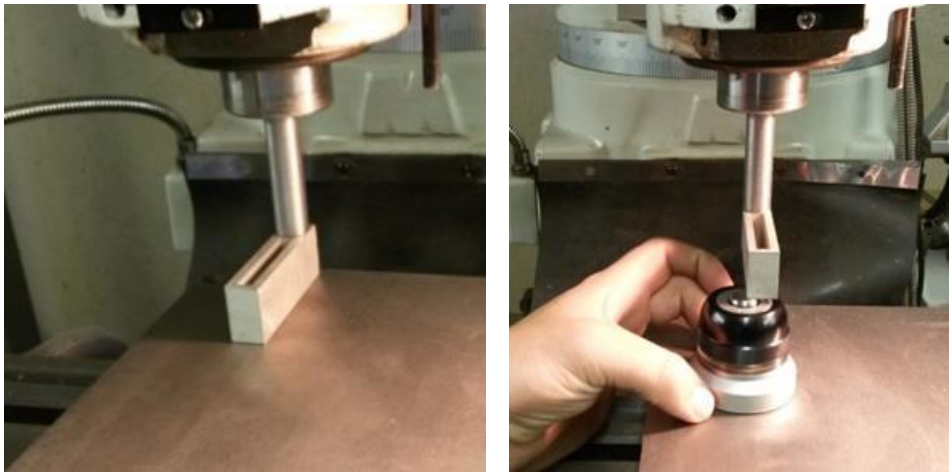

(a) (b)

Figure 4.5.2 (a) Prototype hopper connected to the X-Y controlled table; (b) Vertex height gauge

To deposit two materials onto a substrate the following experimental procedure was followed:

1. Clean substrate with compressed air and alcohol.
2. Clean milling machine with compressed air and wipe the bed clean. This is to ensure that there is no dirt or dust to affect the accuracy.
3. Clamp substrate onto the working area of the milling machine.

4. Clamp the experiment hopper onto the milling machine. The milling machine connects to the hopper with a 16 mm collet.
5. The hopper is straightened using a dial gauge.
6. The hoppers height relative to the substrate is determined using the 50 mm height gauge and the DRO.
7. The hopper is moved accurately to the correct position using the DRO.
8. The first material is deposited in the desired areas.
9. The experimental hopper is cleaned using tissue paper. This is to remove all the previous powder.
10. The second material is deposited in the desired area.
11. A camera with a microscopic lens is used to record the material interface and layer homogeneity.
12. The same procedure was followed for both the 20° and 60° hoppers.

4.5.2. Results and discussion

Two hoppers from Al were manufactured with 20° and 60° angles to investigate the effects of hopper flow rate on powder surface morphology and the interface created between the two powders. Ti6Al4V powder was deposited onto Ti6Al4V substrate at different layer thicknesses (50–350 µm). The substrate was placed on CNC controlled table. The CNC table had a constant speed of 0.008 m/s. When depositing the 50 mm wide powder layer strips it was noticed that the edges of the strips slightly crumbles for the 20° hopper (Fig. 4.5.3). For thicker layers the shedding effect was more significant, which subsequently could lead to undesirable effects when depositing the next powder. When comparing the powder stripes delivered with the 60° hopper and the 20° hopper it is clear that the 60° hopper had more accurate powder stripe edges. Hence it can be concluded that insufficient unstable flow rates lead to undesired surface morphology and inaccurate powder interfaces.

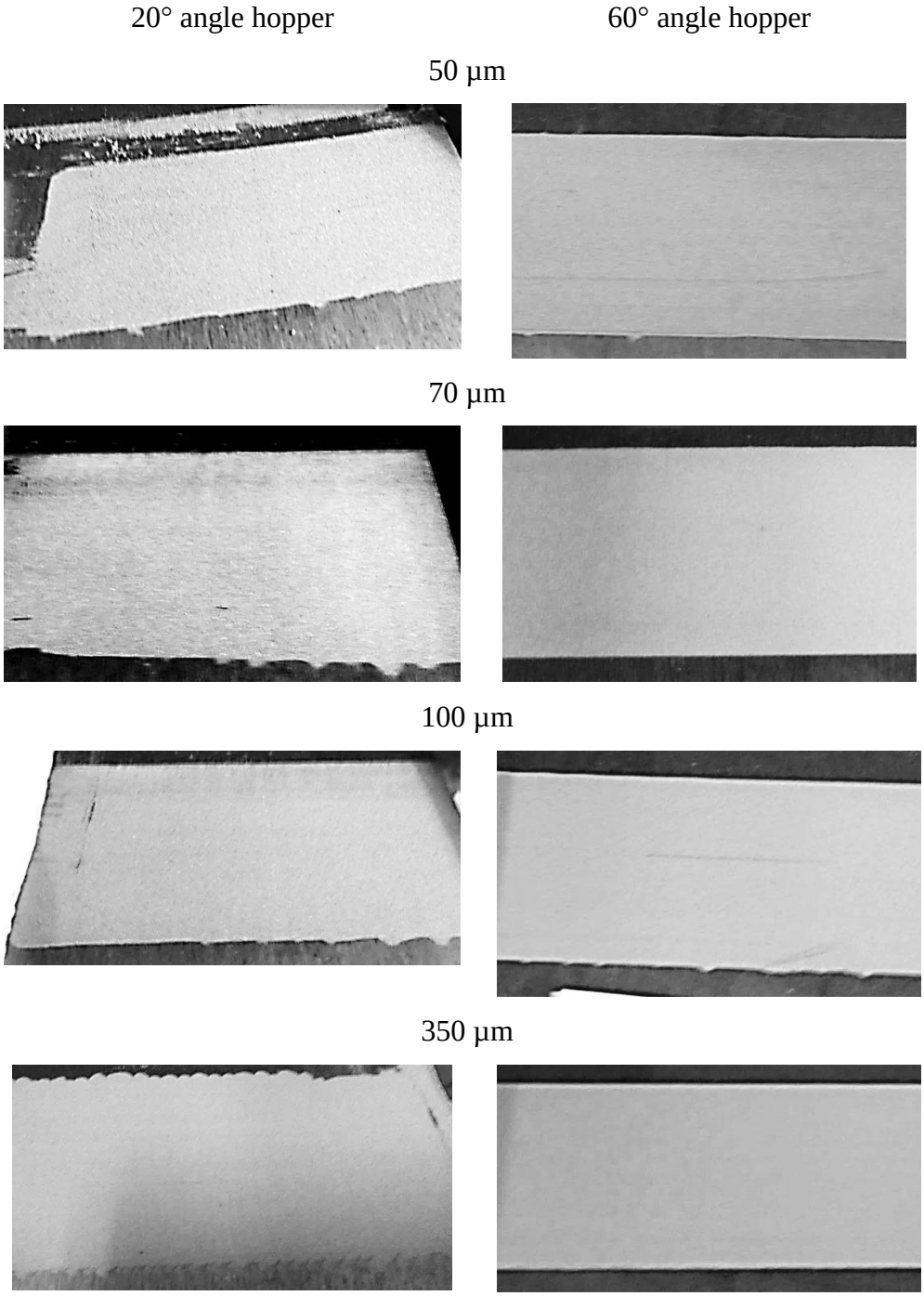

Fig. 4.5.3. Delivered Ti6Al4V powder layer at different layer thickness by 20° and 60° angle hoppers

A sharp interface is visible when depositing powder strips next to each other. When the Ti6Al4V powder followed the Cu powder on the same track and inadequate interface is noted. The Cu powder was deposited for the first 60 mm of the strip from the substrate edge and then retracted

till past the substrate edge. The hopper was then emptied, cleaned and moved to 63 mm (the slot has a 3 mm width) from the substrate edge so that there would be no Cu powder below the hopper, and so theoretically forming a sharp interface when introducing the Ti6Al4V powder. The hopper's back edge that was still over the Cu powder dragged some of the Cu powder particles over the interface causing the deformed interface (Fig. 4.5.4). The surface area between the hopper and the substrate should be as small as possible to reduce the dragging of the powders particles. In general, the elaborated multiple material powder delivery system based on hopper deposition, produced smooth, consistent powder thickness layers from different powders.

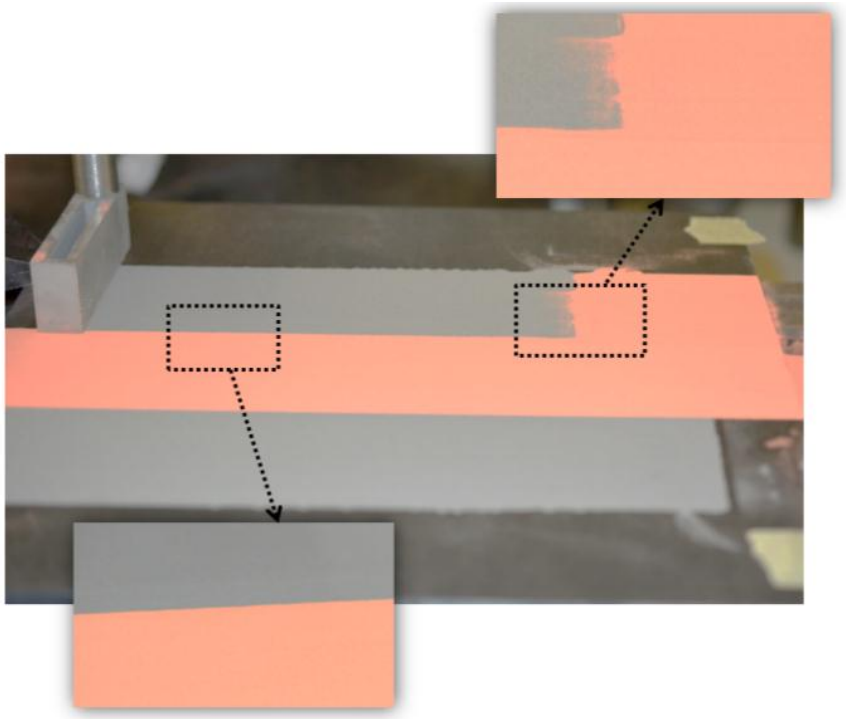

Figure 4.5.4. A consistent deposition of Ti6Al4V and Cu powders

Deposited layers of Ti6Al4V and Cu powders were homogenous, without visible naked spots or voids (Figure 4.5.5). In the first attempt to deposit multiple powders a small step was noted on the Ti6Al4V stripe of powder. Closer investigation showed that this step was caused from the hopper not being aligned exactly parallel to the substrate (Figure 4.5.5c). For the final multiple hopper powder deposition system care should be taken to create a system that is easily aligned to remove such inaccuracies.

(a) (b) (c)

Figure 4.5.5. (a,c) 50 µm deposited layers: Ti6Al4V alloy and (b) Cu powder

4.6. Final hopper design

From the experiments a clear design specification was formed:

- The hopper needs a 3 mm slot width and 60° hopper angle.
- The slot length must vary between 0-30 mm to ensure a time efficient yet accurate process.
- Minimal contact of the variable slot on the powder surface is required to reduce surface imperfections.
- A mechanism is needed to accurately align the hopper with the substrate.

Figure 4.6.1 indicates the critical dimensions of the variable hopper.

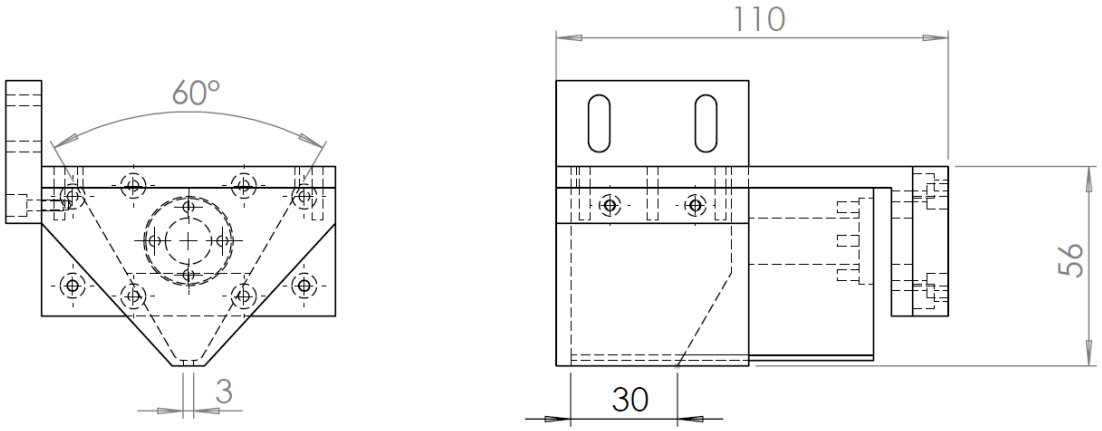

Figure 4.6.1. Final hopper dimensions

To form a final design, SolidWorks was used to create a CAD model. The final design will consist of a hopper, variable hopper wall, mounting plate, aligning plate as well as Nema17 stepper motor with lead screw (Figure 4.6.2a). The section view of the hopper assembly can be seen in Figure 4.6.2b.

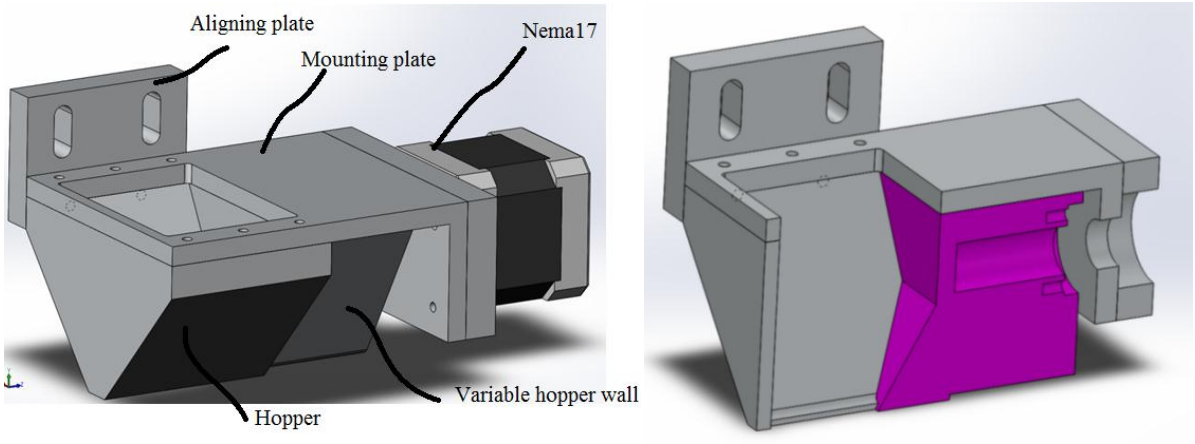

(a) (b)

Figure 4.6.2. (a) Assembled powder hopper with variable slot length; (b) Section view of powder hopper

The variable hopper wall moves within the hopper. This allows for minimal contact with the powder surface. The hopper wall is varied with a lead screw and NEMA17 stepper motor. The NEMA17 has holding torque 0.65 Nm and a 1.8 degree step angle. The 8 mm lead screw has a 2 mm pitch. This implies that the system has a 10 µm resolution on the slot length. By rotating the stepper motor a linear motion is caused between the hopper and the hopper wall via the lead screw. This linear motion selectively changes the slot length as required. The hopper and Nema17 stepper motor are kept in place with the mounting plate. The hopper is aligned to the substrate via the slots on the aligning plate and 5 mm hex socket bolts. Multiple hoppers are bolted to a CNC controlled platform.

4.7. Conclusion

A multiple hopper powder deposition system is proposed for multi material powder delivering for DMLS. The system deposits a homogeneous powder layer with a sharp interlocking powder interface.

When considering a hopper system for multiple powder deposition, the flow of powder becomes an important factor. If hopper parameters are incorrect, rat-holing or arching occur, which, in turn, cause no-flow or irregular unstable flow of the powder. To compare powder flow, Hauser ratio, Carr index, angle of response and powder flow factor are methods used to predict powder flow. However, these methods only take into account the powder flow properties and not the equipment used to handle the material. To make relevant design decisions and to find optimal hopper parameters for employed powders, series of experiments were conducted. It was determined that Cu powder had better flowability than Ti6Al4V for the specific hopper design. Since the Cu and Ti6Al4V powder had similar particle size distribution, both powders were spherical in shape. The final conclusion is that the better flowability of Cu powder was due to its higher density.

After noting the flow rate of different powders at different intervals of slot width and hopper angles the following conclusions can be deduced. Firstly, the flow rate and stability of flow increases with an increase in slot width. The larger the slot width becomes the easier it is to handle and predict the flow of powder. Secondly, the larger the hopper angle becomes the greater the flow rate, but only up and till a point where powder stays behind on the hopper wall. Thirdly, the optimal hopper parameters for both Cu and Ti6Al4V were found to be a 3 mm slot width and 60° hopper angle. The 3 mm slot width produced the most repeatable results and the 60° hopper wall angle provided good flow rates with no rat-holing or arching. The flow rate of Cu and Ti6Al4V at 3 mm slot width and 60° hopper angle was 8.5-9.0 ml/s.

Successfully depositing Cu and Ti6Al4V powder patterns on a substrate validates the idea of multi material hopper deposition with different thickness (50–350 μm). It was noted that thinner layer thicknesses produce more accurate powder deposition. Laying powder strips next to each other leads to a sharp powder interface line in depositing direction (X-direction). Further study is

needed to produce sharp interfaces where one material continues on the same powder strip (Y-direction).

A final hopper design was produced from the design specification determined in the experiments. The hopper has a variable wall that moves with in the hopper to allow for minimal friction between the powder surface and the hoppers variable slot. The hopper has a 3 mm slot width, 60° hopper wall angle and a maximum slot length of 30 mm.

4.8. References

Behera, S., Das, S., Hatvani, Z. & Pahl, M.H., 2002. Flowability-Flowability Studies of Bulk Materials for Design of Hopper Using a Jenike Shear Cell. Powder Handling and Processing, 14(2), pp.96-101.

Bell, T.A., 1999. Powder handling-industrial needs in solids flow for the 21st Century. Powder Handling and Processing, 11(1), pp.9-12.

Cain, J., 2002. Flowability testing-an alternative technique for determining ANSI/CEMA Standard 550 flowability ratings for granular materials. Powder Handling and Processing, 14(3), pp.218-221.

Carr, R.L., 1965. Classifying flow properties of solids. Chemical Engineering, 72 (3), pp. 69-72.

Cheng, X. & Roscae, S.G., 2005. Corrosion behavior of titanium in the presence of calcium phosphate and serum proteins. Biomaterials, 26, pp. 7350-7356.

Cooke, A. & Slotwinski, J., 2012. Properties of metal powders for additive manufacturing: a review of the state of the art of metal powder property testing. US Department of Commerce, National Institute of Standards and Technology.

Feng, B., Weng, J., Yang, B.C., Chen, J.Y., Zhao, J.Z., He, L., Qi, S.K. & Zhang, X.D., 2002. Surface characterization of titanium and adsorption of bovine serum albumin. Materials Characterization, 49(2), pp.129-137.

Freeman Technology, 2014. Introduction to Powders. Available at: http:// www.freemantech.co.uk/ [Accessed May, 2015].

Gemelli, E. & Camargo, N.H.A., 2007. Oxidation kinetics of commercially pure titanium. Revista Matéria, 12 (3), pp. 525-531.

Hassan, M.S. & Lau, R.W.M., 2009. Effect of particle shape on dry particle inhalation: study of flowability, aerosolization, and deposition properties. AAPS PharmSciTech, 10(4), pp.1252-1262.

Hausner, H.H., 1967. Friction conditions in a mass of metal powders. International Journal of Powder Metallurgy, 3(4), pp. 7-13.

Jiang, Y., Matsusaka, S., Masuda, H. & Qian, Y., 2009. Development of measurement system for powder flowability based on vibrating capillary method. Powder Technology, 188(3), pp.242-247.

Kumar P., Beck, E. & Das, S., 2003. Preliminary investigations on the deposition of fine powders through miniature hopper-nozzles applied to multi-material solid freeform fabrication, Proc. Solid Freeform Fabrication, Austin, TX, USA..

Lumay, G., Boschini, F., Traina, K., Bontempi, S., Remy, J.C., Cloots, R. & Vandewalle, N., 2012. Measuring the flowing properties of powders and grains. Powder Technology, 224, pp.19-27.

Marinelli, J. & Carson, J.W., 1992. Solve solids flow problems in bins, hoppers, and feeders. Chemical Engineering Progress, 88, pp.22–28.

Oshima, T., Zang, Y. L., Hirota, M., Suzuki, M. & Nakagawa, T., 1995. The effect of the types of mills on the flowability of ground powders, Advanced Powder Technology, 6 (1), pp. 35-45.

Popov, K.I., Krstajic, N.V. & Cekerevac, M.I., 1996. The mechanism of formation of coarse and disperse electrodeposits. Modern Aspects of Electrochemistry, 30, pp.261-312.

Popov, K.I., Živković, P.M. & Krstić, S.B., 2003. The apparent density as a function of the specific surface of copper powder and the shape of the particle size distribution curve. Journal of the Serbian Chemical Society, 68(11), pp.903-907.

Pouilleau, J., Devilliers, D., Garrido, F., Durand-Vidal, S. & Mahé, E., 1997. Structure and composition of passive titanium oxide films. Materials Science and Engineering: B, 47(3), pp.235-243.

Royal, T.A. & Carson, J.W., 2000. Fine powder flow phenomena in bins, hoppers and processing vessels. Available at: http:// chemicalprocessing.com/ [Accessed April, 2015].

Seville, J., Tüzün, U. and Clift, R., 2012. Processing of particulate solids (Vol. 9). Springer Science & Business Media.

Thalberg, K., Lindholm, D. & Axelsson, A., 2004. Comparison of different flowability tests for powders for inhalation. Powder Technology, 146, pp.206–213.

Visagie, N. & Smal, C.A., 2014. Hopper design for metallic powders used in additive manufacturing processes. Proc. 15th RAPDASA, Stellenbosch, South Africa.

White, A.H. & Germer, L.H., 1942. The rate of oxidation of copper at room temperature. Transactions of The Electrochemical Society, 81(1), pp.305-319.

Yablokova, G., Speirs, M., Van Humbeeck, J., Kruth, J.P., Schrooten, J., Cloots, R., Boschini, F., Lumay, G. & Luyten, J., 2015. Rheological behavior of β-Ti and NiTi powders produced by atomization for SLM production of open porous orthopedic implants. Powder Technology, 283, pp.199-209.

Chapter 5. Ti6Al4V(ELI)-Cu STRUCTURES FOR BIOMEDICAL APPLICATIONS

5.1. Introduction

The way a material reacts with the surrounding biological tissue is all dependent on the properties of the specific material. Biomaterial properties such as mechanical properties, biocompatibility, wear and corrosive resistant properties, toxicity and antibacterial properties are important when selecting a biomaterial for a specific medical implant. Very rarely will a material contain all the properties needed for a medical implant. Materials with high corrosive and wear resistance commonly are toxic to the human body and have much higher mechanical properties than that of bone. Biocompatible materials often show signs of wear early after implantation. By applying more than one material on a medical implant a multiple property implant can be manufactured. Bacterial infections can occur immediately or years after orthopaedic or dental surgeries causing serious implications for the patients. Functionalizing implant interface surfaces with antibacterial properties may represent a promising strategy to reduce the risk of infections. By applying multiple material onto a single implant, multi-functional areas can be produced improving the body's response to the implant. It is challenging task to form multi biomaterial implants with conventional manufacturing techniques such as CNC machining and forging due to the complexity of the implant geometry. With the development of multi material DMLS a new world of antibacterial implant interfaces can be achieved. The layer by layer nature of DMLS will allow for the appropriate amount of material to be placed in the exact areas were infection is most likely to occur. Multi material implants will inhabit multiple properties making them more biocompatible and less harmful to the area of implantation while reducing the risk of bacterial infection.

This chapter is divided into two sections. Firstly, the processing of Ti6Al4V(ELI)-Cu structures; determining the optimal process-parameters for Cu single tracks on a Ti6Al4V substrate, as well as investigation of their effect on single track geometry. Secondly, Ti6Al4V(ELI)-Cu structures will be manufactured to validate the concept of a multi material implant interface that can reduce the risk of bacterial infection.

5.2. Applications of Ti6Al4V and Cu as biomedical materials

Biomedical materials are defined by the American National Institute of Health as "any substance or combination of substances, other than drugs, synthetic or natural in origin, which can be used for any period of time, which augments or replaces partially or totally any tissue, organ or function of the body, in order to maintain or improve the quality of life of the individual".

There are three main types of biomaterial namely, bio-tolerant materials, bio-active materials and bio-inert materials. Bio-tolerant materials refer to a material where the interface between the bone tissue and implant is separated by a fibrous layer of tissue. Bio-active materials refer to materials where chemical bonds with bone tissue are established. In other words, surrounding bone forms directly on to the interface surface of the implant. However bio-inert materials have direct contact with the surrounding bone tissue but there is no chemical reactions between the implant and the tissue (Bergmann & Stumpf, 2013). Alumina, zirconia, tantalum, niobium and titanium are all examples of bio-inert biomaterials.

Ti and its alloys are communally used in medical implants. Ti provides strong mechanical strength and good biocompatible that can be applied to orthopaedic and dental fields. Increased use of Ti alloys as biomaterials is occurring due to their superior biocompatibility and enhanced corrosion resistance when compared to more conventional stainless steels and cobalt-based alloys.

Williams (1999) Dictionary of Biomaterials refers to biocompatibility as "the ability of a biomaterial to perform its desired function with respect to a medical therapy, without eliciting any undesirable local or systemic effects in the recipient or beneficiary of that therapy, but generating the most appropriate beneficial cellular or tissue response to that specific situation, and optimizing the clinically relevant performance of that therapy".

Ti and its alloys have a higher elastic module than that of bone thus causing break down of the bone due to stress shielding. Stress shielding refers to the reduction in bone density as a result of removal of normal stress from the bone by an implant. By constructing a porous structure using the DMLS process the elastic modulus is reduced. The interconnected pores also reduce the weight of the implant and bone tissue grows in the pores increasing the integration of the bone and implant (Pattanayak *et al.*, 2011; Niinomi, 2008) .

Bandyopadhyay *et al.* (2010) produced samples of porous Ti structures to investigate the interaction between the Ti implant and the bone. After being implanted for 12 days, newly formed bone was observed on the porous Ti samples, which was directly bonded to the Ti walls of the samples.

Porous Ti structures are within the range of mechanical properties of bone, which reduces stress shielding. High-porous Ti structures (68–88% porosity) provide ample space for bone regeneration and secure fitment of the implant making Ti a well-established biomaterial. However, the poor fatigue strength and wear resistance of Ti alloys have nevertheless limited their biomedical use (Andani et al., 2014).

Yavari *et al.* (2013) studied the fatigue behavior of porous Ti alloy manufactured using DMLS which is commonly found in medical implants. A hydraulic test frame (Max 25 kN load at 15 Hz) was utilized to perform compression–compression fatigue tests. Loads were applied at 20-80% of the yield strength of the samples. The study concluded that the endurance limit of the porous structures are lower than that of solid Ti and that of some other porous Ti structures manufactured using other manufacturing techniques. This is due to the formation of regions of non-melted powder associated with the manufacturing DMLS process (Lipinski *et al.*, 2013). The endurance limit however increased with a decrease in porosity.

The most serious complication in implantation surgery is bacterial infection at the interface between the implant and the bone. By coating the interface with materials that inhabit antimicrobial properties is a promising method of preventing infection. Material such as silver, zinc and Cu have shown such antibacterial properties. The main advantage of using antibacterial materials is that it acts locally at the site of infection.

In the past silver fibres have been used to fight infection in wounds of burn victims. The local administration of silver was proven to reduce bacterial growth at the area of application. However silver has been found to have toxic effects towards human cells. Cu, unlike silver is a trace metal and is an essential component of several enzymes. However, Cu in excess is also toxic to the human body but in less effect compared to silver (MacKeen *et al.*, 1987).

Shirai *et al.* (2009) investigated the possibility of Cu coated implants as a method of reducing bacterial infection at the interface of medical implants. Firstly pure Cu coated pins were tested for biocompatibility. Test results proved that Cu-coated implants are unable to function as an anti-bacterial interface. The Cu-coated pins cause toxicity not only to the bacteria, but also to the healthy human cells. This toxicity was caused by the large amount of Cu-ions released at the interface. Shirai *et al.* (2009) suggested the use of a Ti-Cu alloy that only contained 1% Cu. The use of the alloy would decrease the amount of Cu-ions released but still be effective in bacterial breakdown at the implant interface while remaining biocompatible. The biocompatibility was tested by comparing the Ti-1%Cu pin with a pin made of pure Ti, which is known to inhabit good biocompatible properties. It was concluded that bone cellular formation had occurred normally on the Ti-1%Cu sample and was similar to that observed for pure Ti. In vivo studies of the Ti-1%Cu implanted into eight fully grown rabbits, showed good antibacterial properties as well as good biocompatibility. Blood tests also proved that the difference between the pre-operative and the post-operative blood Cu values was not statistically significant for the Ti-1%Cu. Due to the good biocompatibility and low cytotoxic activity, Ti-1%Cu shows particular promise as a biomaterial to decrease infection at the implant interface.

Jung *et al.* (2012, 2014) electrochemically deposited small amounts of Cu onto Ti discs to show the effect of Cu as an antibacterial agent. After 10 days of exposure to the Cu, bacteria such as *E. coli* K12 DH5α and *S. aureus* that cause infection experienced a dramatic decrease in growth. Demonstrating that antibacterial fictionalization of Ti implants by Cu is possible.

5.3. Processing Ti6Al4V–Cu structures with EOS M280

5.3.1. Experimental setup

Samples were manufactured with the EOS patented DMLS process utilizing an EOS M280 machine situated and operated at the CRPM at the Central University of Technology, Free State (Figure 5.3.1a, Table 5.3.1). A powder layer is deposited with a hard tool steel blade or soft carbon fibre brush from the powder platform to the build platform (Figure 5.3.1b). A laser then selectively melts the desired regions of powder on the build platform. By solidifying layers onto each other a 3D part is formed.

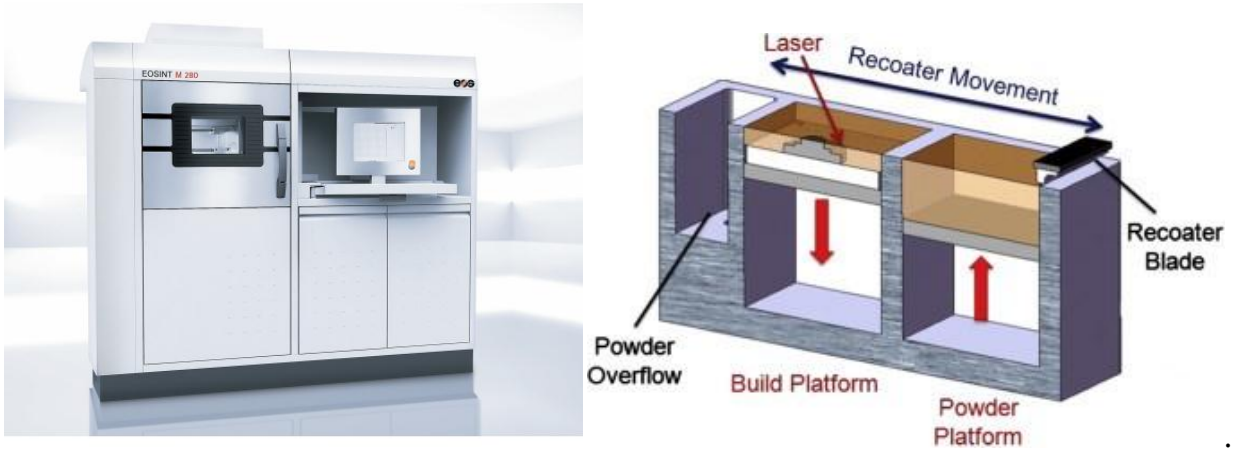

(a) (b)

Figure 5.3.1. EOS M28 machine (a) and delivering system (b)

EOS offers a range of application-optimized process-parameters for certain powders, such as Ti6Al4V, maraging steel MS1, Co-Cr alloys MP1 and SP2, Nickel alloys IN718 and IN625, AlSi10Mg and two stainless steel powders. The build strategy, laser power, scanning speed, hatch distance, layer thickness as well as build atmosphere (nitrogen/argon) are predetermined by EOS and cannot be changed by the user. EOS guaranties approximately 100 % relative density with prescribed standard parameters. With an open parameter set, the operator could change any of the machine parameters as needed and could be used for a variety of powders.

Table 5.3.1 Characteristics of EOS M280 machine (EOS, 2015)

EOS M280	
Building volume (incl. building platform)	250 mm x 250 mm x 325 mm
Laser type	Yb-fibre laser, 400 W power and 1075 nm wavelength
Precision optics	F-theta-lens, high-speed scanner
Scan speed during build process	up to 7.0 m/s (23 ft/s)
Laser beams profile	TEM00 Gaussian profile
Laser spot size	80 µm spot diameter
Power supply	32 A
Power consumption	maximum 8.5 kW / typically 3.2 kW
Nitrogen generator	integrate
Compressed air supply	7 000 hPa; 20 m3/h

Manufacturing procedure for EOS M280 System:

1. Clean Ti6Al4V substrate with Ethanol.
2. Attach the substrate to the M280 build platform with four allen cap bolts.
3. Level the platform and substrate using a dial gauge and the toggle switches below the build platform.
4. Determine starting height using the M280 interface and a feeler gauge.
5. Ensure recoater blade is damage free.
6. Deploy powder into powder delivery platform.
7. Compact powder.
8. Level powder.
9. Install Duct in front of building chamber and close chamber door.
10. Prepare slice data from CAD data using EOS RT tools.
11. Load slice data into EOS M280 interface via USB.
12. Flood chamber with Argon until oxygen content is below 0.01%.
13. The DMLS process then starts automatically via the EOS interface.

As stated in Chapter 3, the quality of single track formation is majorly influenced by laser power, scanning speed and layer thickness. For this experiment the layer thickness remained constant at 70 µm. The laser power and scanning speed were varied to determine the optimal process-parameters. In Figure 5.3.2 the experimental design can be seen. The scanning speed was increased with an interval of 0.1 m/s for seven intervals starting at 0.7 m/s and ending at 1.3 m/s. The scanning speed was varied over three different laser powers: 150 W, 170 W and 190 W. In addition, 2 mm- wide surfaces (placing single tracks next to each other) with a hatch distance of 100 µm at three different scanning speeds (0.7, 1.0 and 1.3 m/s) for the three different laser powers (150, 170 and 190 W) were also produced. The quality of the surface is majorly influenced by laser power, scanning speed and hatch distance.

The following experimental procedure was used to manufacture the single tracks and surfaces at different scanning speeds and laser powers:

1. A 6 mm thick Ti6Al4V plate (100 mm x 50 mm) was attached to the substrate with two M5 counter sink cap screws.
2. The attached plate was surface grinded to ensure a homogeneous surface.
3. The substrate and attached plate were fastened into the M280 and aligned.
4. The recoating arm was positioned 70 µm above the Ti6Al4V plate.
5. Cu powder was placed on the plate and the recoating arm was moved back and forth till a homogeneous layer of powder was formed.
6. The 3D sliced data was loaded onto the EOS M280 interface and specific parameter sets were assigned to each single track interval.
7. The chamber is flooded with Argon until oxygen content was below 0.01%
8. The DMLS process starts automatically via the EOS interface
9. The un-melted powder was removed with a vacuum cleaner.
10. The substrate was removed from the EOS M280 and the plate was detached from the substrate.
11. The plate was placed in an ultrasonic bath for 30 min at 25°C to dislodge all remaining unmelted power.

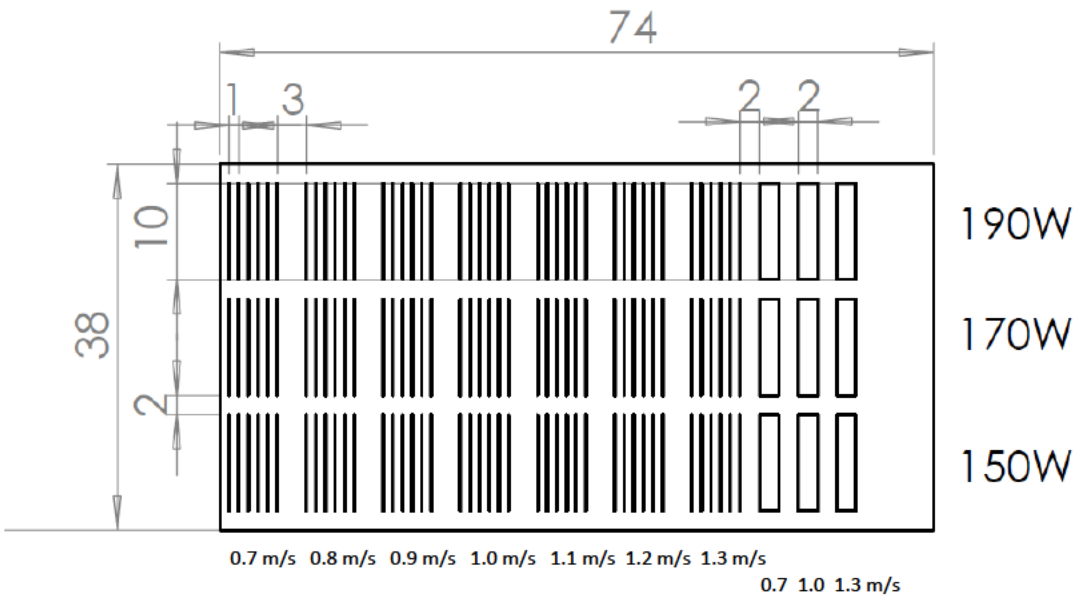

Figure 5.3.2. Design of the experiments with single tracks and surfaces

5.3.2. Results and discussion

To determine the optimal process parameters for Cu powder on a Ti6Al4V substrate the following three aspects were investigated:

1. Characterization of single tracks at various parameter sets.
2. Effect of laser power and scanning speed on track width.
3. Investigation of produced Cu surface at various parameters.

Cu single tracks on the Ti6Al4V substrate

Single tracks produced with DMLS can be characterized into continuous tracks with regular geometrical characteristics (Figure 5.3.3, zone B) and undesired irregular tracks (Fig. 5.3.3, zones A and C). Single track formation is directly influence by the process parameters. If the scanning speed decreases, it results in a higher power input (power per unit speed). Irregular tracks in zone A are formed at higher power input because the heat effected zone becomes larger involving more powder particles. Tracks in zone A tend to have satellites or dislodged sections that form during solidification. Excessive energy input can also lead to keyhole mode resulting in deep remelting of the substrate and pores inside the molten pool. Drop formation (balling effect) occurs at insufficient power input because the surface tension breaks the melting single track into individual droplets (zone C). At low effective power the powder experiences lower temperatures, thus the surface tension coefficient as well as melt viscosity increase leading to drop formation (Yadroitsev *et al.*, 2007).

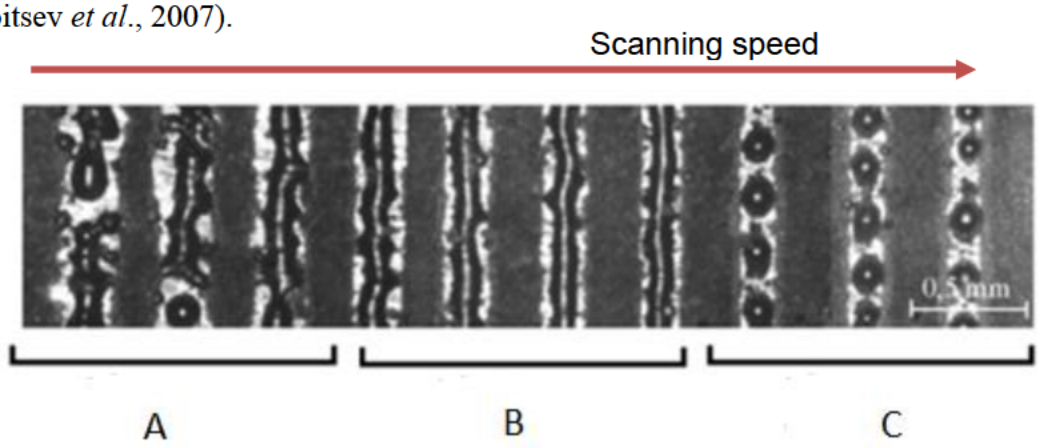

Figure 5.3.3. DMLS single tracks at the substrate (Yadroitsev, 2009)

Powder layer thickness defines the quantity of powder material involved in the molten pool formation (Yadroitsev *et al.*, 2012). The effective powder layer thickness is a combination of the distance moved by the build platform in the Z-direction, the roughness and shrinkage of the

previously processed layer. At standard EOS process-parameters for Ti6Al4V, 30 µm powder layer thickness is utilized (Z-movement of build platform). The average surface roughness of Ti6Al4V samples were found to be *Rz*=30.2±5.52 µm and *Ra*=6.9±1.37 µm (perpendicular to the scanning direction). However the maximum measured *Rz* value was 40 µm (Figure 5.3.4). Thus, a 70 µm powder layer thickness was utilized for the optimal process parameter investigation of Cu on Ti6Al4V substrate. Shrinkage is not taken into account because only one layer of powder is deposited.

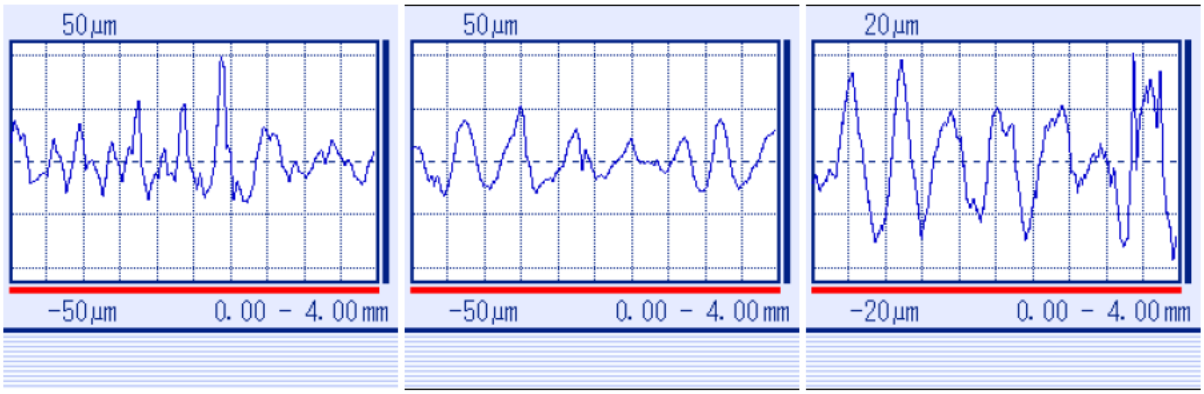

Figure 5.3.4. Surface roughness profiles of the DMLS Ti6Al4V surface at standard EOS process-parameters

Analysis of the manufactured single tracks showed, that at a 150 W laser power the balling effect started to be noticed at scanning speed of 1.2 m/s. The surface tension starts to deform the track though the track is still continuous. At 1.3 m/s the drop formation is fully visible. For scanning speeds lower than 1.1 m/s the tracks are fully continuous and stable with no signs of irregularity. As predicted, the drop formation becomes less with the increase in laser power (170–190 W). An optical microscope was used to measure the single track width. It was found that with an increase in scanning speed the single track width decreased. From Figure 5.3.6 it is clear that laser power has very little effect on single track width. This may indicate that the variation in power was not large enough (150-190 W) to notice a distinct difference in single track width. It is also noted that for single tracks with higher scanning speeds more Cu is visible on the surface of the single track (by colour).

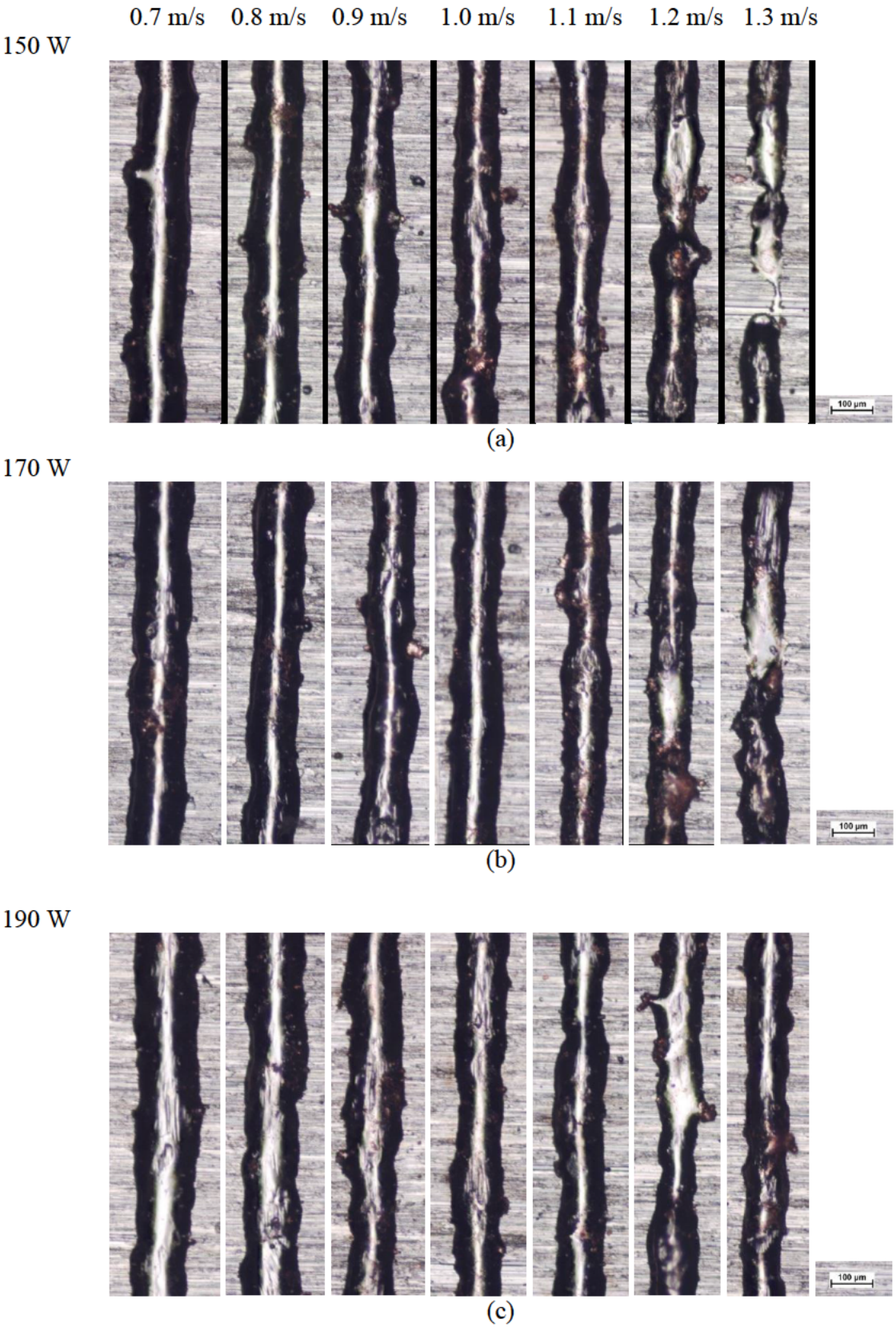

Figure 5.3.5. Single tracks at different laser power: 150 W (a), 170 W (b) and 190 W (c)

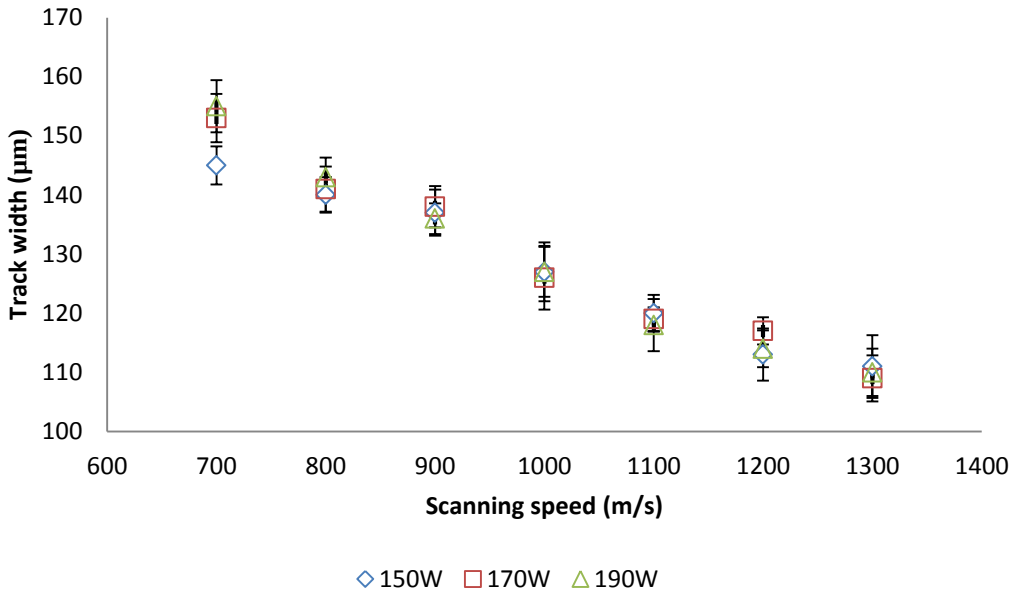

Figure 5.3.6. Effect of process parameters on Cu single track width on a Ti6Al4V substrate

Single layer Cu coating of the Ti6Al4V

In this experiment a Cu surface 2 mm wide and 10-mm long was manufactured with a constant hatch distance of 100 µm. A flat surface was observed for 0.7 m/s scanning speeds at all three intervals of laser power (Figure 5.3.7). Although small cracks were observed perpendicular to the scanning direction. These cracks further indicate the high stresses induced in the scanning direction by the DMLS process. These high stresses and cracks could be a result of the different cooling rates and shrinkages of Cu and Ti6Al4V. Another reason may be different metallic phases formed when processing Cu powder and Ti6Al4V by laser melting. These phases such as intermetallic phases ($CuTi_2$, CuT_i, Cu_3Ti_2, Cu_4Ti_3), are known to be very brittle.

For surfaces produced with 1.0 m/s–1.3 m/s scanning speeds gaps are noticed between tracks. With an increase in laser power the gaps became smaller. The hatch distance was initial estimate at 100 µm due to the fact that the smallest track width established in the previous experiment was 110 µm. This is due to the denudation effect, where the first track is wider than the next (Yadroitsev, 2009). The zone of powder consolidation does not have sufficient powder to form a fully developed single track. At 0.7 m/s scanning speed, single tracks were about 150 µm wide, thus 100 µm hatch distance was a reasonable estimation. To form a suitable surface at 1.0-1.3 m/s scanning speed, the hatch distance must be reduced.

Scanning speed 0.7 m/s 1.0 m/s 1.3m/s

150 W

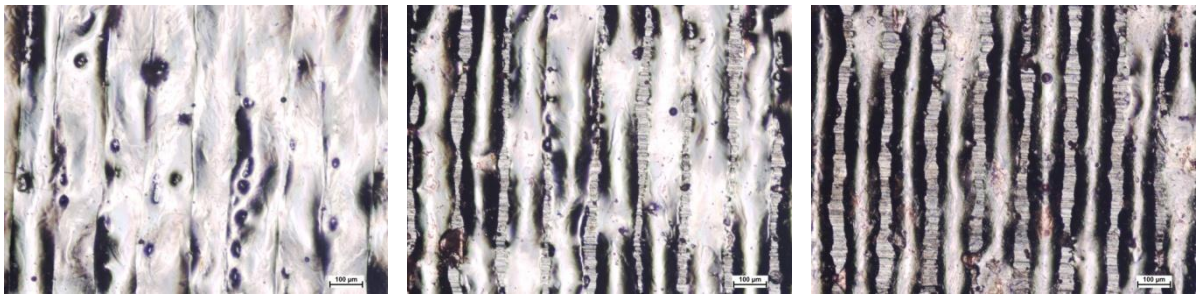

(a)

170 W

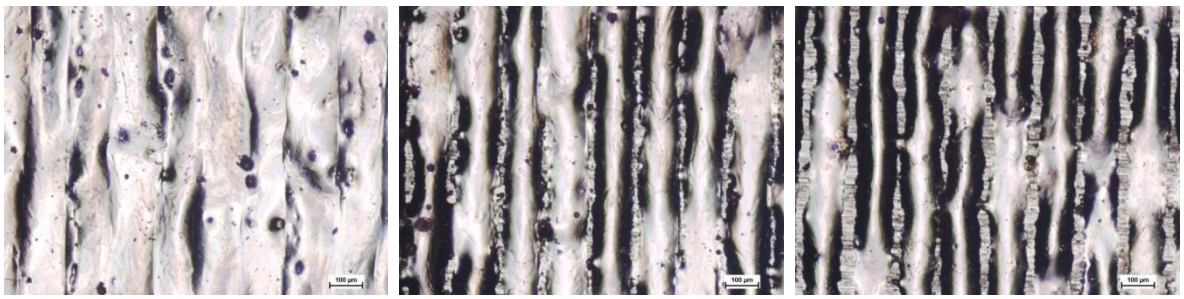

(b)

190 W

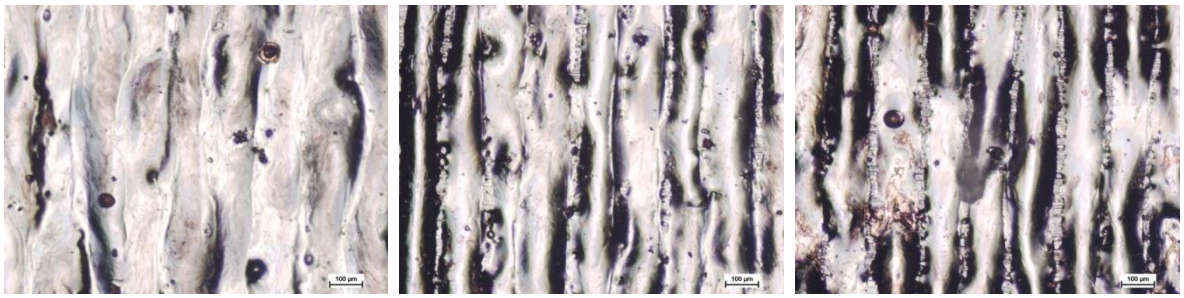

(c)

Figure 5.3.7. Surface morphology of Cu layer on Ti6Al4V substrate at different laser power: (a) 150 W, (b) 170 W and (c) 190 W

5.4. Validation of Ti6Al4V–Cu structures for biomedical applications

5.4.1. Experimental setup

To validate the hypothesis of a Ti6Al4V and Cu multi material implant interface that reduces the risk of bacterial infection two methods of application were investigated. Firstly, by alloying the Ti6Al4V and Cu powder and melting a complete layer. Secondly, by directly melting the Cu powder to 1% of the Ti6Al4V surface. All samples were 10 mm in diameter and 3 mm high. The samples were manufactured from Ti6Al4V and only the last layer was modified. All samples were produced on an EOSINT M280 system.

The Ti6Al4V sample acts as a baseline to determine the effect of the Cu and the effectiveness of the various surfacing strategies to reduce bacterial growth. To manufacture the 1% Cu surface samples, pure Cu was deposited one layer thick (30 µm) on the previously produced Ti6Al4V discs. As suggested by Shirai *et al.* (2009) 1% Cu would be introduced to the Ti6Al4V surface, as it would ensure bacterial death but not be cytotoxic. The laser selectively melted the Cu powder at 1.2 m/s scanning speed and 170 W laser power in argon atmosphere. The specific parameter set was determined from the previous experiment (Chapter 5.3). The pure Cu additions are designed to be 30 µm thick, 150 µm wide and 600 µm long (Figure 5.4.1a). The surface area of the 10 mm diameter disc was 78 mm^2 and the sum of the surface area of the eight Cu single tracks amounted to 0.78 mm^2. Therefor the surface contains 1% Cu on the Ti6Al4V surface in regard to surface area.

To manufacture the 1% (atomic weight) Cu alloy samples pure Cu powder was mixed with Ti6Al4V powder (Figure 5.4.1b). A layer thickness of the alloyed powder was deposited on to the Ti6Al4V disc and the entire surface of the sample was melted. To produce the surface standard Ti6Al4V process parameters were utilized (1.2 m/s scanning speed, 170 W laser power). The alloy powder was mixed according to atomic weight. Cu and Ti6Al4V have an atomic mass of 63.546 and 45.859 respectively. 1.38 g of Cu with 98.62 g of Ti6Al4V powders were mixed for 1 hour.

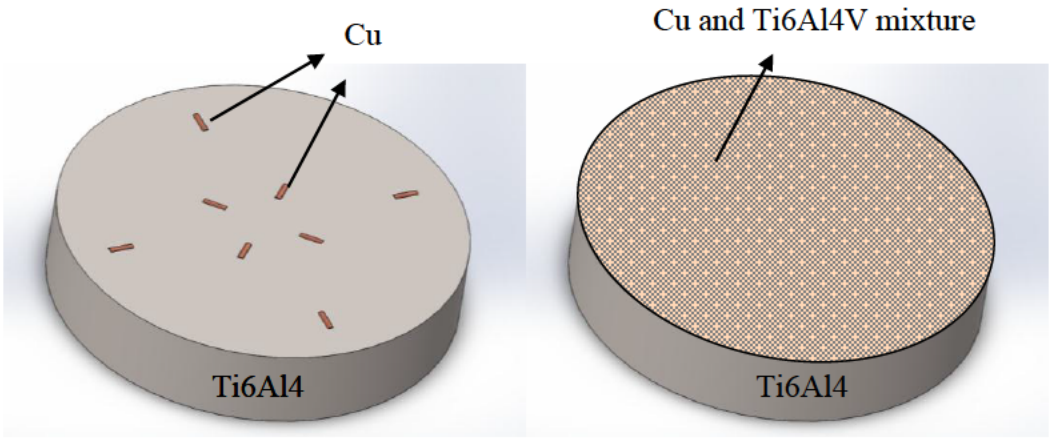

Figure 5.4.1. 1% Cu surface (a) and 1% Cu alloy samples (b)

The Ti6Al4V discs with the substrate were heat treated at 650˚C for 3 hours in an argon atmosphere for stress relieving. After heat treatment the substrate with the discs was placed into the EOSINT M280 and the surface modification completed. The samples were then cut with a EDM wire cut machine from the substrate and placed in an alcohol bath at 25˚C for 30 min to remove fine powder particles. Three series of samples were manufactured namely; 1% Cu surface, 1% Cu alloy and control samples. For each series of samples 12 discs were manufactured.

Two different microbes were used namely *Escherichia coli* ATCC 10536 (Gram-negative rod shaped) and *Staphylococcus aureus* ATCC 25923 (Gram-positive cocci). Suspensions of actively growing bacterial cells (pure or mixed) at a concentration of 10^5 CFU/ml were applied to the discs at time 0 h. Cells were incubated at 37°C in a 24 well culture plate without aeration for 24 h. Pure cultures were performed in triplicate and bacterial mixtures performed in duplicate. Bacterial counts (CFU/ml) were determined from the suspension after incubation. Pure cultures were enumerated on nutrient agar plates. Mixed cultures were enumerated on selective agar; Chromocult (*E. coli*) and Baird-Parker (*S. aureus*). To determine the effect of the Cu additions two control conditions were utilized. Firstly, to show the growth of microbes without any influences, a sterile nutrient broth where no disks were present (control ND in Fig. 5.4.2) was

employed. Secondly, Ti6Al4V discs were placed in a sterile nutrient broth. This condition showed the effect of the Ti6Al4V disc on the microbes without any effect from the Cu additions.

5.4.2. Results and discussion

To study the produced Ti6Al4V-1%Cu samples, EDX analysis was performed with a JOEL Scanning Electron Microscope (SEM) at the University of the Free State (UFS). The control Ti6Al4V sample had a typical DMLS surface layer with a surface roughness *Rz*=30.2±5.52 μm, *Ra*=6.9±1.37 μm (perpendicular to the scanning direction).

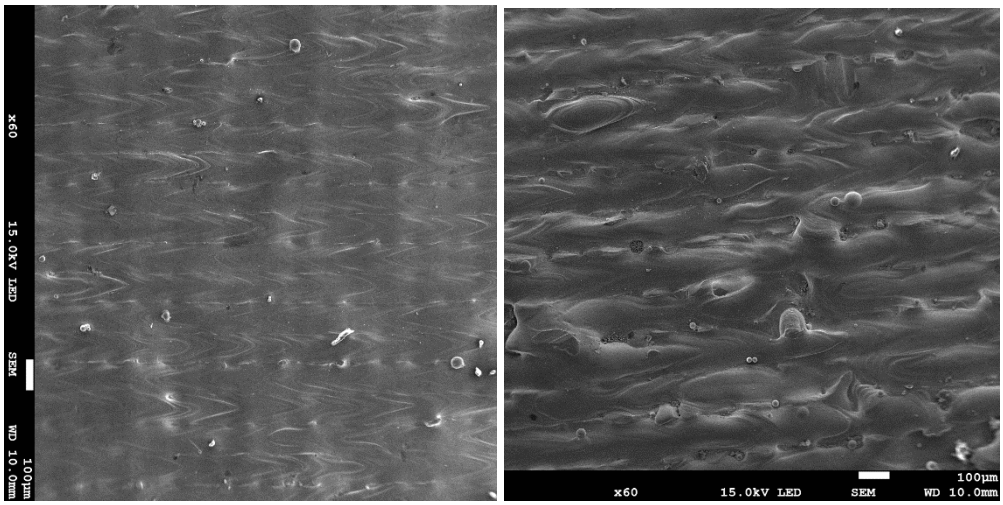

(a) (b)

Figure 5.4.2. Single layer surface morphologies: Ti6Al4V sample (a) and Ti6Al4V-1% Cu alloy

SEM and energy dispersive X-ray (EDS) analysis was performed on the samples. This was done to investigate the elemental distribution near the surface of the manufactured DMLS samples. Six element maps with magnification x200 (2 maps for 3 discs, Figure 5.4.3) confirmed the chemical composition of the control Ti6Al4V samples: 90.55±0.09% Ti, 5.65±0.05 Al and 3.79±0.13%V. The final material chemistry is satisfactory to ASTM standard (F2924-14). The elemental analysis was conducted on a rough unpolished surface, which may have influenced the results slightly. However, it is important to note that no impurities and spectra of other elements were detected.

The Ti6Al4V-1% Cu alloy had an non-homogeneous surface layer; an average surface roughness was *Rz*=38.0±4.17 µm, *Ra*=8.0±0.69 µm (perpendicular to the scanning direction). These imperfections were not expected due to the small percentage of Cu added to the Ti6Al4V, therefore standard Ti6Al4V process parameters were used. Although from the SEM analysis it is clear that optimal process parameters will have to be determined for Ti6Al4V-1%Cu powder mixture separately.

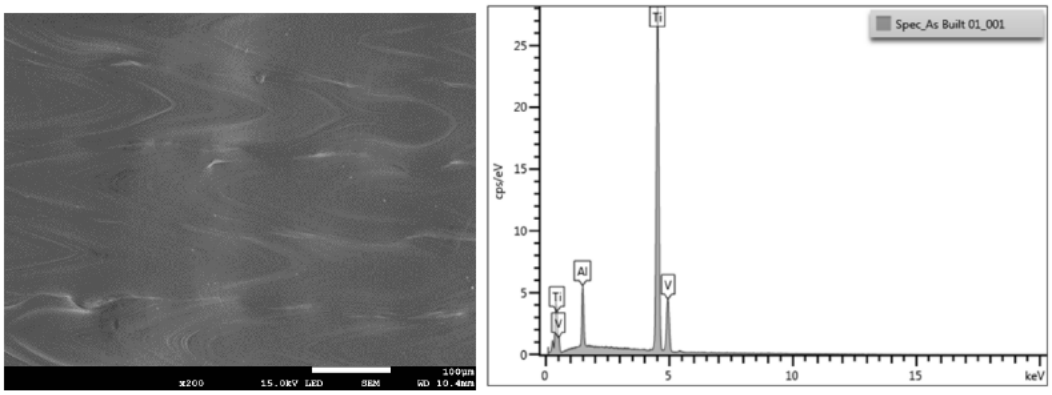

(a) (b)

Figure 5.4.3. (a) Back scatter detector (BSE) surface morphology images and (b) EDS spectra for Ti6Al4V sample

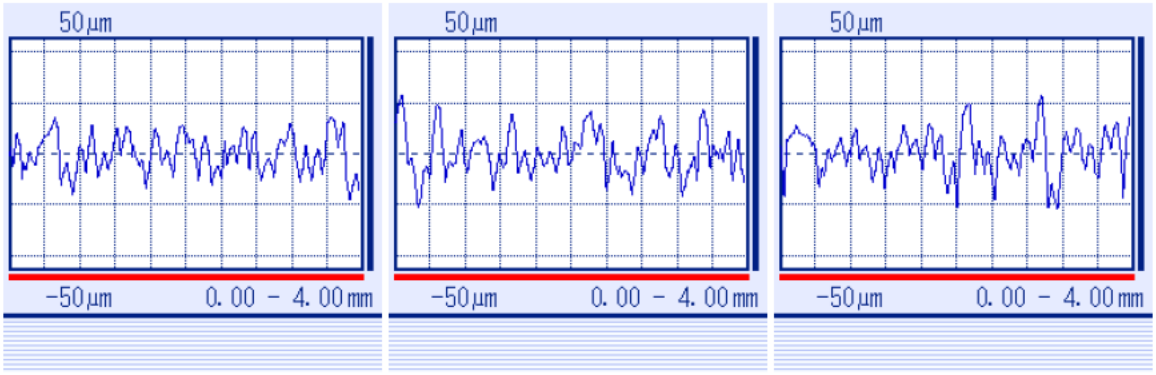

Figure 5.4.4. Surface roughness profiles of the DMLS Ti6Al4V-1% Cu alloy surface at standard EOS process-parameters for TiAl4V

For the Ti6Al4V-1%Cu powder mixture, an element map indicated that 4.31±2.19% of Cu was present near the surface. The element map indicated that the Cu was more or less homogeneously spread throughout the entire surface (Figure 5.4.5). Additional EDS analysis of the cross-sections

of the disks is needed to investigate the dilution of Cu in the layer and how Cu particles melted with Ti6Al4V powder and the substrate.

The 1% Cu surfaces were successfully manufactured to the desired dimensions. The prescribed pure Cu additions had a 150 µm width and 600 µm length. Examining the Cu additions showed that quality single tracks were produced however small cracks were visible on the Cu surface. An element map indicated that the Cu was concentrated over the desired regions and not the entire surface.

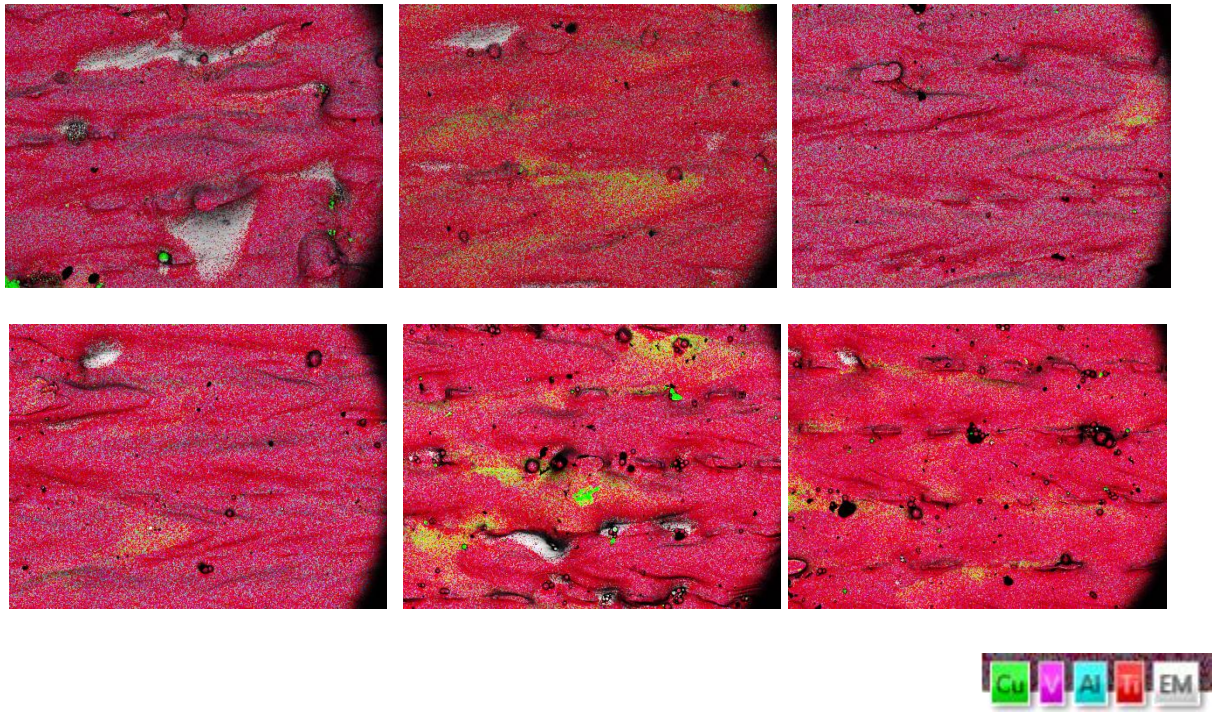

Figure 5.4.5. Elemental maps and photos of Ti6Al4V-1%Cu alloy samples

A line scan indicated that the surface composition of the Cu additions was a mixture of Ti6Al4V and Cu since Cu powder was melted with the substrate. Utilizing an element map, the percentage of Cu on the surface can be estimated (Figure 5.4.6). The surface area of the map (0.466 mm^2) consisted of 17.4% Cu and 82.6% Ti6Al4V. This implies that the total Cu on the entire surface (78.54 mm^2) was not in fact 1% but 0.81%.

Microbiological results shown in Fig. 5.4.7 indicate that the presence of all discs lead to growth inhibition of the *S. aureus.* All changes observed were statistically significant ($p<0.05$, *t-test*). It

is important to note that the adhesion of the bacteria to the surface was not considered, thus less cells can be counted in the suspension.

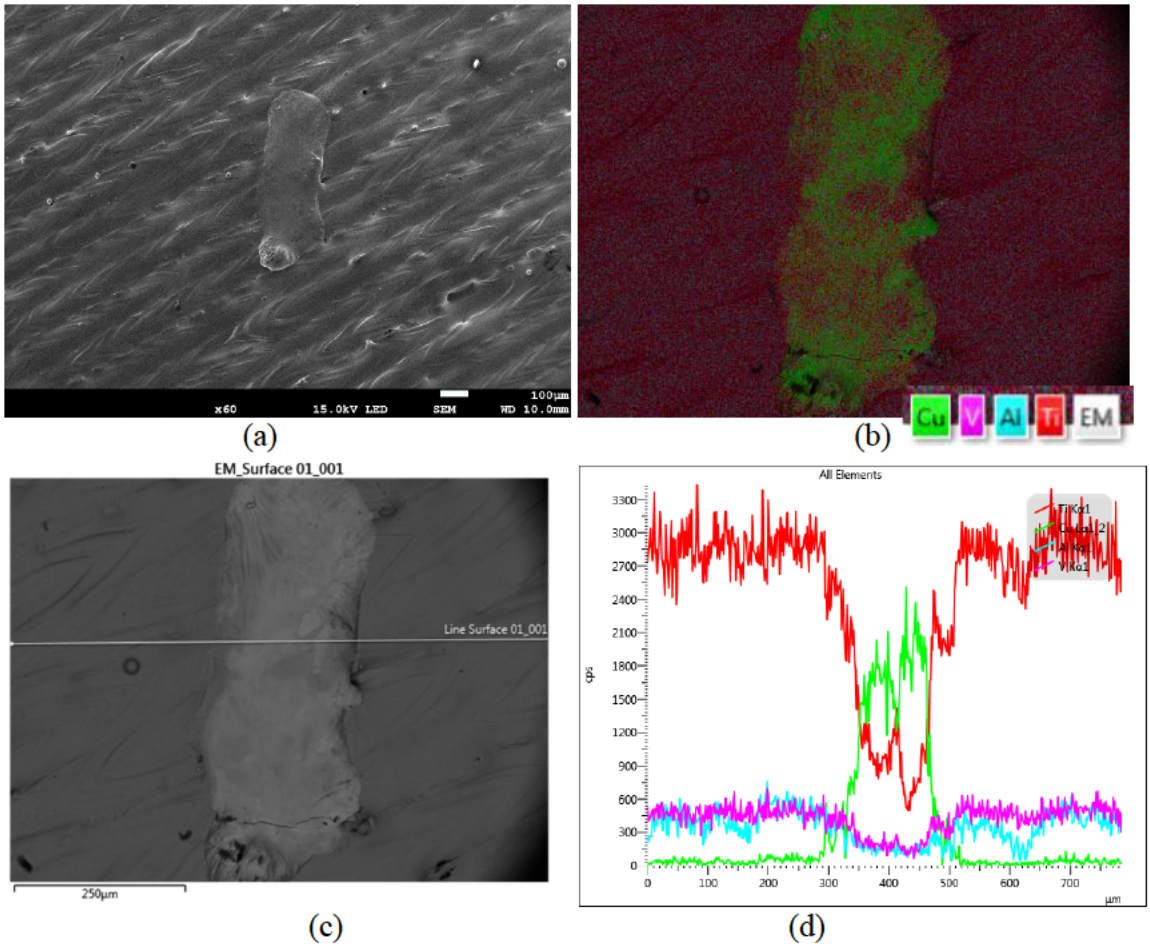

Figure 5.4.6. (a) SE photo of Ti6Al4V-1%Cu surface sample; (b) elemental map, (c) BSE photo and (d) elemental line scan

The presence of Cu in the alloy had a more profound effect on *S. aureus* than on *E. coli*. The bacteriostatic effect (growth inhibition of *S. aureus*) in the mixed culture was also attributed to the presence of Cu in the alloy (Figure 5.4.7). The Ti6Al4V-1%Cu alloy had a greater influence on growth inhibition for both *S. aureus* and *E. coli* compared to the Ti6Al4V-1%Cu surface. An EDX analysis showed that 4.31% and 0.81% Cu were present on the top area of the Ti6Al4V-1%Cu alloy and Ti6Al4V-1%Cu surface disks respectively. More profound antibacterial effect of the Ti6Al4V-1%Cu alloy disks compared to the Ti6Al4V-1%Cu surface disks can be linked with the higher Cu content on the Ti6Al4V-1%Cu alloy

disks top areas. Also different roughness of the samples can have an influence on the microbe's adhesion to the surface and, finally, on the count of the cells in the suspension.

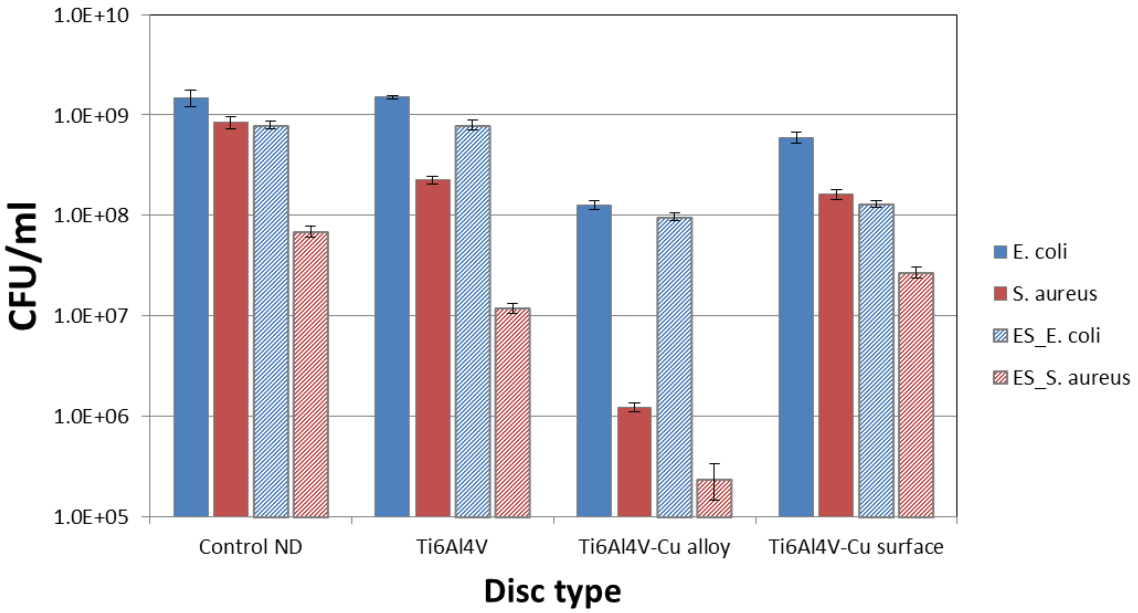

Figure 5.4.7. Antibacterial activity of Cu. ES – bacterial cell mixture of *E. coli* and *S. aureus*; CFU – colony forming unit

5.5. Conclusion

In this chapter Ti6Al4V-Cu structures were investigated as an antibacterial implant interface. The Ti6Al4V-1%Cu structures were manufactured in two proposed processes. Firstly, by in-situ alloying of Ti6Al4V powder with 1%Cu powder. Secondly, by producing pure Cu regions on a Ti6Al4V substrate, so that the surface contains 1% Cu by means of surface area. Before producing Cu single tracks on a Ti6Al4V substrate, optimal process parameters needed to be determined. It was found that a laser power of 170 W and scanning speed of 1.2 m/s were the optimal process parameters to produce stable continuous single tracks. Further investigation of the Cu single tracks showed that the track width reduced with an increase in laser scanning speed and that the optimal hatch distance was approximately 70µm.

The produced Ti6Al4V-1%Cu alloy structure showed a rough surface finish and further investigation needs to be conducted on optimal process parameters for the Cu additions to

Ti6Al4V. Furthermore the Ti6Al4V-1%Cu surface structure exhibited continuous single tracks but small cracks were notice perpendicular to the scanning direction.

A microbiological experiment suggested that the Ti6Al4V-1%Cu alloy structure was more effective as an antibacterial interface than the Ti6Al4V-1%Cu surface structure. Ti6Al4V-1%Cu alloy structure successfully inhibited the growth of both *S. aureus* and *E. coli*, having a greater effect on *S. aureus*.

The greater percentage Cu on the Ti6Al4V-1%Cu alloy may be the reason for the larger effect on bacterial growth inhibition. However, the Cu on the Ti6Al4V-1%Cu surface was not homogeneous over the entire surface, rather in selected regions. It may be that the bacteria avoids the prescribed Cu areas of the Ti6Al4V-1%Cu surface and grows on the Ti6Al4V substrate. This is not possible when considering the Ti6Al4V-xCu alloy as the Cu addition is homogeneous over the entire surface. Rescanning strategy can be used to produce in-situ homogenous DMLS layer from a mixture of Ti6Al4V and Cu powder. Further experiments are needed to conclude on the effect of percentage Cu addition and surface roughness on bacteria growth inhibition and adhesion.

5.6. References

Andani, M.T., Moghaddam, N.S., Haberland, C., Dean, D., Miller, M.J. and Elahinia, M., 2014. Metals for bone implants. Part 1. Powder metallurgy and implant rendering. Acta biomaterialia, 10(10), pp.4058-4070.

ASTM F2924-14, Standard Specification for Additive Manufacturing Titanium-6 Aluminum-4 Vanadium with Powder Bed Fusion, ASTM International, West Conshohocken, PA, 2014.

Bandyopadhyay, A., Espana, F., Balla, V.K., Bose, S., Ohgami, Y. & Davies, N.M., 2010. Influence of porosity on mechanical properties and in vivo response of Ti6Al4V implants. Acta Biomaterialia, 6(4), pp.1640-1648.

Bergmann, C.P. & Stumpf, A., 2013. Dental Ceramics: Microstructure, Properties and Degradation. Springer Science & Business Media.

Jung, C., Straumann, L., Kessler, A., Pieles, U. & de Wild, M., 2014. Antibacterial copper deposited onto and into the oxide layer of titanium implants. BioNanoMaterials, 15, pp.110.

Jung, C., Ryter, N., Köser, J., Hoffmann, W., Straumann, L., Balimann, N., Meier, F., de Wild, M., Schlottig, F., Martin, I. & Pieles, U., 2012. Antibacterial functionalization of the

surface of titanium implants by electrochemical copper deposition. European Cells and Materials, 23, pp.16.

Lipinski, P., Barbas, A. & Bonnet, A. S., 2013. Fatigue behavior of thin-walled grade 2 titanium samples processed by selective laser melting. Application to life prediction of porous titanium implants. Journal of the Mechanical Behavior of Biomedical Materials, 28, pp.274–290.

MacKeen, P.C., Person, S., Warner, S.C., Snipes, W. & Stevens, S.E., 1987. Silver-coated nylon fiber as an antibacterial agent. Antimicrobial agents and chemotherapy, 31(1), pp.93-99.

Niinomi, M., 2008. Mechanical biocompatibilities of titanium alloys for biomedical applications. Journal of the Mechanical Behavior of Biomedical Materials, 1, pp.30–42.

Pattanayak, D.K., Fukuda, A., Matsushita, T., Takemoto, M., Fujibayashi, S., Sasaki, K., Nishida, N., Nakamura, T. & Kokubo, T., 2011. Bioactive Ti metal analogous to human cancellous bone: fabrication by selective laser melting and chemical treatments. Acta Biomaterialia, 7(3), pp.1398-1406.

Shirai, T., Tsuchiya, H., Shimizu, T., Ohtani, K., Zen, Y. & Tomita, K., 2009. Prevention of pin tract infection with titanium-copper alloys. Journal of Biomedical Materials Research Part B: Applied Biomaterials, 91(1), pp.373-380.

Williams, D.F., 1999. The Williams dictionary of biomaterials. Liverpool University Press.

Yadroitsev, I., 2009. Selective laser melting: Direct manufacturing of 3D-objects by selective laser melting of metal powders. LAP Lambert Academic Publishing, Saarbrücken, Germany.

Yadroitsev, I., Bertrand, P. & Smurov, I., 2007. Parametric analysis of the selective laser melting process. Applied Surface Science, 253, pp.8064–8069.

Yadroitsev, I., Yadroitsava, I., Bertrand, P. & Smurov, I., 2012. Factor analysis of selective laser melting process parameters and geometrical characteristics of synthesized single tracks. Rapid Prototyping Journal, 18(3), pp.201-208.

Yavari, S.A., Wauthlé, R., van der Stok, J., Riemslag, A.C., Janssen, M., Mulier, M., Kruth, J.P., Schrooten, J., Weinans, H. & Zadpoor, A.A., 2013. Fatigue behavior of porous biomaterials manufactured using selective laser melting. Materials Science and Engineering: C, 33(8), pp.4849-4858.

CHAPTER 6. CONCLUSION AND FUTURE WORK

In this work DMLS multi material structure for biomedical applications were investigated. The study was divided into major two sections:

1. The conceptual development and validation of a multi material powder deposition system for DMLS
2. The manufacturing and validation of Ti6Al4V-Cu structures that reduce the risk of bacterial infection.

In the literature review the current DMLS process, existing multi material powder deposition systems and applications of multi material structures by DMLS were described. The layer by layer nature of the DMLS process allows parts to be manufactured that previously weren't possible with conventional manufacturing methods. The ability to produce complex structures from predetermined CAD data in a time efficient manner makes DMLS ideal for biomedical application. Process parameters play a major role in the accuracy and quality of the parts being manufactured. For each powder a set of optimal process parameters (laser power, scanning speed, layer thickness, laser spot size, etc.) need to be determined.

Currently multi material structures are possible with DMLS. However, the powder variation is between layers and not on a specific layer. An ideal multi material powder deposition system forms a homogeneous powder layer with a sharp interlocking powder interface on a specific layer. Accurately depositing powder to form complex geometry yet time efficiently. There are many conceptual prototypes to deposit multiple powders on a single layer but none exhibit all the necessary attributes. Multi material structures from DMLS do not only have applications in the biomedical field but also the tool making and aerospace industries.

Ti6Al4V is widely accepted as biomaterial that is commonly used to manufacture medical and dental implants. Ti6Al4V exhibits excellent biocompatible and corrosive resistant properties. As indicated in literature, Cu has antibacterial properties and in small percentages is not toxic to the human body.

For the experiments in this dissertation only Ti6Al4V and pure Cu powder were considered. Both the Ti6Al4V and Cu powder were sourced from TLS Technic. The powders are spherical in shape and –45 µm in size.

A multiple hopper powder deposition system is proposed to produce multi material structures for biomedical applications. The powder deposition system utilizes multiple hoppers with a dynamically varied outlet to form a homogeneous powder layer that has a sharp interlocking interface. By varying the slot length as the hopper moves over the substrate accurate powder deposition occurs time effectively. To determine the optimal hopper parameters an experimental hopper was manufactured to similar sizes and composition as the intended final design. This experimental hopper had a variable slot width and hopper wall angle. The experiment showed that for both Ti6Al4V and Cu powder repeatable and stable flow occurred at 3 mm slot width and 60° hopper wall angle. The experiment also proved that flow properties are not sufficient in estimating powder flow through hoppers. The Hauser ratio and Carr index indicated that Ti6Al4V has better flow properties than that of Cu. However Cu showed better flow rates through the experimental hopper than that of Ti6Al4V. Furthermore, multiple powders were deposited on a Ti6Al4V substrate with a prototype hopper, which validated the concept of multiple hopper powder deposition. A homogeneous powder layer was formed with a sharp interlocking interface. With the data received from various experiments a final hopper design was produced.

To validate Ti6Al4V-xCu structures as a multi material implant interface that reduces the risk of bacterial infection, two methods were proposed: 1) in-situ DMLS alloying Ti6Al4V and Cu powders as top layer of the sample; 2) surface modification of DMLS Ti6Al4V substrate by deposition pure Cu directly onto the desired regions. EDX analysis showed that Cu was successfully melted with the Ti6Al4V powder, exhibiting a final Cu percentage of 4.31% on the top surface of the structure. Selected Cu areas were produced on 0.81% of the Ti6Al4V substrate surface. To determine the more effective structure, microbiological experiments were conducted. These experiments showed that the in-situ alloying process was the most effective and a viable concept as an antibacterial implant interface. Further experiments are needed to conclude on the effect of percentage Cu addition on bacteria growth inhibition.

Future work entails further investigation of Ti6Al4V-Cu alloys as an antibacterial agent at the implant interface. The effect of varies percentages of Cu additions on the mechanical properties, microstructure, antibacterial affectivity and cytotoxicity of Ti6Al4V-xCu structures will also need to be investigated. Optimal process parameters will need to be determined for each addition of Cu to the alloy. The final task will be to manufacture advanced implants that will be clinically tested. Bacterial testing will not be limited only to *S. aureus* and *E. coli* but immerging pathogens causing anaerobic infections associated with implants (for example, *Prerotella intermedia, Porphgromonas gingivalis, Tannerella forsgthia, Fusobacterium nucleatum* and *Aggregatibacter achnomycetemcomitans*). It is also necessary to conduct tests with not only laboratory strains but also isolated strains from failed implants.